AD-A110 212 HUGHES HELICOPTERS CULVER CITY CA F/G 1/3
ADVANCED CONCEPTS FOR COMPOSITE STRUCTURE JOINTS AND ATTACHMENT--ETC(U)
NOV 81 J V ALEXANDER, R H MESSINGER DAAJ02-77-C-0076
UNCLASSIFIED HH-80-402-VOL-1 USAAVRADCOM-TR-81-D-21A NL

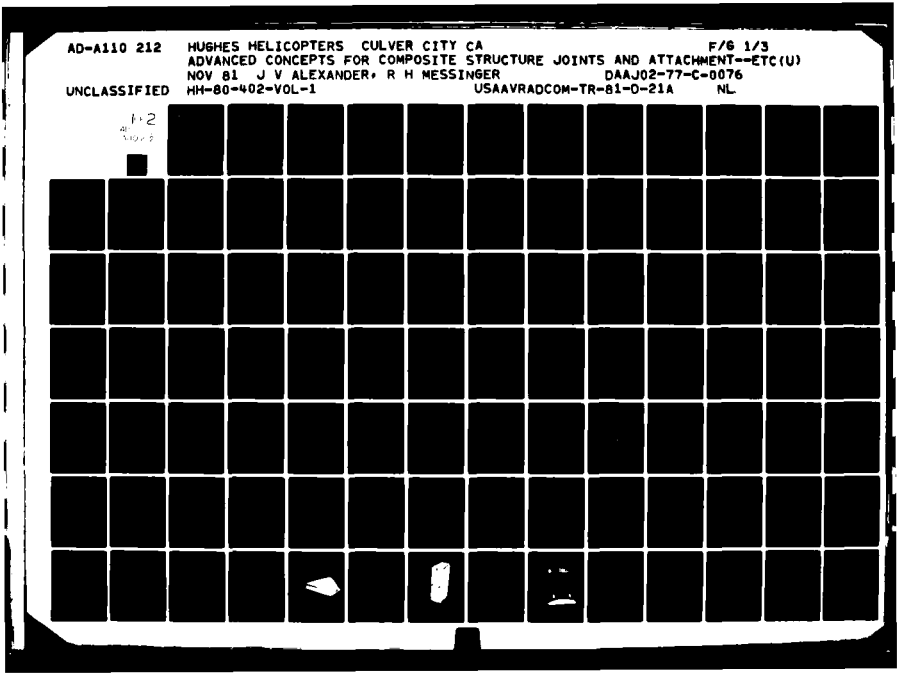

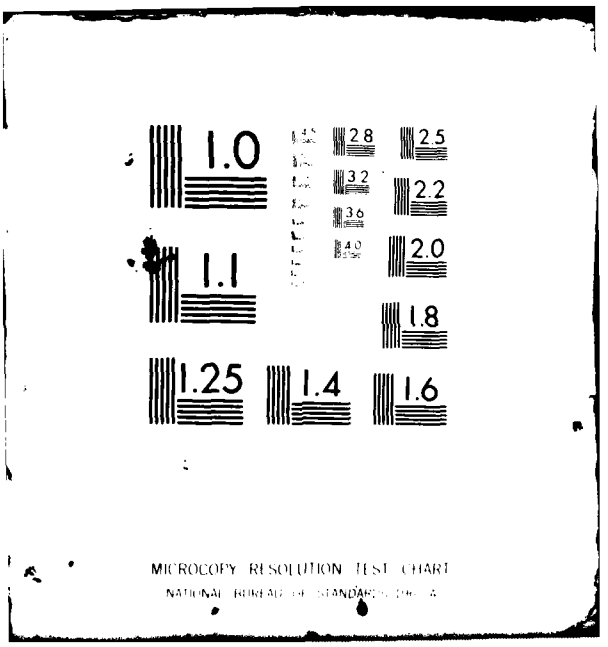
1.0
1.1
1.25
1.4
1.6
2.8
3.2
3.6
4.0
2.5
2.2
2.0
1.8
MICROCOPY RESOLUTION TEST CHART
NATIONAL BUREAU OF STANDARDS

USAAVRADCOM-TR-81-D-21A

AD A110218

LEVEL II

12

ADVANCED CONCEPTS FOR COMPOSITE STRUCTURE JOINTS AND ATTACHMENTS FITTINGS

Volume I - Design and Evaluation

J. V. Alexander and R. H. Messinger
Hughes Helicopters
Division of Summa Corporation
Culver City, CA 90230

November 1981

Final Report for Period July 1977 - October 1980

Prepared for

APPLIED TECHNOLOGY LABORATORY
U. S. ARMY RESEARCH AND TECHNOLOGY LABORATORIES (AVRADCOM)
Fort Eustis, Va. 23604

APPLIED TECHNOLOGY LABORATORY POSITION STATEMENT

This report consists of two volumes and identifies all design considerations, testing, and cost analysis pertinent to composite joints and fittings attachments. The approach used in this program was to identify generic types of joints and fittings applicable to helicopter composite primary structures; the design emphasized reliability and cost effectiveness. The technology developed in this program has been incorporated in the design of new major composite components such as tail sections, and the foundation for future R&D work has been laid.

Mr. Nick Calapodas of the Aeronautical Technology Division served as project engineer for this effort.

AD A110212

UNCLASSIFIED

SECURITY CLASSIFICATION OF THIS PAGE *(When Data Entered)*

REPORT DOCUMENTATION PAGE		READ INSTRUCTIONS BEFORE COMPLETING FORM
1. REPORT NUMBER USAAVRADCOM-TR-81-D-21A	2. GOVT ACCESSION NO. AD-A110 212	3. RECIPIENT'S CATALOG NUMBER
4. TITLE *(and Subtitle)* ADVANCED CONCEPTS FOR COMPOSITE STRUCTURE JOINTS AND ATTACHMENT FITTINGS – Volume I: Design and Evaluation		5. TYPE OF REPORT & PERIOD COVERED Final Report Jul 1977 - Dec 1980
		6. PERFORMING ORG. REPORT NUMBER HH-80-402
7. AUTHOR(s) J. V. Alexander and R. H. Messinger		8. CONTRACT OR GRANT NUMBER(s) DAAJ02-77-C-0076
9. PERFORMING ORGANIZATION NAME AND ADDRESS Hughes Helicopters Division of Summa Corp. Culver City, California 90230		10. PROGRAM ELEMENT, PROJECT, TASK AREA & WORK UNIT NUMBERS 62209A IL262209AH76 00 228 EK
11. CONTROLLING OFFICE NAME AND ADDRESS Applied Technology Laboratory, U.S. Army Research and Technology Laboratories (AVRADCOM), Fort Eustis, Virginia 23604		12. REPORT DATE November 1981
		13. NUMBER OF PAGES 125
14. MONITORING AGENCY NAME & ADDRESS*(if different from Controlling Office)*		15. SECURITY CLASS. *(of this report)* Unclassified
		15a. DECLASSIFICATION/DOWNGRADING SCHEDULE

16. DISTRIBUTION STATEMENT *(of this Report)*

Approved for public release: distribution unlimited.

17. DISTRIBUTION STATEMENT *(of the abstract entered in Block 20, if different from Report)*

18. SUPPLEMENTARY NOTES

Volume I of a two-volume report.

19. KEY WORDS *(Continue on reverse side if necessary and identify by block number)*

Attachment Fittings	Helicopters	Strength
Composite Fittings	Joints	Weight
Design	Nondestructive Inspection	Wet Filament Winding
Fabrication		

20. ABSTRACT *(Continue on reverse side if necessary and identify by block number)*

The purpose of this program was to develop the technology of applying fiber-reinforced composite materials to helicopter joints and attachment fittings that permit disassembly of major components. A generic design methodology approach was used to make the data developed applicable to ongoing and future helicopter programs.

DD FORM 1 JAN 73 1473 EDITION OF 1 NOV 65 IS OBSOLETE

UNCLASSIFIED

SECURITY CLASSIFICATION OF THIS PAGE *(When Data Entered)*

A detail design, analysis, and testing program was carried out on the three joint and fitting concepts selected: wrapped tension fittings, gearbox attachment fittings, and seat attachment fittings.

The scope of the study included analytical design tools, including finite element computer analysis; fabrication techniques, with special emphasis on weight and cost effectiveness considerations; structural integrity testing, including static, dynamic, failsafe/safe-life, and ballistic tolerance considerations; and nondestructive inspection (NDI) techniques.

The analytical results, test results, and Design Guide for each type of joint or fitting tested are presented in Volume II.

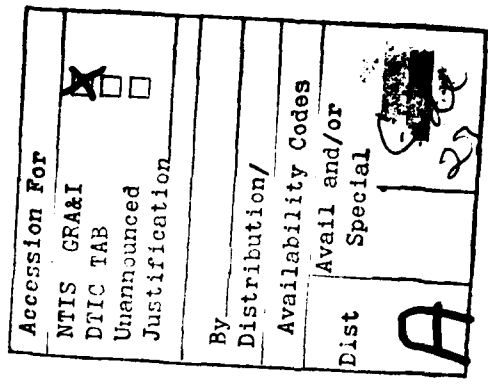

SUMMARY

This report was prepared by Hughes Helicopters, Division of Summa Corporation, Culver City, California, for the Applied Technology Laboratory, U. S. Army Research and Technology Laboratories (AVRADCOM), Fort Eustis, Virginia, under Contract DAAJ-02-77-C-0076.

The purpose of this program was to develop the necessary methodology for applying fiber-reinforced composite materials to helicopter joints and attachment fitting designs that permit disassembly of major components.

Primary joints and fittings representative of high performance helicopters (the YAH-64 in particular) were selected for evaluation. A generic design methodology approach was used so that the data that was developed could be applied to other helicopter programs.

The objective of this program was to develop basic concepts for competitive helicopter joints and fittings using composite materials. The composite components developed were capable of being attached to other components, both composite and metal, such that their weight and cost effectiveness was an improvement over the baseline metal component alternatives.

During preliminary design, the various types of joints used on a modern helicopter such as the YAH-64 were characterized. The state-of-the-art design methodology and fabrication process as it relates to composite joints and fittings was surveyed; conceptual drawings were prepared; analytical tools were selected; testing methods were recommended; and generic joint/fitting concepts, including materials and fabrication methods, were selected.

Six types of joints and fittings were selected for continued evaluation in order to cover as broad a range of design types as possible within the scope of the program. During the detail design activity, these six joint and fitting concepts were designed and analyzed. Strength, weight, and cost comparisons were made with the baseline metallic joints and fittings. Three designs were selected for fabrication and test. Fabrication and Test Plans were prepared for these components.

Sixteen specimens of the three final designs were fabricated and tested. Static strength and endurance limit data obtained from the tests were compared with analytical predictions.

The program was successful in proving that reliable, efficient composite joints are practical in the design of primary aircraft structures.

TABLE OF CONTENTS

LIST OF ILLUSTRATIONS

LIST OF ILLUSTRATIONS (CONT)

LIST OF ILLUSTRATIONS (CONT)

LIST OF ILLUSTRATIONS (CONT)

LIST OF TABLES

INTRODUCTION

This report describes the design of composite structure joints and attachment fittings and the testing necessary to verify that the design concepts are capable of producing reliable, long-life, low-cost, advanced composite helicopter primary structures.

The program began with a survey and evaluation of the problems of designing, fabricating, and testing composite helicopter joints and fittings that were capable of being disassembled. The objective was to select and recommend to the Army a minimum of five relatively generic joint and fitting concepts for detail design, using composite materials integrated into composite components whenever possible. Figure 1 illustrates the locations of the various helicopter structural joints which were considered to be candidates for the application of composite materials. Four types of fittings – tension, lug, shear, and socket – were identified as being appropriate for these joints. Table 1 shows the joints arranged in a matrix by possible fitting types. The alphanumeric codes identify different concepts of each fitting type. That is, A1, A2, etc, are variations of fitting type A.

Rotor blade root end attachments, stiffener-to-panel and -skin joints, and honeycomb panel lap joints are specific types of joints which were not considered.

The first step was establishing generic baselines for the selected joints and fittings. Then composite design concepts were developed.

After the design requirements were defined and the available data were evaluated, a preliminary design study was performed to develop candidate design configurations. The analytical tools required for determining the structural efficiency of each joint and fitting type were evaluated, and a NASTRAN computer program (a three-dimensional, multilayered, finite element model routine in two parts) was developed to determine the interlaminar shear properties in the radius of an angle (Volume II). Test requirements that would yield useful design data were recommended.

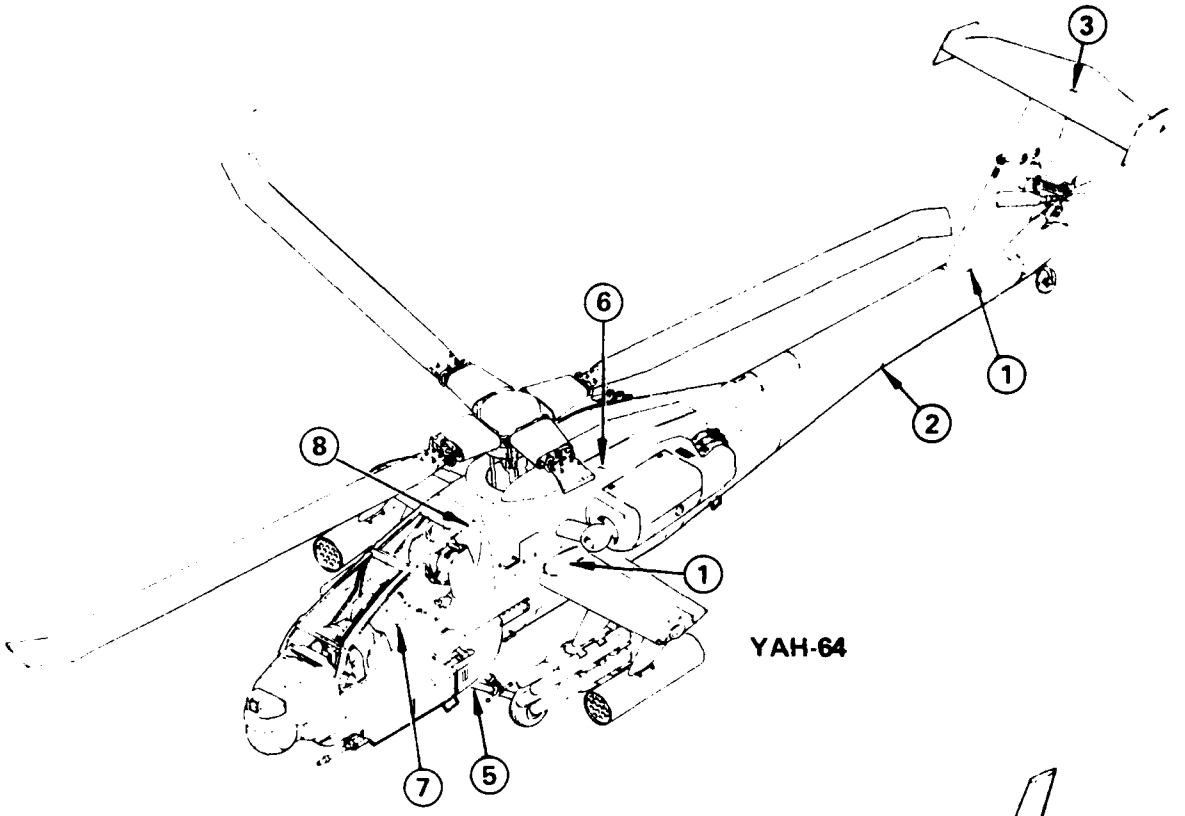

NUMBERS INDICATE JOINT DESIGN TYPES (SEE TABLE 1)

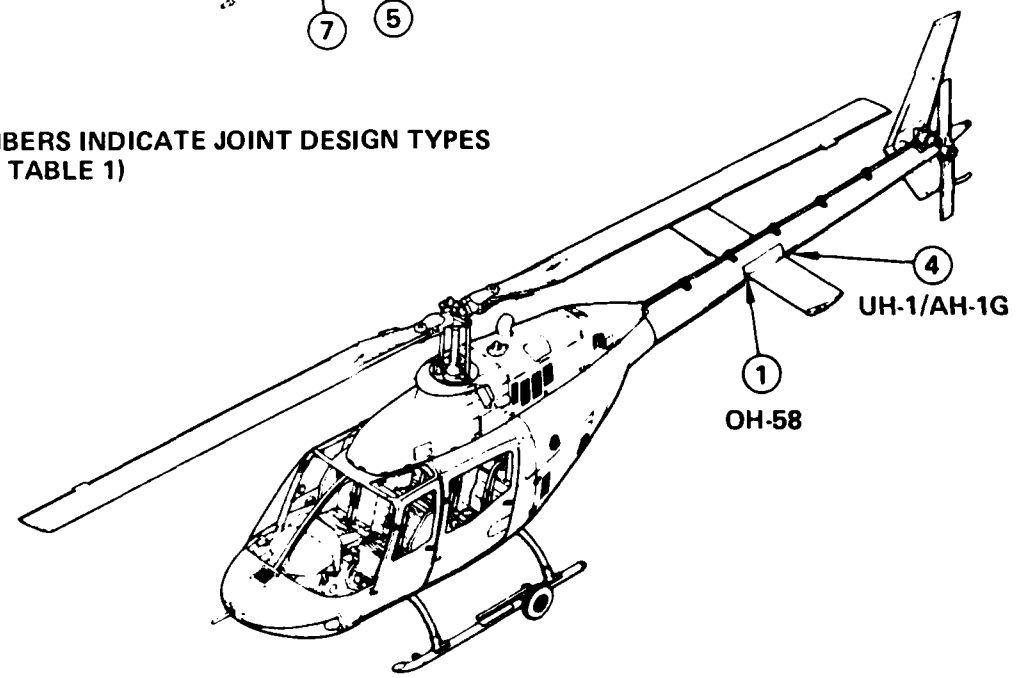

Figure 1. Composite Joints and Attachment Fittings

TABLE 1. COMPOSITE JOINT/FITTING MATRIX

		Joint Type							
		1	2	3	4	5	6	7	8
		Vertical Tail-to-Tailboom Horizontal Stabilizer-to-Fuselage Wing-to-Fuselage	Tailboom-to-Fuselage Fuselage Section-to-Fuselage Section	T-tail Horizontal Stabilizer-to-Vertical Tail	Sync Elevator-to-Tailboom	Landing Gear-to-Fuselage Other Pivots Trunnions Stud Shafts	Transmission Mounts Pylon Platforms Engine Mounts	Seat Mounts Cargo Tiedowns Brackets	Canopy-to-Fuselage Frame Ends Stiffener and Rib Brackets
Fitting Type	Tension	A1, A2, A3, A4	A1, A2, A3, A4	A1, A2, A3, A4			A1, A2, A3, A4	A1, A2, A3	
	Tension	B1, B2, B3, B4	B1, B2, B3	B1, B2, B4	B4		B1, B2	B1, B2	
	Tension	C1, C2	C1, C2	C1, C2, C3		C1, C2	C1, C2	C	
	Tension	D1, D2	D1, D2	D1, D2			D1, D2		
	Lug	E	E	E		E	E	E	
	Complex					F1, F2			
	Socket				G1, G2, G3				
	Lug					H1, H2, H3			
	Lap Shear								I2, I3
	Tension								I1, I3
	Tension						J1, J2		
	Lug							K1, K2	

At the end of the preliminary design effort, a briefing was given to the Army, summarizing the work accomplished and recommending fitting concepts for detail design.

The Army approved six joint and fitting concepts for detail design, and established a priority for each. The order in which the designs appear in this report corresponds to the priority assignments. Metal baselines and loads were established using the YAH-64 and AH-1G helicopters. Five baseline configurations were derived for the YAH-64 and one for the AH-1G.

After the metal baseline was established, layouts of each joint/fitting concept were developed. Numerous design ideas were explored for feasibility, and the final configurations were developed based on requirements for structural efficiency, producibility, cost, weight, and various other design considerations. The principal methods used for fabrication of the composite structure included wet filament winding, tape layup, broadgoods layup, and various combinations of these methods.

Simplified joint/fitting configurations and low-cost manufacturing techniques were used in order to integrate, as much as practical, the joint/fitting attachment systems into the primary structure.

Analysis of the joints/fittings included static and fatigue performance evaluation relative to the metal baseline components, and incorporated computer techniques wherever practical.

The detail design was documented in layouts of the six configurations and six test specimen fabrication drawings.

Fabrication and Test Plans were prepared for the test specimens to be used to determine structural integrity and reliability, and to validate the selected manufacturing processes.

A second briefing was then given to the Army covering the detail design, comparative analysis, Fabrication and Test Plans, and recommendations with regard to selecting three of these six joint/fitting types for fabrication and testing.

The Fabrication Plan was used as a basis for generating tool designs, ordering raw materials, and preparing prototype planning for each of the three types of specimens. Tool proof articles of each specimen type were fabricated to determine if satisfactory parts could be built, and changes were made as necessary to improve the processes before fabricating the components for test.

Testing began with nondestructive inspection of the finished parts, including visual checks, hammer tapping, and use of the harmonic analyzer. Samples with known voids were fabricated for use as references for comparing the bonds of joint/fitting specimens to detect flaws.

Structural testing included both static and fatigue tests. Static tests of each specimen type produced data on ultimate strength as well as modes of failure for each specimen. Fatigue tests were conducted to generate S-N diagrams for two of the three joint/fitting types.

SURVEY AND EVALUATION

PROBLEM DEFINITION

An extensive technology base in composite materials and structures has been established over the past 15 years. Significant strength and stiffness improvements as well as cost and weight savings have been amply demonstrated in numerous DoD-sponsored programs.

Composite structures, including primary joints and fittings made of composite materials, will make improved structural behavior and significant cost reduction possible, and when they become competitive with the light-gauge skin-stringer-frame construction presently used in helicopter airframes, a broader commitment to helicopter production will result.

The problem now is to develop competitive basic concepts using composite materials capable of being integrated into composite components and attached to other components, both composite and metal.

Background

A review of existing helicopters and the literature showed that four basic structural methods are used to transfer load across a demountable joint: lap joints, lugs, tension fittings, and sockets.

To date bonded-in, mechanically attached metal fittings have been used wherever disassembly of mating components is required. As a result, both cost and weight penalties have reduced the overall effectiveness of the composite component. Limited work has been done in developing composite joints and fittings, especially the tension type often used in helicopters.

The design process requires analytical computer methods, including an interlaminar shear routine (NASTRAN) developed for this program; simplified design concepts; low-cost manufacturing procedures; reliable nondestructive evaluation (NDE) techniques; and structural integrity testing to ensure performance and reliability.

Also, design procedures developed for metallic joints cannot be directly applied to composite joints owing to the anisotropy and inhomogeneity characteristic of the composites. Optimum composite joints must therefore start with selection and arrangement of the basic material constituents. This is an important consideration because, for example, an unsymmetrical ply stacking sequence could cause warpage of the cured component.

A major problem in tension fitting design, in addition to the three-dimensional state of stress that complicates analysis, is "turning the corner." One example is an angle with one leg in tension and the adjacent leg in combined bending and shear. A solution to this problem is necessary for any composite tension fitting.

Design Methodology Problems

The design methodologies are based on fabrication cost considerations as generated by manufacturing engineering analysis, and structural efficiency considerations as generated by stress analysis and test. By combining and balancing these considerations, a cost effectiveness criterion that can assist in deciding among the design alternatives can be developed. This will minimize costs and retain joint/fitting serviceability (safety and durability).

Analytical Problems

2
F

Tension joint analysis is complex owing to the multiple discontinuities present in the joint system, such as cutouts for fasteners in tension and shear and turning-the-corner stress flow (which introduces both interlaminar shear and interlaminar tension). The analysis is also influenced by other factors such as bolt location, washer/bolt size, fastener pattern, laminate thickness, corner radius, and lamina stacking sequence.

The literature search did not yield any useful interlaminar shear computer programs, so one was developed (Volume II). To obtain comparative experimental data to check out the NASTRAN interlaminar shear routine, special tests were performed using basic back-to-back angle joints (Volume II).

Fabrication Problems

The fabrication problem is essentially one of selecting, from among the various geometries available, the least costly design that still maintains the joint's effectiveness, structural integrity, and efficiency.

The primary producibility consideration is selecting the most cost effective methods for fabrication by low-skilled shop personnel. For maintenance economy and minimum downtime, ease of disassembly in the field must be

considered. There is also considerable debate over whether the detail parts should be precured or cocured with the primary structure; the choice of manufacturing method will affect both production economy and the strength of the part. Finally, the type of fasteners to be used (captive, fixed, or floating) must be determined.

Nondestructive Evaluation/Inspection (NDE/NDI)

NDE/NDI methods that provide adequate quality control and ensure manufacturing integrity without prohibitive production cost must be established. Increases in safety and durability (serviceability) requirements mean increases in NDE costs. The problem is to establish an accept/reject criterion that is economical and yet ensures structural integrity.

Testing Problems

The basic testing problems are:

- How much preliminary design testing is necessary, and what types of mechanical and physical tests are needed to support the design process?
- How much post-design laboratory testing is necessary to establish reliability prior to flight demonstrations?
- How much flight testing is necessary to qualify the components?
- How much proof testing is necessary during the production run to ensure manufacturing integrity and reliability?

LITERATURE SEARCH

A systematic literature search was conducted for state-of-the-art design methodology, fabrication, and test techniques for composite joints and fittings to avoid duplicating work already done by others. This search identified the usable existing data in the areas of design theory, fabrication, cost effectiveness, testing, similar joints and fittings, analytical tools (including computer programs), inspection, and NDE/NDI techniques that apply to composite joints and fittings.

Library files were searched for papers, books, magazines, and symposium proceedings (Table 2). Eight search reports from NASA and the Defense Technical Information Center (DTIC) were received and evaluated. Over 1,000 reports were cited, and over 400 were evaluated (Table 3). Reports considered pertinent to this program are listed in the Bibliography.

TABLE 2. DATA SOURCES SEARCHED

Sources	Design Theory	Composite Joints	Composite Fittings	Testing Techniques	NDI	Analytical Tools	Fabrication Techniques	Cost Effective No.
NASA	X	X	X	X	X	X	X	X
DTIC	X	X	X	X	X	X	X	X
AFML	X			X	X	X	X	X
Navy (GIDEP)	X			X		X	X	X
AFFDL	X			X	X	X	X	X
Applied Sci. and Tech. Index	X					X		
USAAMRDL, USAMMRC	X	X	X	X		X	X	X
TAB, STAR	X	X	X	X	X	X	X	X
SAMPE Publications				X	X		X	
Journal of Composites	X			X		X		
ASTM				X	X			
AIAA	X					X		
Manufacturers' Publications			X				X	X
National Technical Information Center	X					X		
AHS Papers	X	X	X	X	X	X	X	X
AGARD (NATO)	X			X		X		

See Appendix N for acronym definitions.

TABLE 3. LITERATURE SEARCHES

Search No.		Reports Cited	Reports Evaluated
NASA	DTIC		
36581		244	85
36801		187	62
36746		204	103
37234		69	15
	062761	69	30
	CW9384	37	12
	062250	260	89
	063101	21	6
		1,091	402

The search was continued throughout the program to ensure that all pertinent available data were utilized.

DESIGN

PRELIMINARY DESIGN

The preliminary design consisted of four interrelated tasks:

- Conceptual design using preliminary angle test results (see Volume II)
- Test recommendations
- Fabrication recommendations
- Configuration recommendations for detail design

Generic Concepts

The generic joints and fittings consist of eight joint types and four fitting types derived from the YAH-64, UH-1, and OH-58 helicopters:

- Joints:

  Aerodynamic surface-to-fuselage /tailboom

  Tailboom-to-fuselage

  T-tail surface joining

  Sync elevator-to-fuselage

  Landing gear-to-fuselage

  Assorted tension-type mounts-to-airframe

  Assorted shear-type mounts-to-airframe

  Longeron/canopy bow-to-airframe

- Fittings:

  Tension

  Lug

  Shear

  Socket

These eight helicopter joints were considered good candidates for composite materials. Arranging these joint types and the four fitting types in a matrix resulted in 29 design concepts (Table 1). Only six of these concepts (Figures 2 through 7) survived the screening rationale for baseline consideration:

- Acceptability: Likelihood of concept being accepted for incorporation into a production helicopter
- Data resource: Potential for yielding new or required test data and for gaining more confidence in composite fitting design
- Low cost: Simplicity, affordable costs, and high producibility
- Generic adaptability: Possession of features that are generic, cut across the borders between joint types, and can be readily and logically adaptable to as wide a set of design situations as possible
- Risk and uncertainties: Possible relegation to later consideration when uncertainties are cleared up

Test Recommendations

It was recommended that the following test articles be fabricated and tested:

	Number of Specimens			
Configuration	Tool Proofing	Static Test	Fatigue Test	Total
X	1	2	3	6
Y	1	2	4	7
Z	1	2	-	3
				16

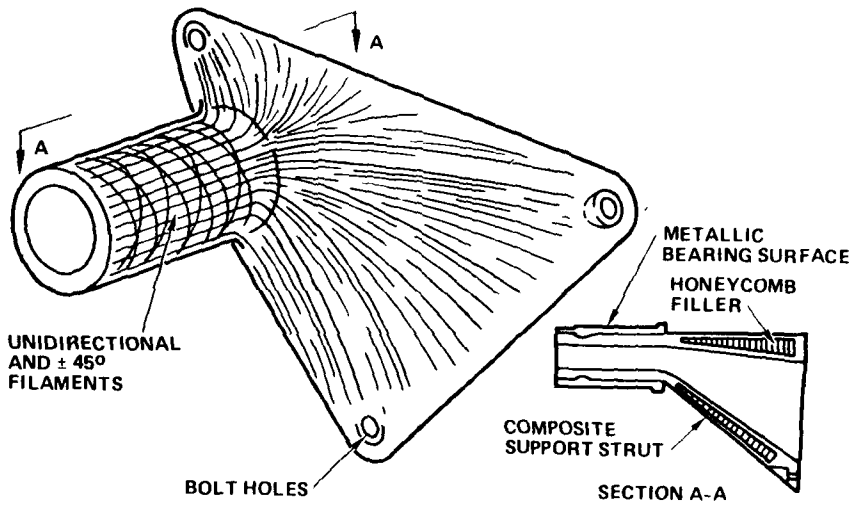

Figure 2. Type F – Composite Landing Gear Fitting

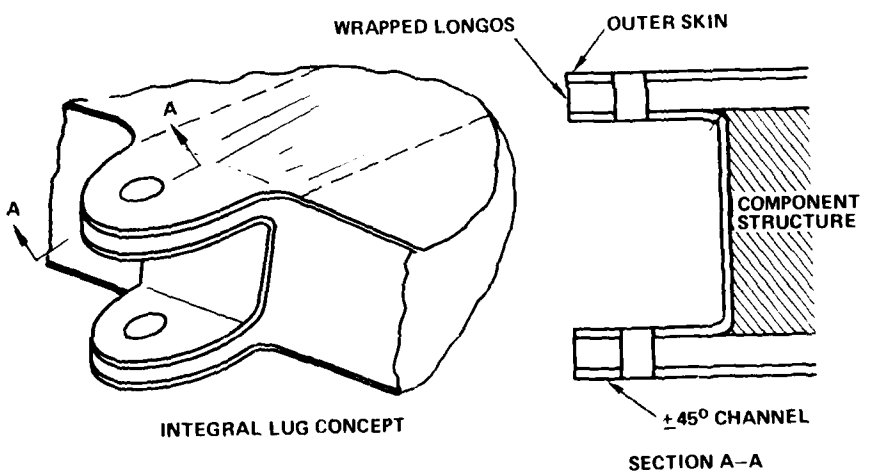

Figure 3. Type E – Integral Lug Fitting

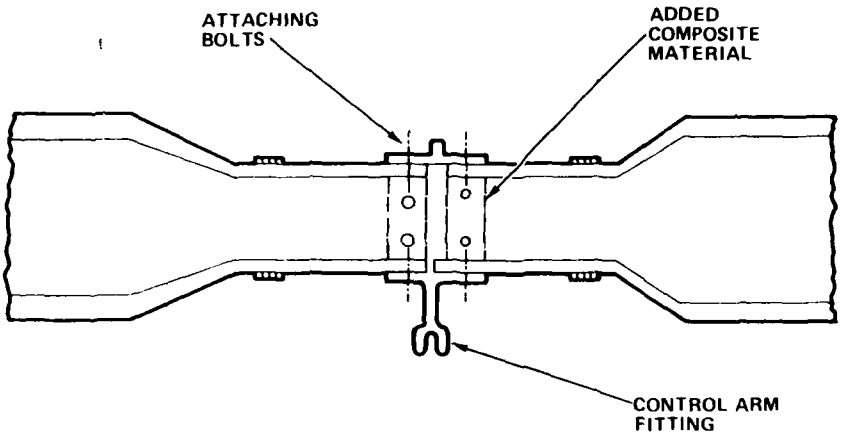

Figure 4. Type G – Socket Attachment Fitting

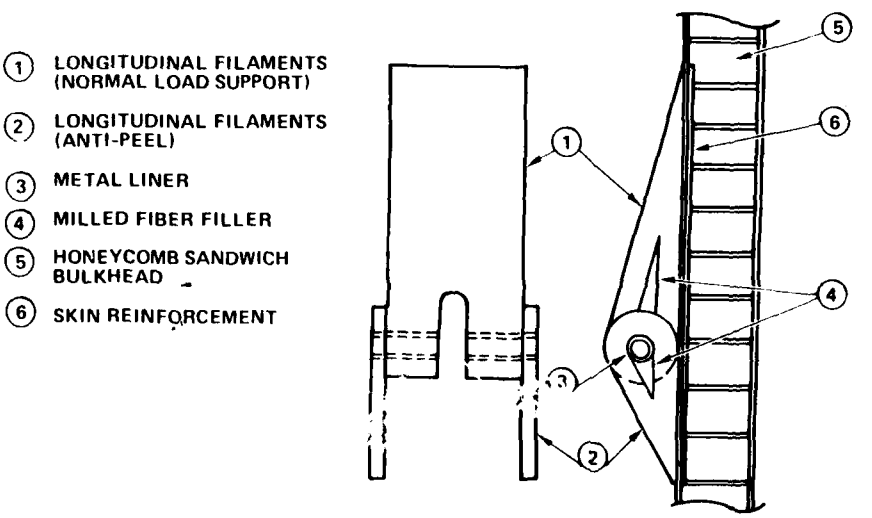

Figure 5. Type K – Seat Attachment Fitting

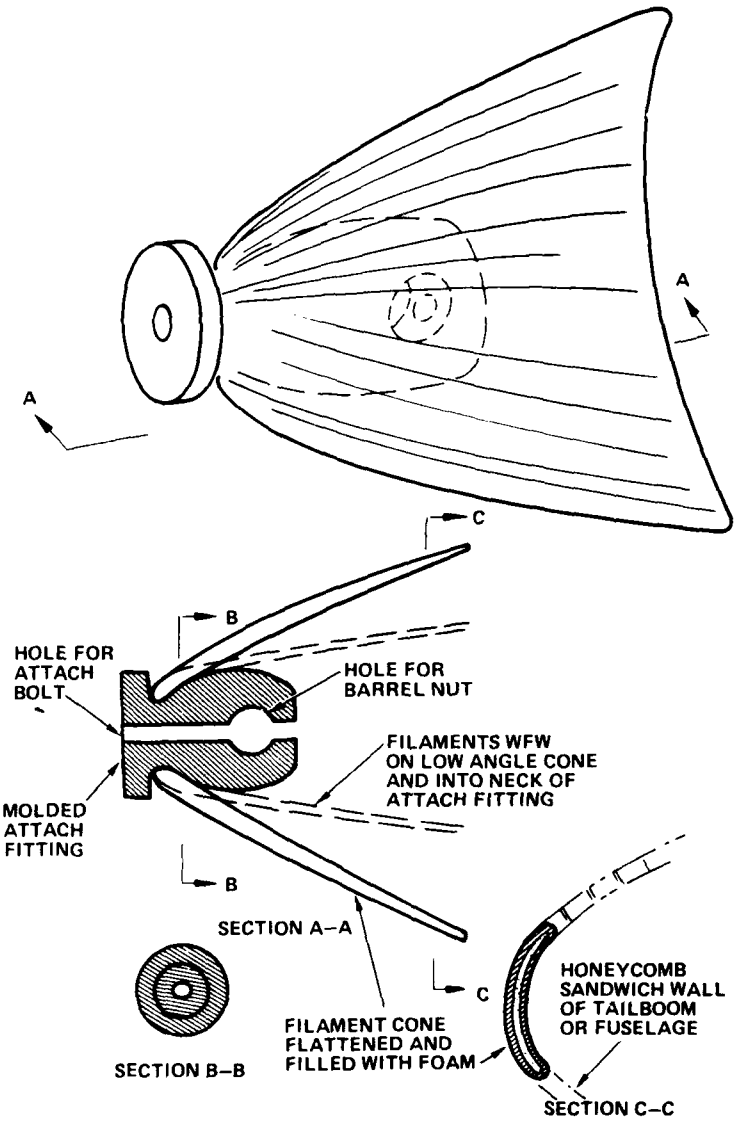

Figure 6. Type D – Gearbox Attachment Fitting

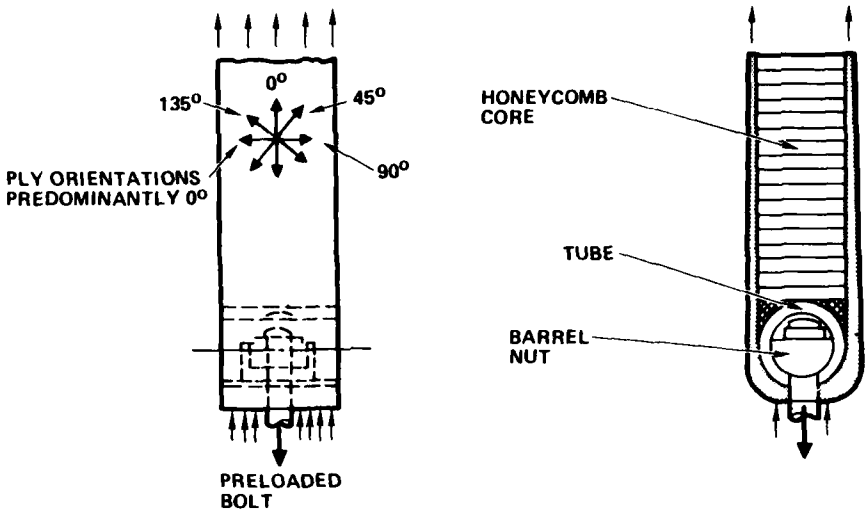

Figure 7. Type A – Wrapped Tension Fitting

Fabrication Considerations

Several techniques for fabricating composite attachment fittings and joints were considered: wet filament and tape winding; automated, semiautomated, and manual layup of tape and fabric; roll forming; post-formed pultrusions; and block and sheet molding compounds.

Trends and developments that tend to reduce the cost of tooling were also studied. These include:

- Pultrusion dies for under $5,000
- Stable, accurate, low-cost chopped-fiber phenolic tooling in lieu of steel
- Internal mandrels that expand into hard cavity tools needing only ovens for pressure curing with pressure-expanded ABS vessels or pressurized silicone rubber bags

Selected Concepts

Of the 29 concepts considered, 16 were evaluated according to design capability, potential resource for generic data, simplicity, low cost, producibility, and cost effectiveness. Of these, six configurations were selected for detail design:

- Type F – composite landing gear fitting (Figure 2)
- Type E – integral lug fitting (Figure 3)
- Type G – socket attachment fitting (Figure 4)
- Type K – seat attachment fitting (Figure 5)
- Type D – gearbox attachment fitting (Figure 6)
- Type A – wrapped tension fitting (Figure 7)

DETAIL DESIGN

After the six joint/fitting generic concepts were selected, a detail design effort was undertaken to develop final designs using the analytical tools and methods recommended during the preliminary design. These included the analysis of static and fatigue strength, weight, structural efficiency, producibility, cost, failure modes, access, and ballistic tolerance.

Analytical Tools

The analytical tools used to size the composite joints/fittings were state-of-the-art methods developed for laminated composite plates, shells, beams, and columns as used in analyses of discontinuities, edge effects, and joints. The individual analyses were governed by the complexity of the design and the required accuracy. Each analysis considered factors such as fits, clearances, eccentricity, torque-induced loads, bearing surface requirements, edge distance, materials, and the influence of bushings and liners.

No economical NASTRAN program was found that would assist or could be modified to assist in the sizing efforts except for the finite element interlaminar shear models developed during preliminary design (Volume II).

However, parametric studies were conducted with finite element models C-1 and C-2, which can determine the interlaminar shear present in the radius of an angle. Using the half-symmetrical C-1 model, variations in

washer diameter, washer distance from the bend, lamina orientations and thicknesses, and bend radius:thickness ratios were investigated. With the strip C-2 model, variations in stacking sequence were investigated. The influence of these variations on interlaminar shear stress induced in the radius of an angle is discussed in Volume II.

The detail design effort began with the selection of six existing metal helicopter components to serve as a baseline from which composite components would be designed, using the six selected generic concepts as a starting point.

In this section, the six components are described individually, starting with the metal baseline and continuing through the evolution of the generic concepts to the final design. Each type is discussed separately in chronological order to show clearly the development process.

Differences in concept between the composite components and the metal baselines were permitted as follows:

- The existing metal airframe may be assumed to be replaced by a composite airframe.
- Minor changes in joint geometry (thickness of skins, number and location of fasteners, etc.) may be made in order to improve the composite design.
- Composite fittings, whether direct replacements or modifications of the metal fittings, must perform the same functions and carry the same loads.

Type F – Composite Landing Gear Fitting

Figure 8 illustrates the metal baseline part which was to be redesigned using composite materials wherever practical. The fitting carries a shear load from the main landing gear shock strut into the fuselage shell on the YAH-64. Kick loads created by the offset of the shock strut from the fuselage are carried as a bending moment through the fitting and are reacted by bulkheads in the fuselage.

Figure 9 illustrates Concept 1. The trunnion has been extended to allow a continuous filament wound graphite/epoxy shell to carry axial and shear loads into the fuselage structure. However, the concept is not capable of carrying the load intensities present in this application. (The shear load applied to the trunnion by the shock strut is 130,800 pounds.) Access holes through the upper shell for the attachment bolts would also weaken the shell.

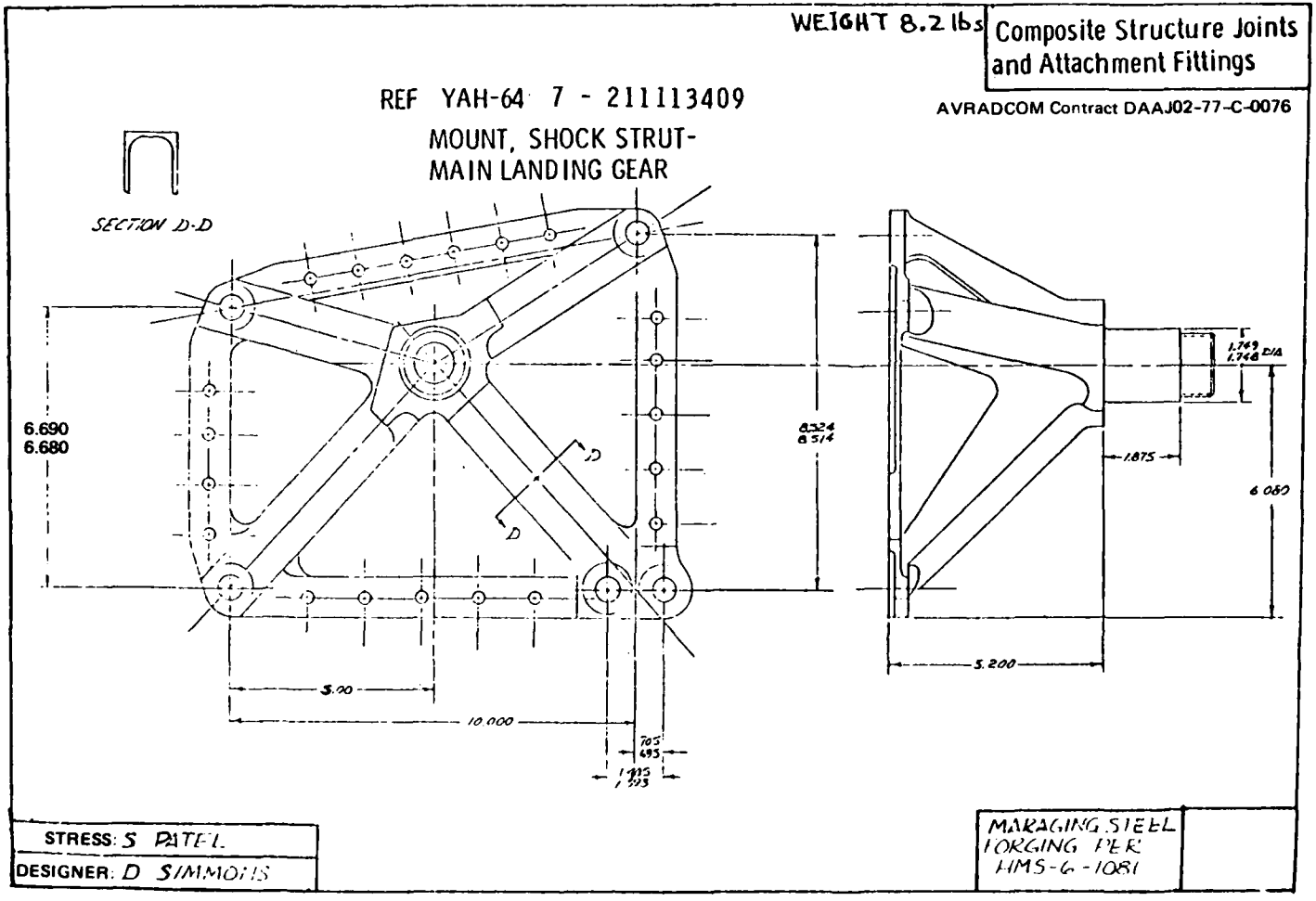

Figure 8. Baseline Metal Part Design: Composite Landing Gear Fitting (Type F)

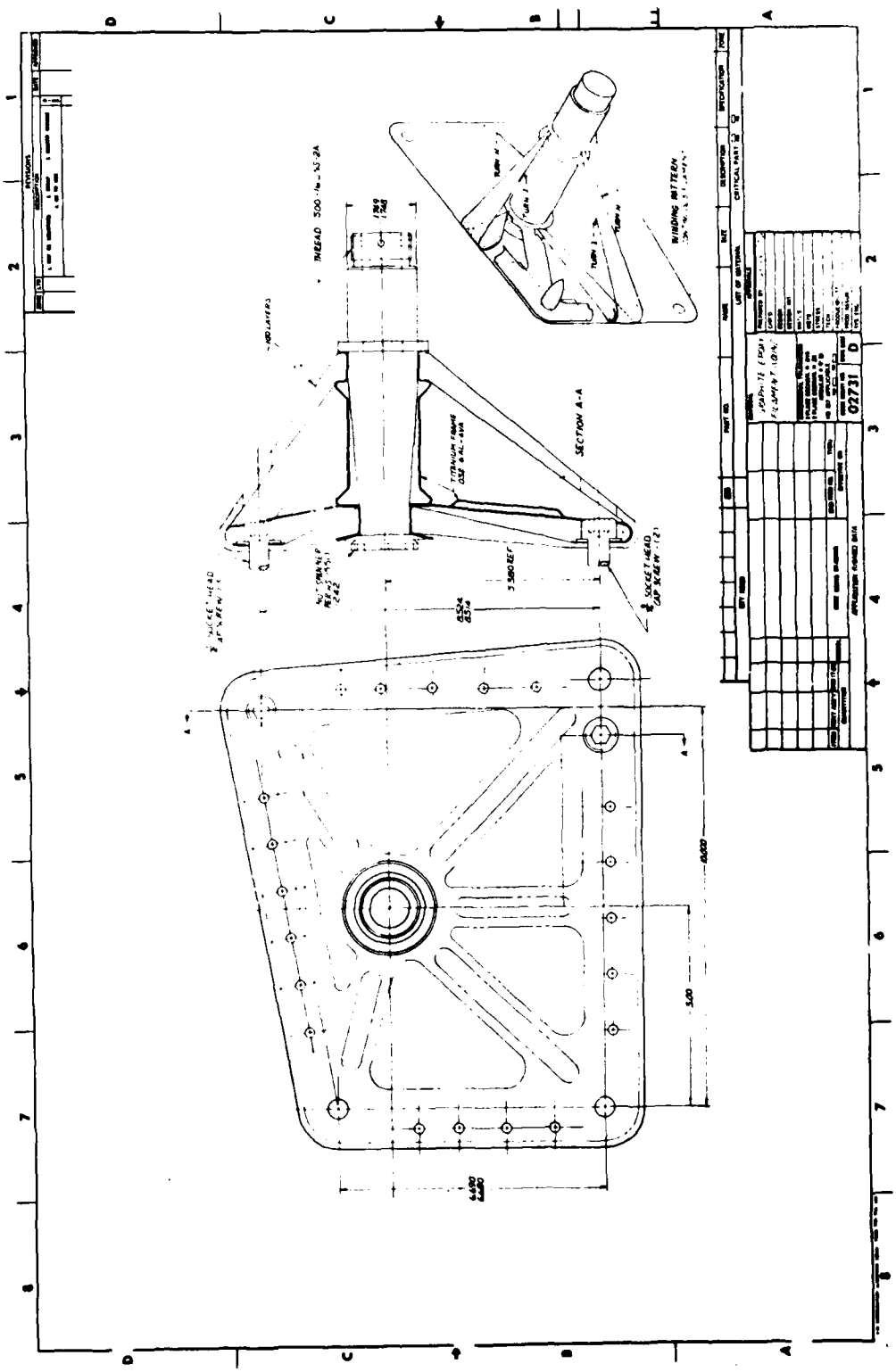

Figure 9. Type F Concept 1

Figure 10 illustrates Concept 2. The shell of Concept 1 has been replaced by one which wraps around spools at each bolt location, thereby eliminating the need for access holes through the shell. The design is inadequate to carry the shear loads.

Figure 11 illustrates Concept 3. The continuous shell has been replaced by individual beam elements with shear webs inserted between the upper and lower caps. The attachment of the beams to the trunnion is impractical, and the concentrated bolt loads are too large to apply to the composite.

Figure 12 illustrates Concept 4. The beam elements of Figure 11 have been modified by replacing the caps with "fan belts" which are wrapped around the trunnion and attachment bolts. The transverse shear stresses at the bolts and the trunnion are excessive, and the shear webs are insufficient in area.

Figure 13 illustrates the final detail design of Type F. The design has returned to a continuous shell, with the addition of titanium inserts around the trunnion and the corner attachment bolts. The inserts permit the loads to be distributed to the composite more evenly, allowing higher average shear stresses. The trunnion is still 300-M maraging steel to resist the loads imposed by the shock strut.

Type E – Integral Lug Fitting

Figure 14 illustrates the metal part which was used as a baseline for developing a composite replacement. This bracket carries a tail rotor driveshaft support bearing on the YAH-64.

Figure 15 illustrates Concept 1, which is essentially a duplicate of the baseline made with graphite/epoxy molding compound and employing beveled stiffeners. Without draft angles on the deep section, this concept would require a segmented tool to permit removal.

Figure 16 illustrates the second concept: a manual layup made from graphite fabric. Isolating the lugs would allow the bracket to be integrally wound into the tailboom skin; however, the part would not be replaceable. Lateral stability is provided by secondarily bonded supports.

Figure 17 illustrates Concept 3. This design is also based upon using three individual lugs rather than a continuous fitting. The fitting is made from graphite/epoxy molding compound as in Concept 1. The attachment bolt holes have been relocated to line up with the lugs.

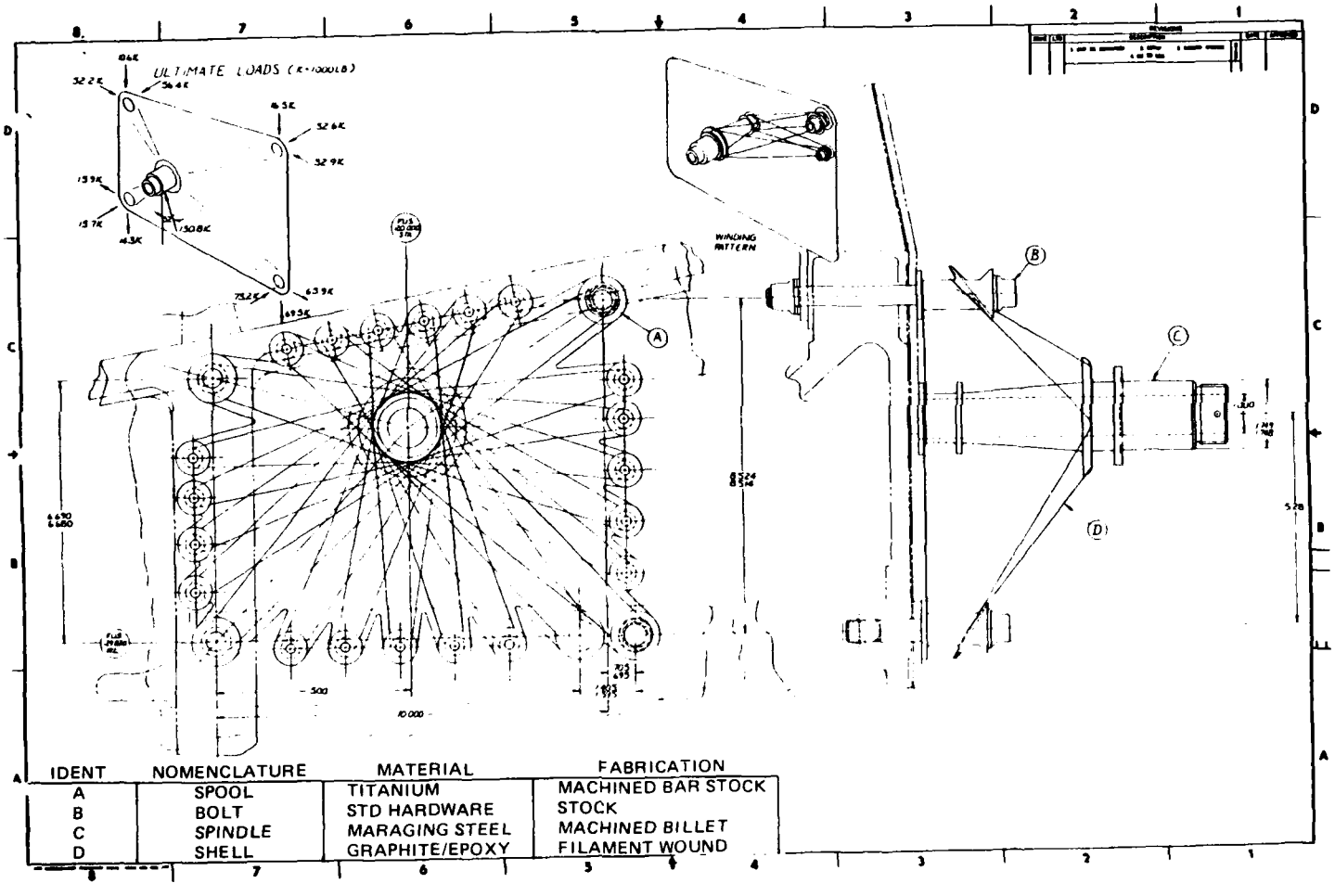

IDENT	NOMENCLATURE	MATERIAL	FABRICATION
A	SPOOL	TITANIUM	MACHINED BAR STOCK
B	BOLT	STD HARDWARE	STOCK
C	SPINDLE	MARAGING STEEL	MACHINED BILLET
D	SHELL	GRAPHITE/EPOXY	FILAMENT WOUND

Figure 10. Type F Concept 2

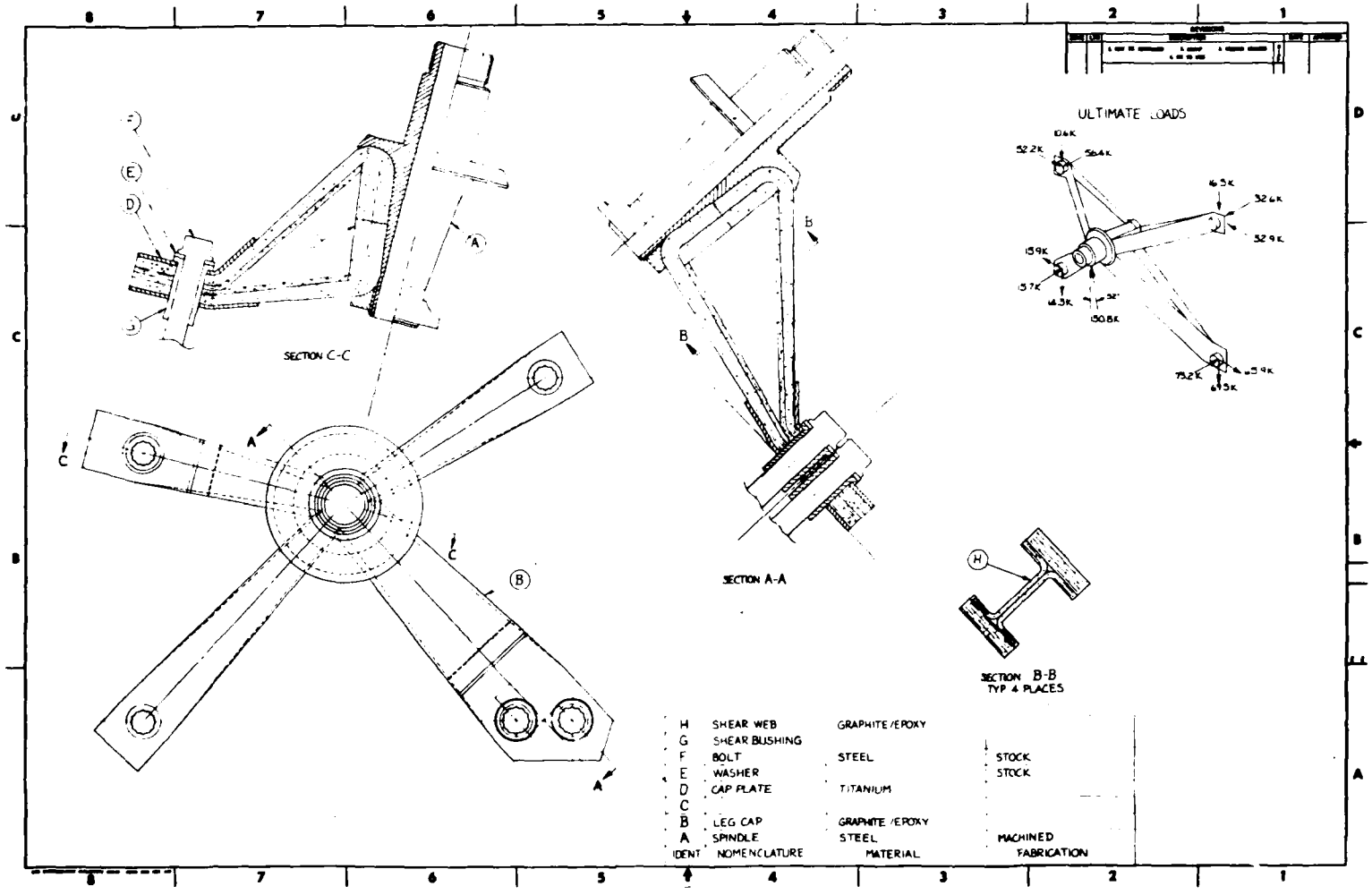

Figure 11. Type F Concept 3

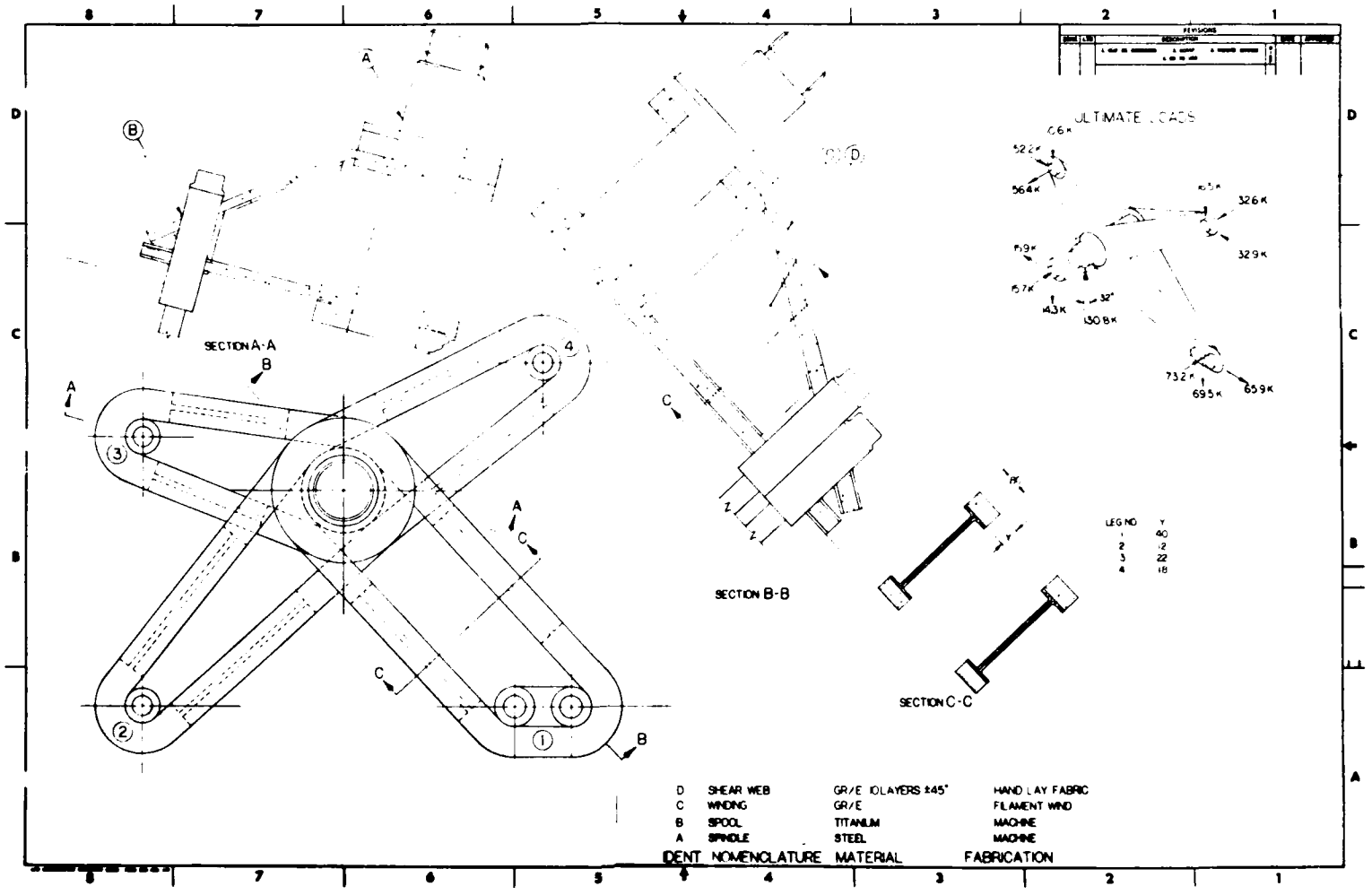

Figure 12. Type F Concept 4

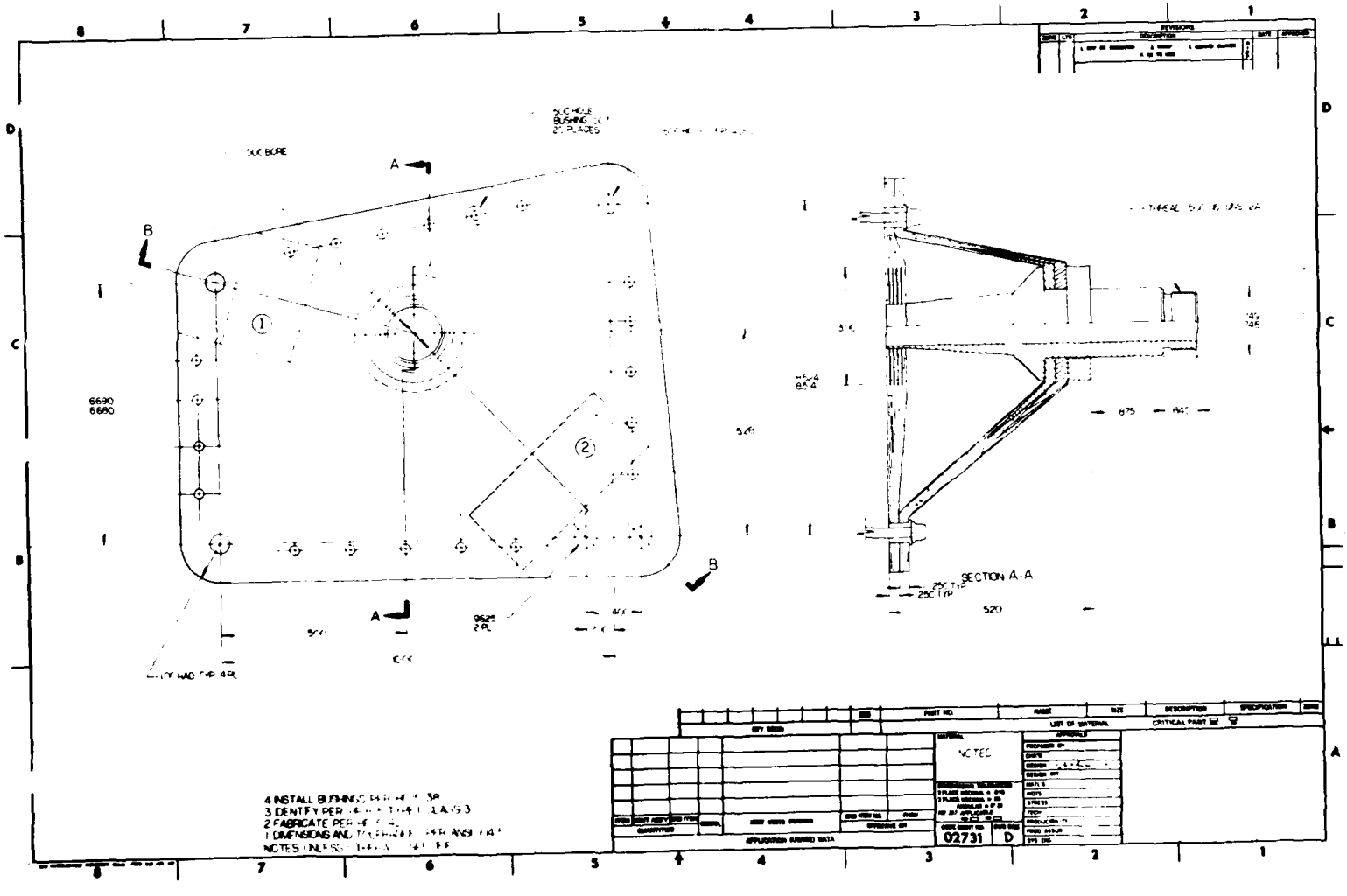

Figure 13. Final Detail Design: Type F (Sheet 1 of 2)

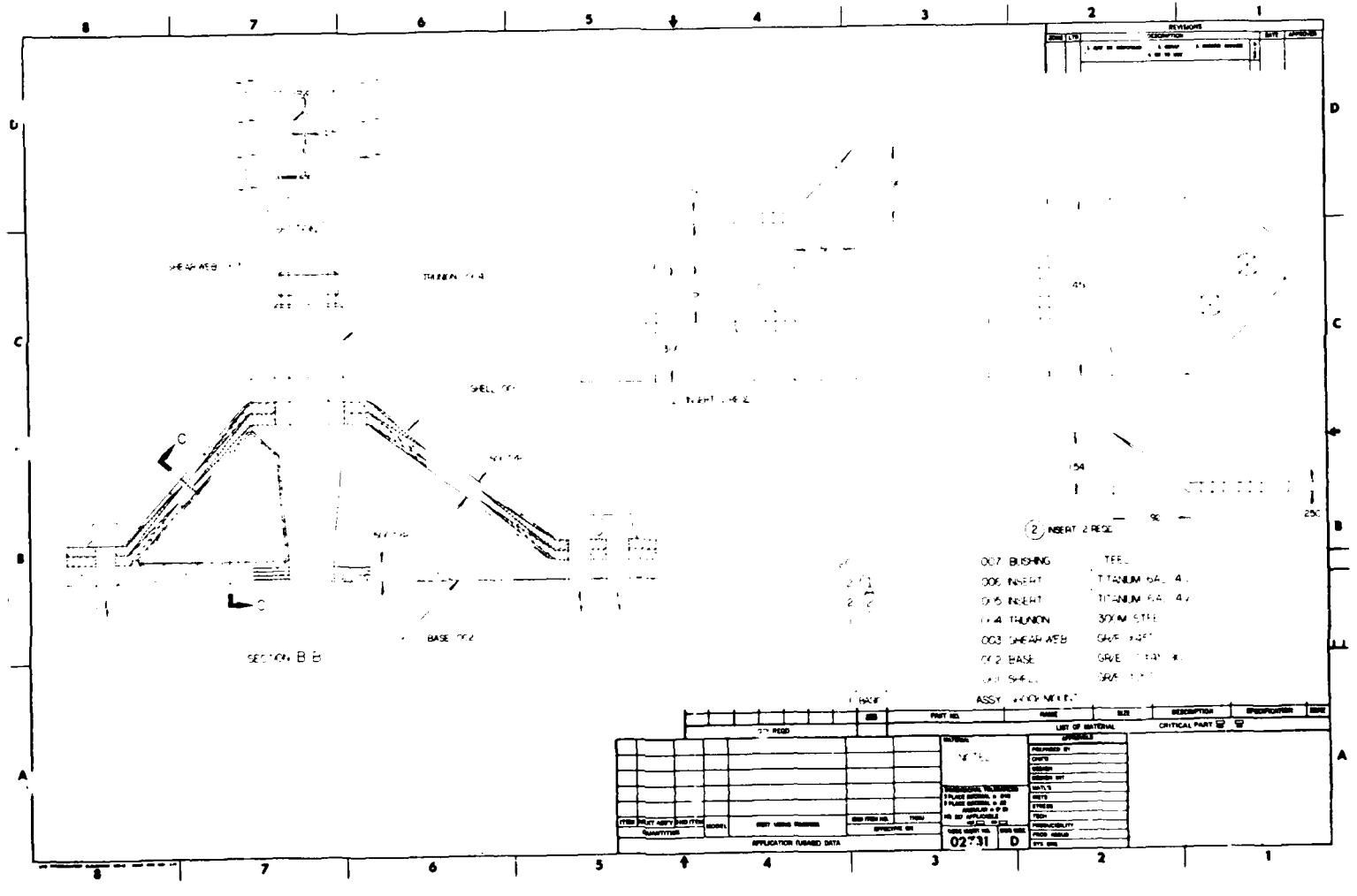

Figure 13. Final Detail Design: Type F (Sheet 2 of 2)

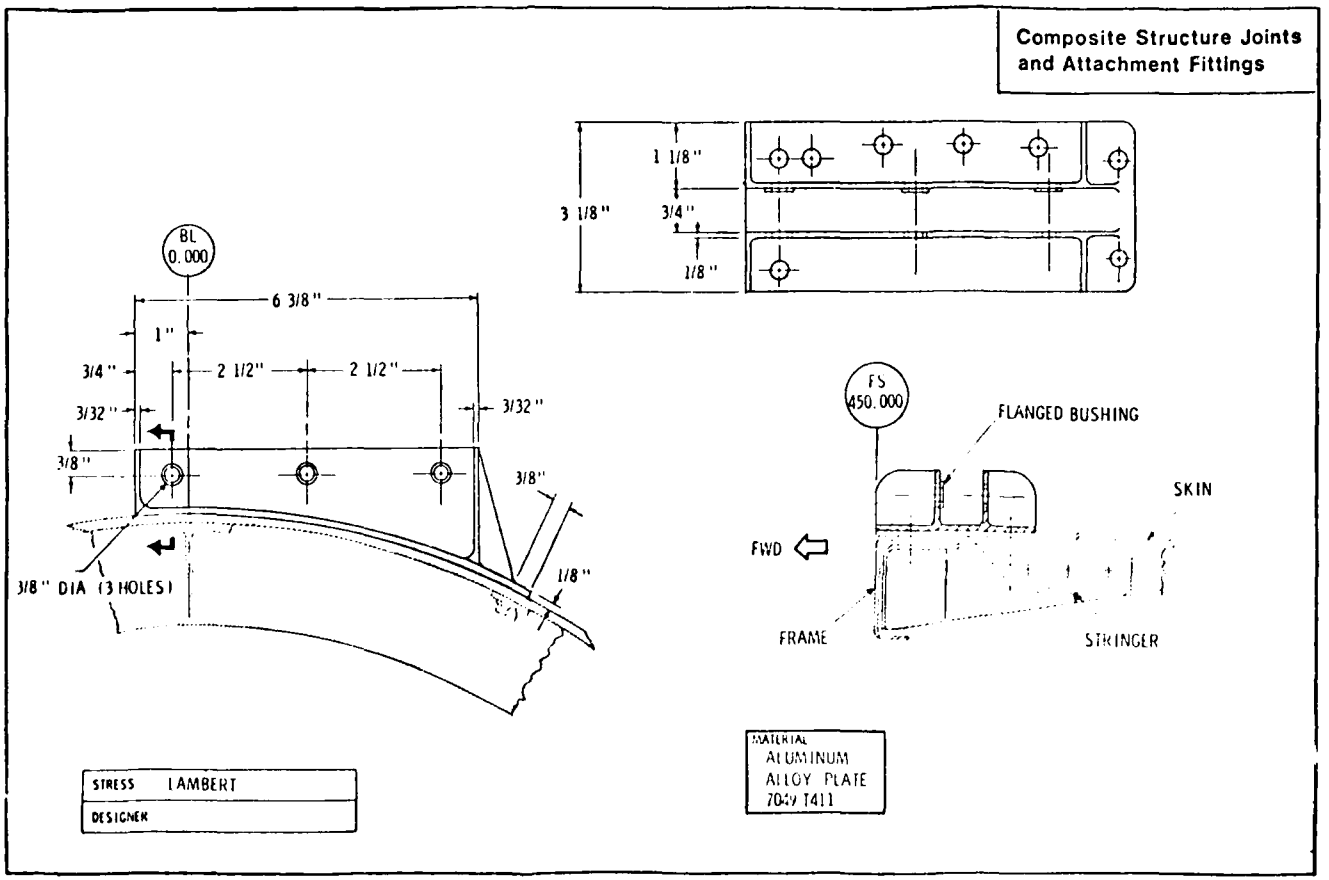

Figure 14. Baseline Metal Part Design: Integral Lug Fitting (Type E)

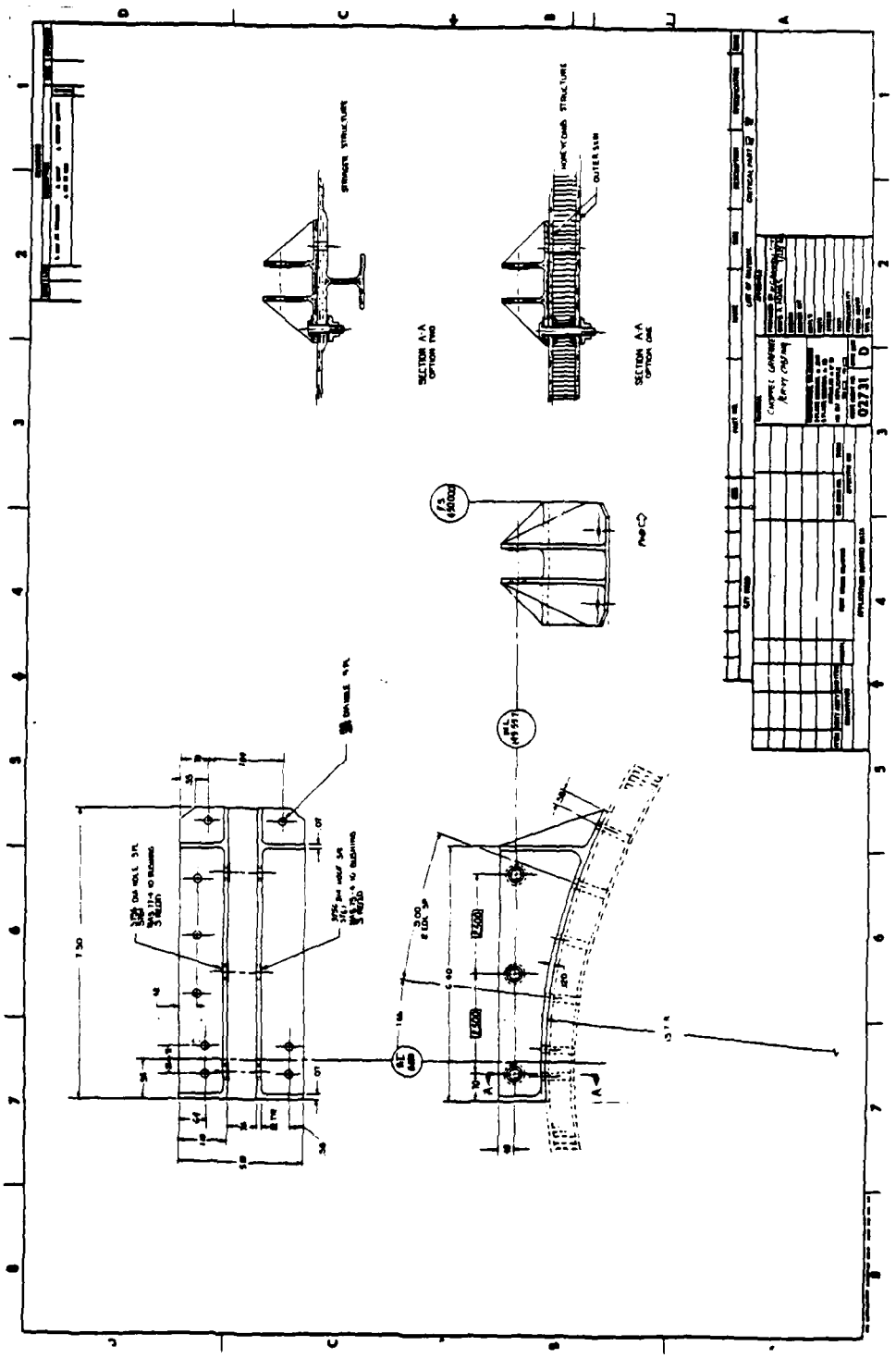

Figure 15. Type E Concept 1

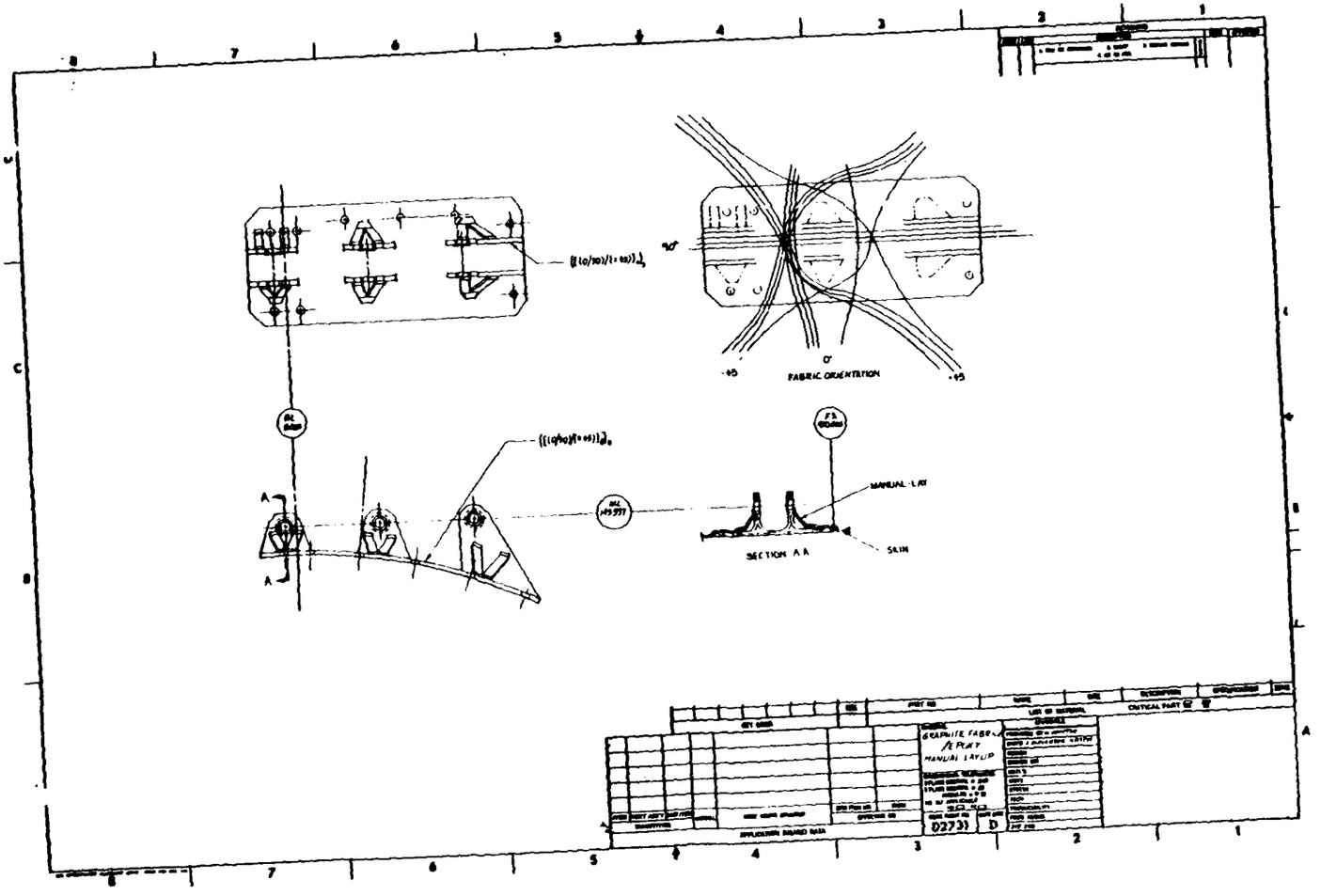

Figure 16. Type E Concept 2

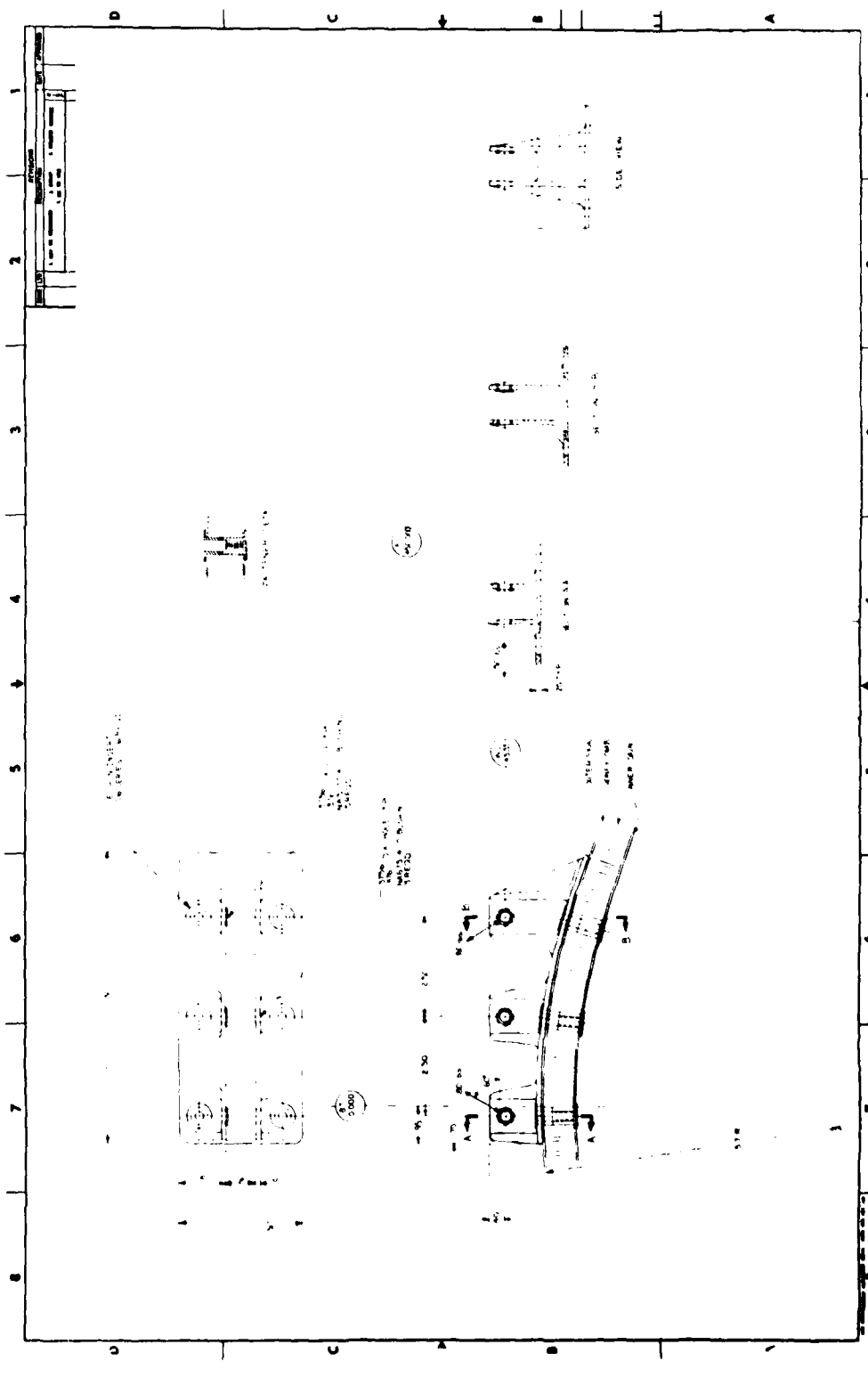

Figure 17. Type E Concept 3

Figure 18 shows the Type E final design, which is also a graphite/epoxy molding. The lugs have been connected with a continuous flange and the center pocket is closed out at both ends for lateral stability.

Type G – Socket Attachment Fitting

Figure 19 illustrates the existing metal component design for the elevator torque tube installation on the AH-1G helicopter. The left and right elevator torque tubes slip into the center tube. The center tube is supported at both ends by bearings attached to the tailboom. A forged aluminum crank arm is welded to the center tube for the actuator rod attachment.

Figure 20 illustrates Concept 1. Two filament-wound torque tubes are flanged on the inboard end. A filament-wound crank arm is sandwiched between the tubes and through-bolted with integrally wound studs. A metal insert at the end of the crank arm accepts a rod end bearing. The large bolt circle diameter adds weight, and the flanges would have to be formed after winding.

Concept 2 is shown in Figure 21. The 90-degree flange of Concept 1 has been reduced to 45 degrees in an effort to reduce the bolt circle diameter. Build-ups have been provided on the torque tubes for machining bearing surfaces and retainer grooves. The torque tubes are an improvement; however, the crank arm is heavier.

Figure 22 illustrates Concept 3. The two-piece torque tube has been replaced by a single unit, and the crank arm is integrally wound around the tube and cocured. The crank arm would be difficult to wind, and the weight has not been reduced significantly.

Concept 4 is illustrated in Figure 23. The integrally wound crank arm is now an I-section rather than honeycomb. Metal sleeves are installed on the tube for bearing surfaces, and a metal insert is bonded to the web halves for a press-in bearing.

The final design for the Type G fitting is illustrated in Figure 24. The metal sleeves on the torque tube have been replaced by buildups that can be machined to serve as bearing surfaces.

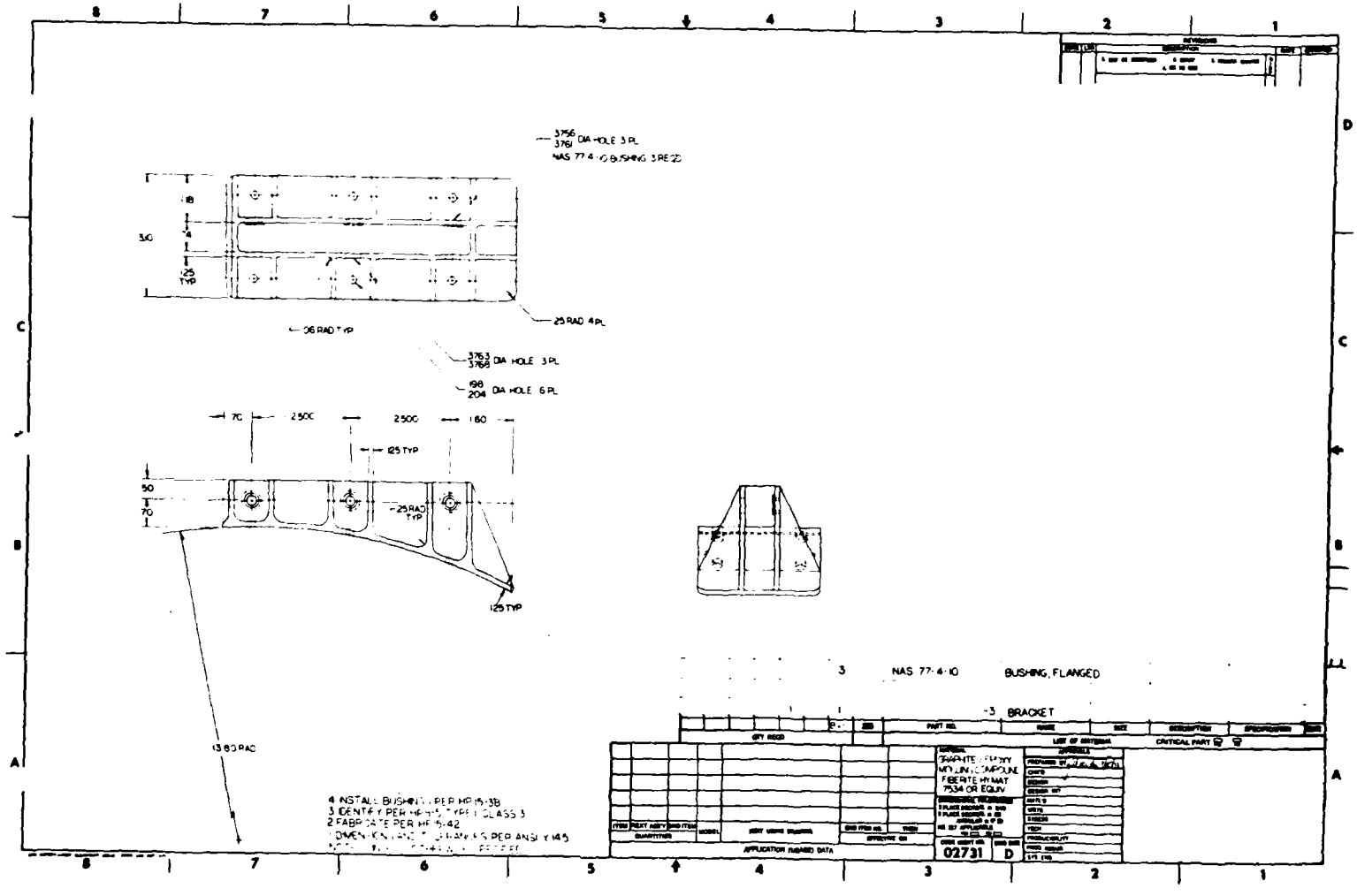

Figure 18. Final Detail Design: Type E

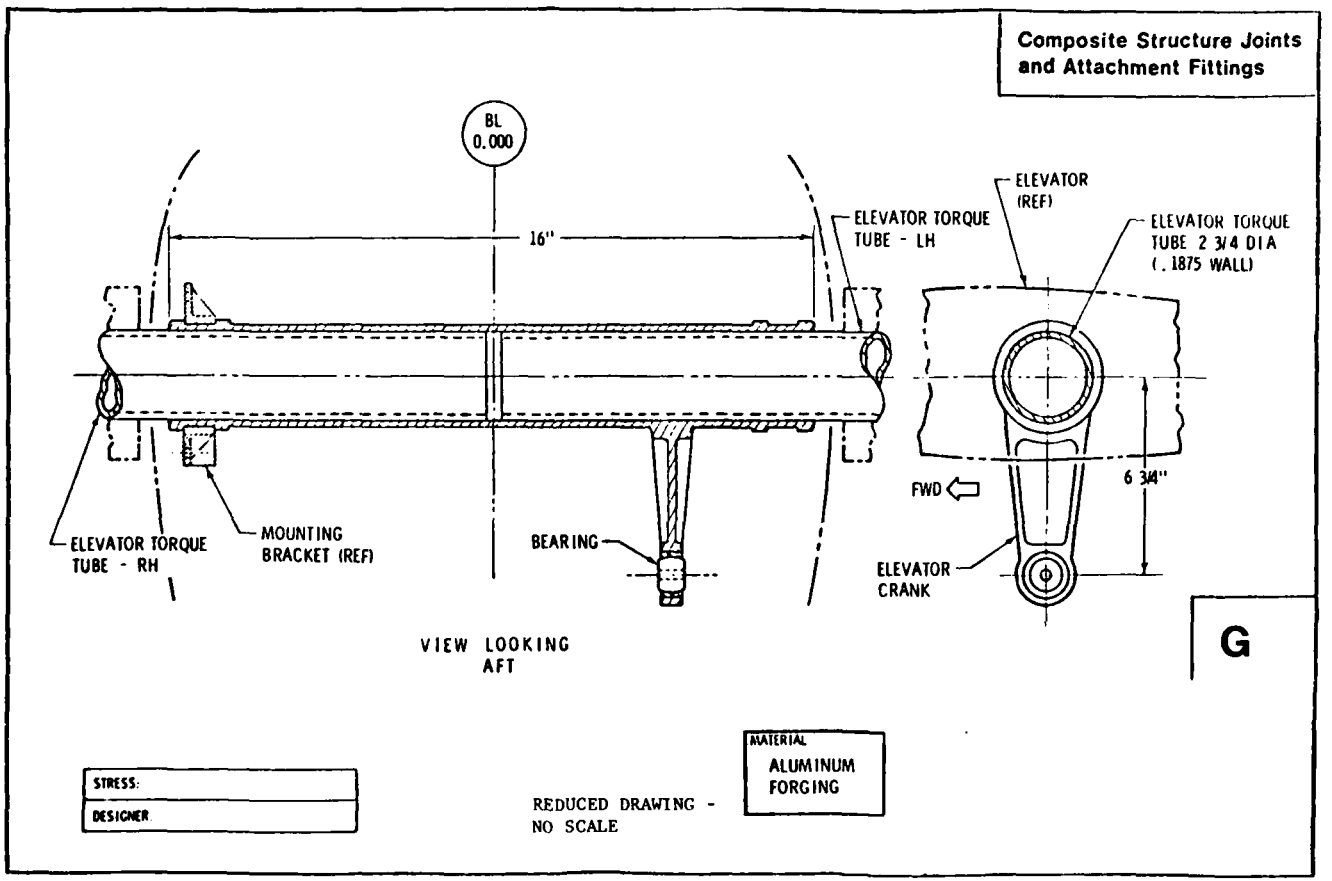

Figure 19. Baseline Metal Part Design: Socket Attachment Fitting (Type G)

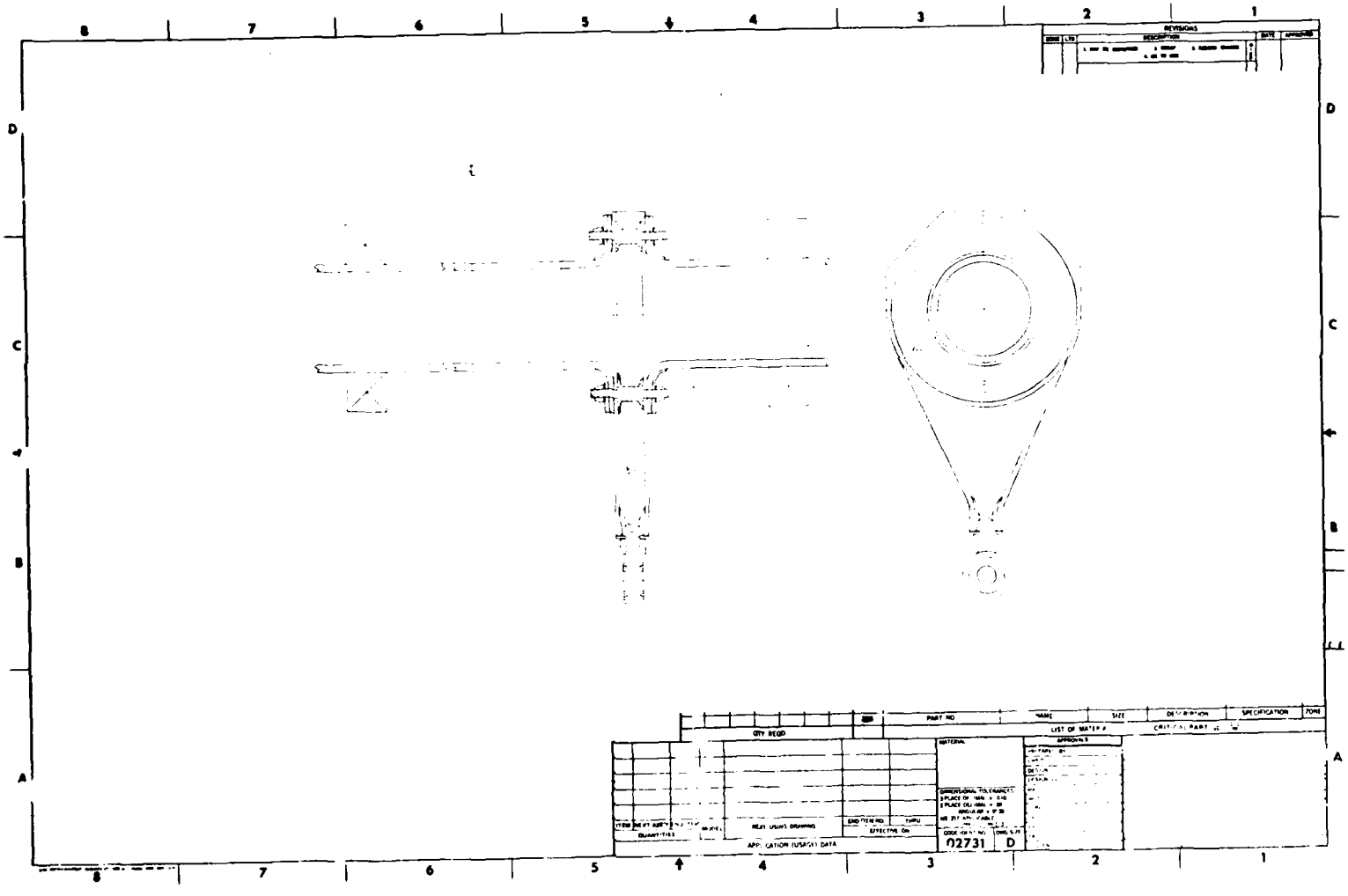

Figure 20. Type G Concept 1

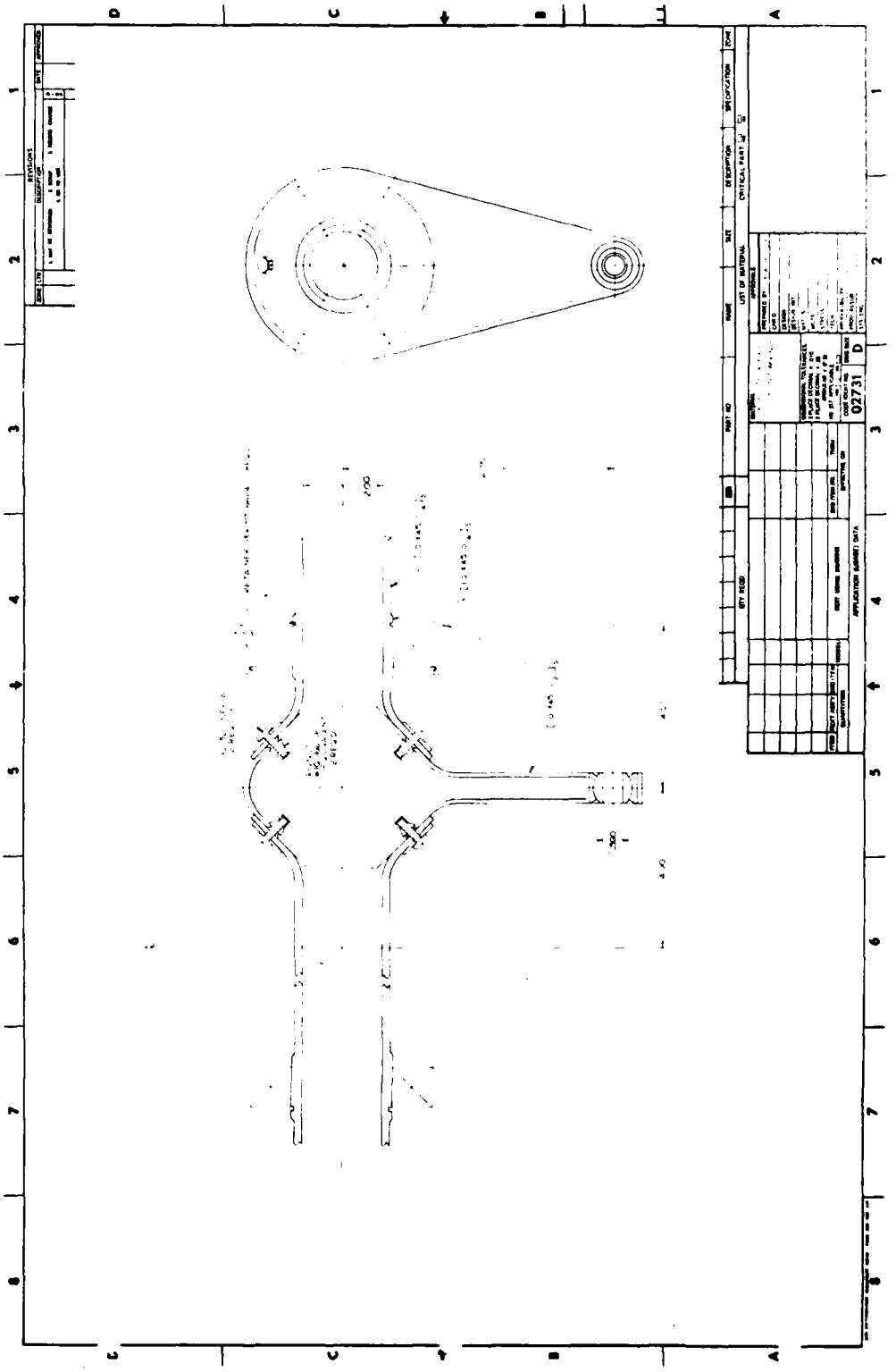

Figure 21. Type G Concept 2

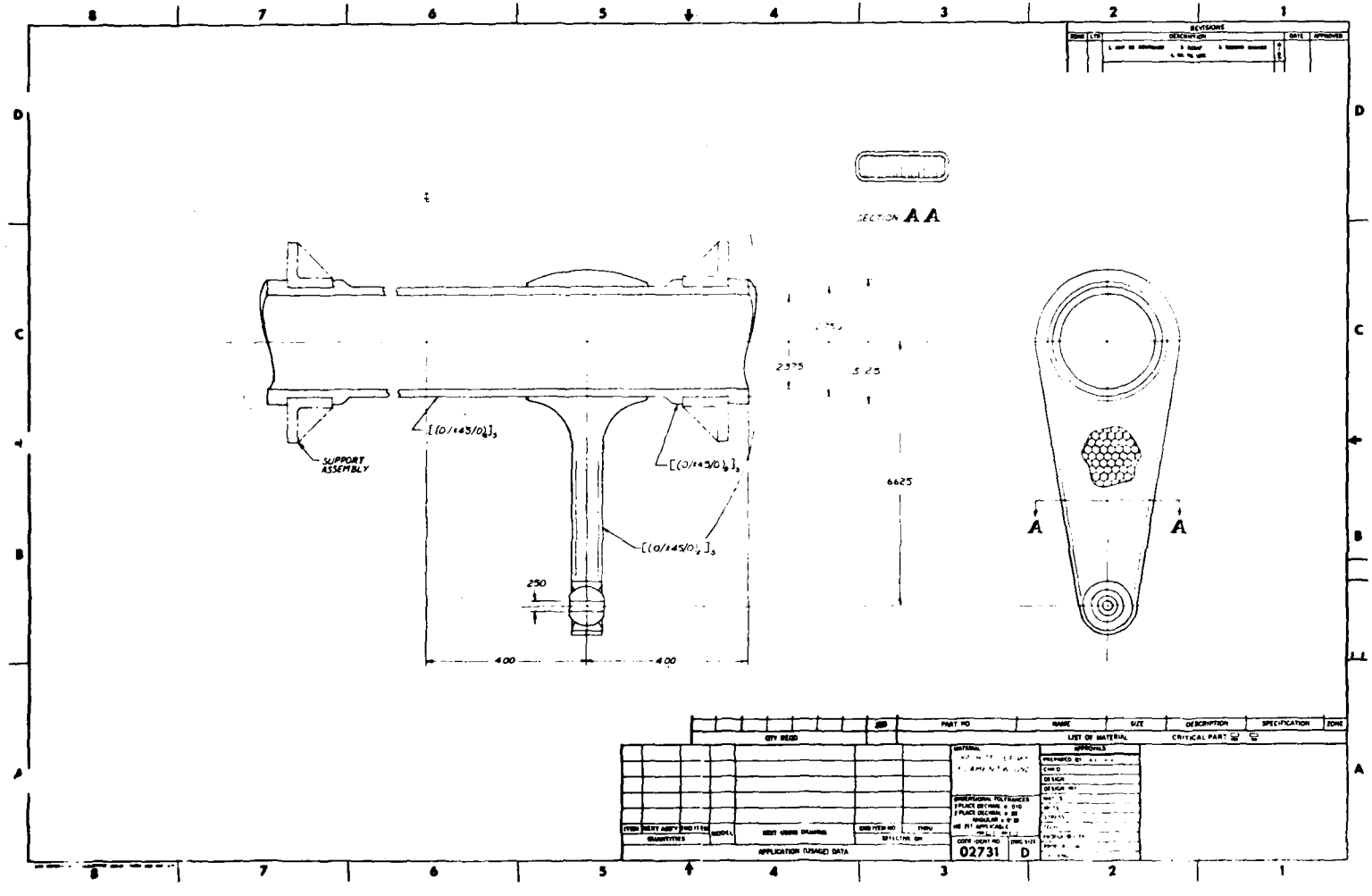

Figure 22. Type G Concept 3

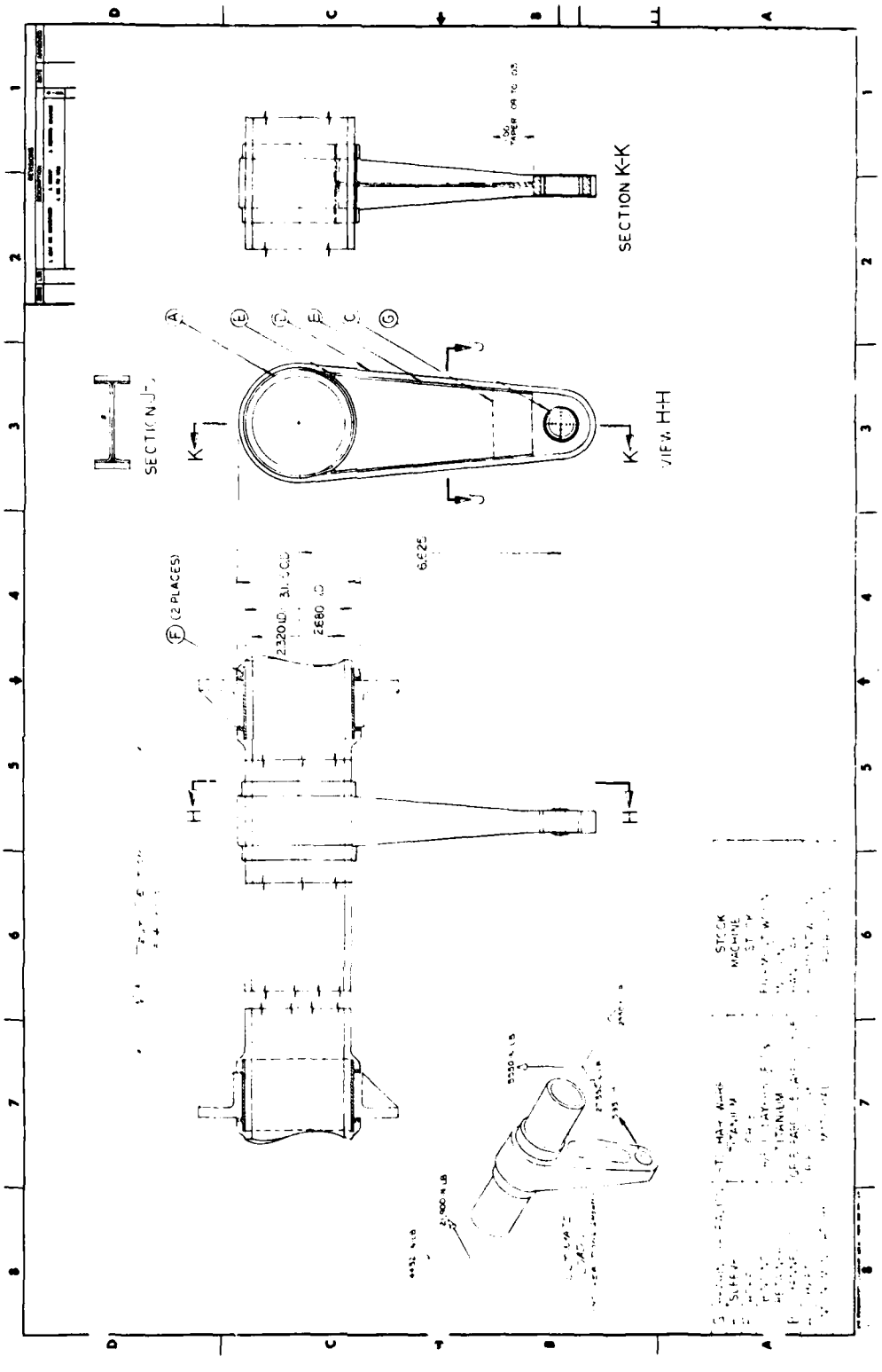

Figure 23. Type G Concept 4

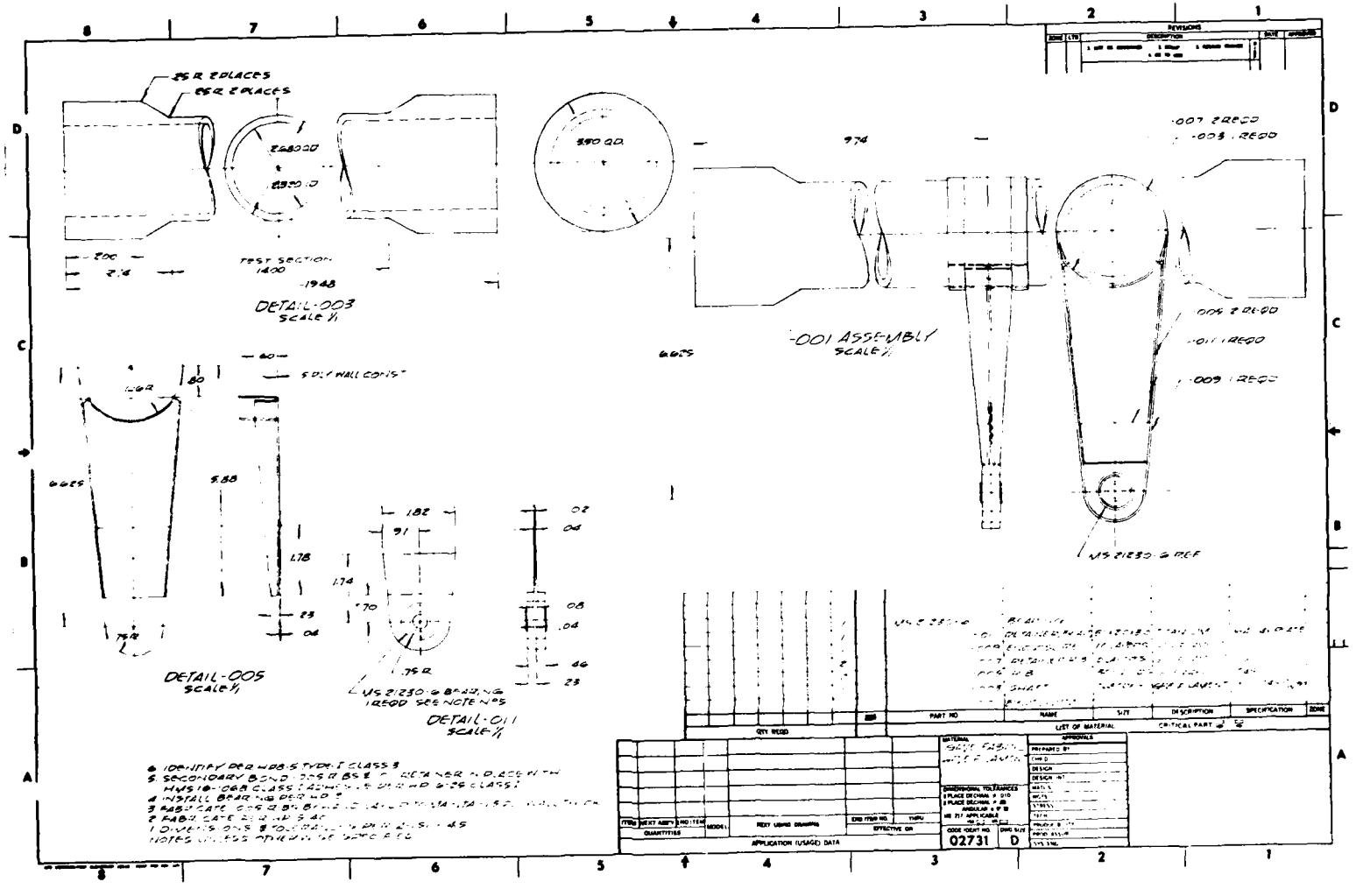

Figure 24. Final Detail Design: Type G

Type K – Seat Attachment Fitting

Figure 25 shows the baseline fitting design. This part is machined from a 4340 steel bar for the YAH-64. Four of these fittings are mounted to a bulkhead behind the copilot's compartment and support the copilot's seat. Loads are from the inertia of the seat/occupant mass during a crash landing condition.

Concept 1 is illustrated in Figure 26. This concept is a copy of the metal design using a graphite/epoxy pultrusion. The lug edge distance is insufficient for lug tearout.

Concept 2 is shown in Figure 27. The lug has been extended in the direction of load to prevent tearout, and the material changed to a graphite/epoxy fabric. Manual layup is used. The single lug configuration is insufficient due to interlaminar tension stresses in the corners.

Figure 28 shows Concept 3. The manual layup fabric construction of Concept 2 has been retained; however, a double lug has been substituted for the previous single lug. Fasteners in the center channel are necessary to prevent peeling.

The final Type K fitting design is shown in Figure 29. The lug has been lengthened to extend to the end of the base, and the stacking sequences and number of plies have been changed. Two fastener holes have been added in the center channel, plus a bearing block to reduce the tensile stress in the bond to the base plate.

Type D – Gearbox Attachment

Figure 30 illustrates the metal baseline part from the YAH-64. This rib is one of two that support the tail rotor 90-degree gearbox on the vertical stabilizer. The ultimate loads are the result of a blade strike condition.

Concept 1 is illustrated in Figure 31. The steel attach stud threads into an asymmetrical metal anchor, which is bonded to the graphite/epoxy and honeycomb rib. Kick loads generated by the asymmetry are reacted by the six tie-down bolts. The bond area available is insufficient to carry the loads, and the stiffness of the anchors is not compatible with the graphite/epoxy skins.

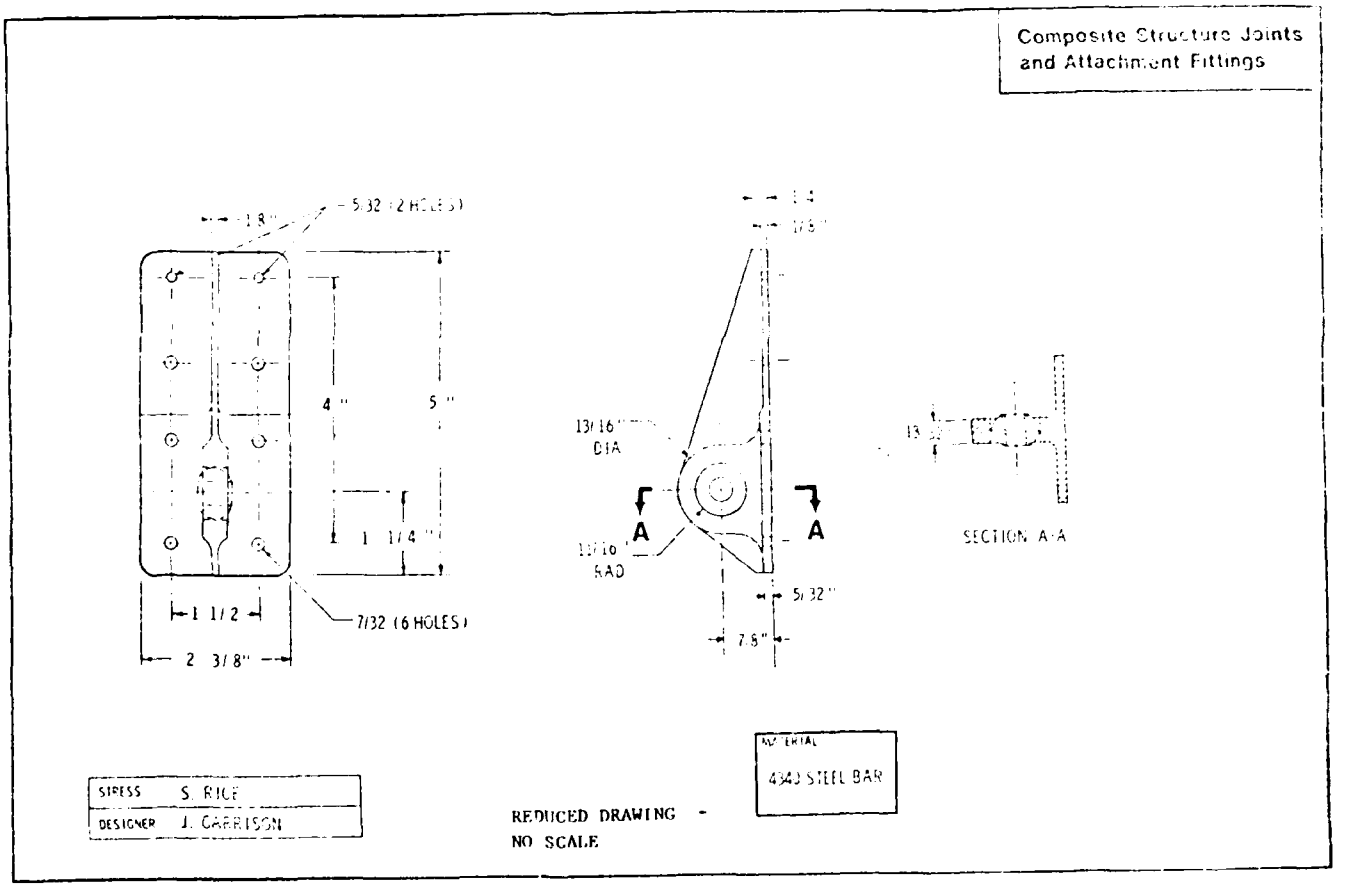

Figure 25. Baseline Metal Part Design: Seat Attachment Fitting (Type K)

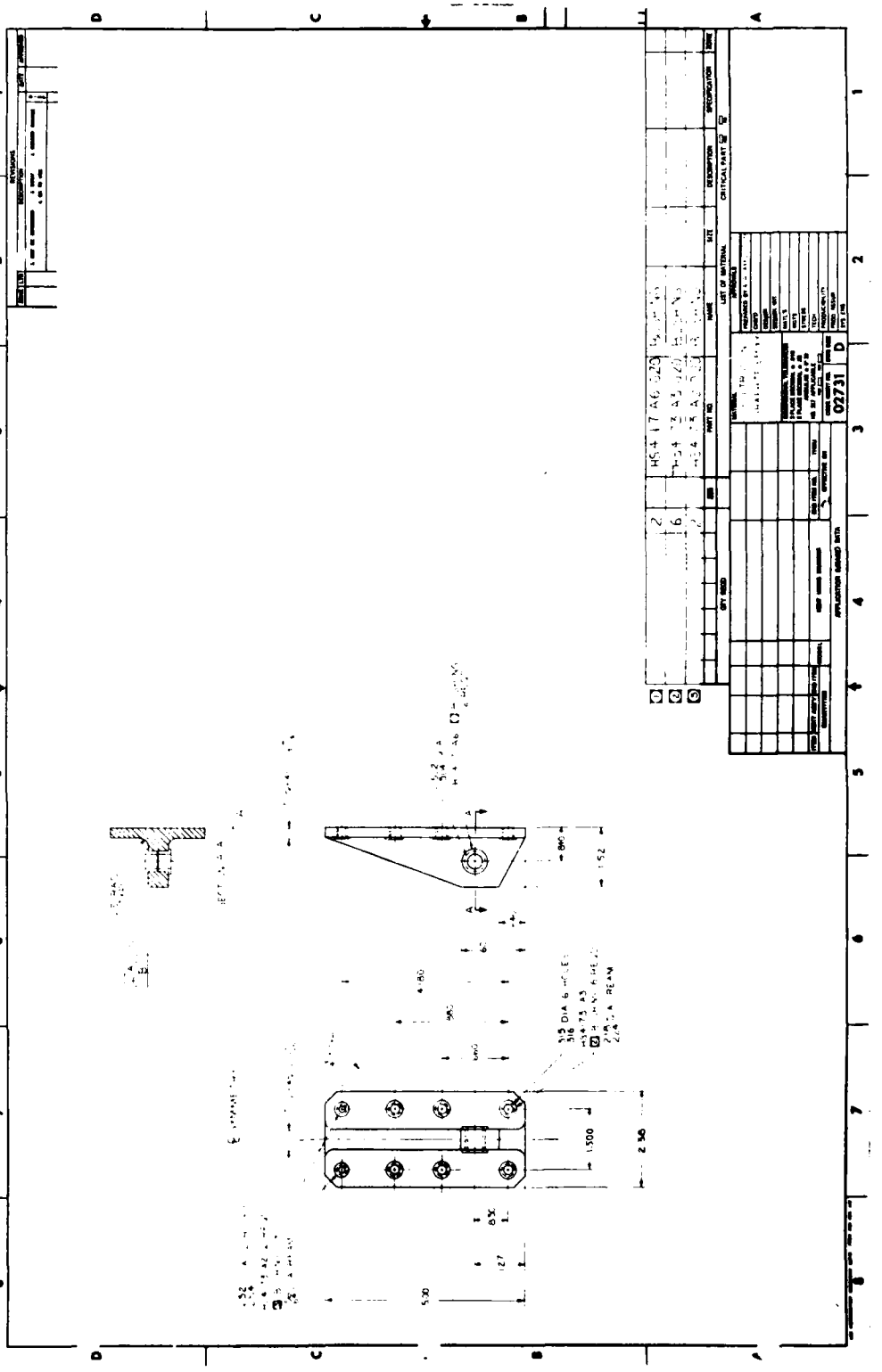

Figure 26. Type K Concept 1

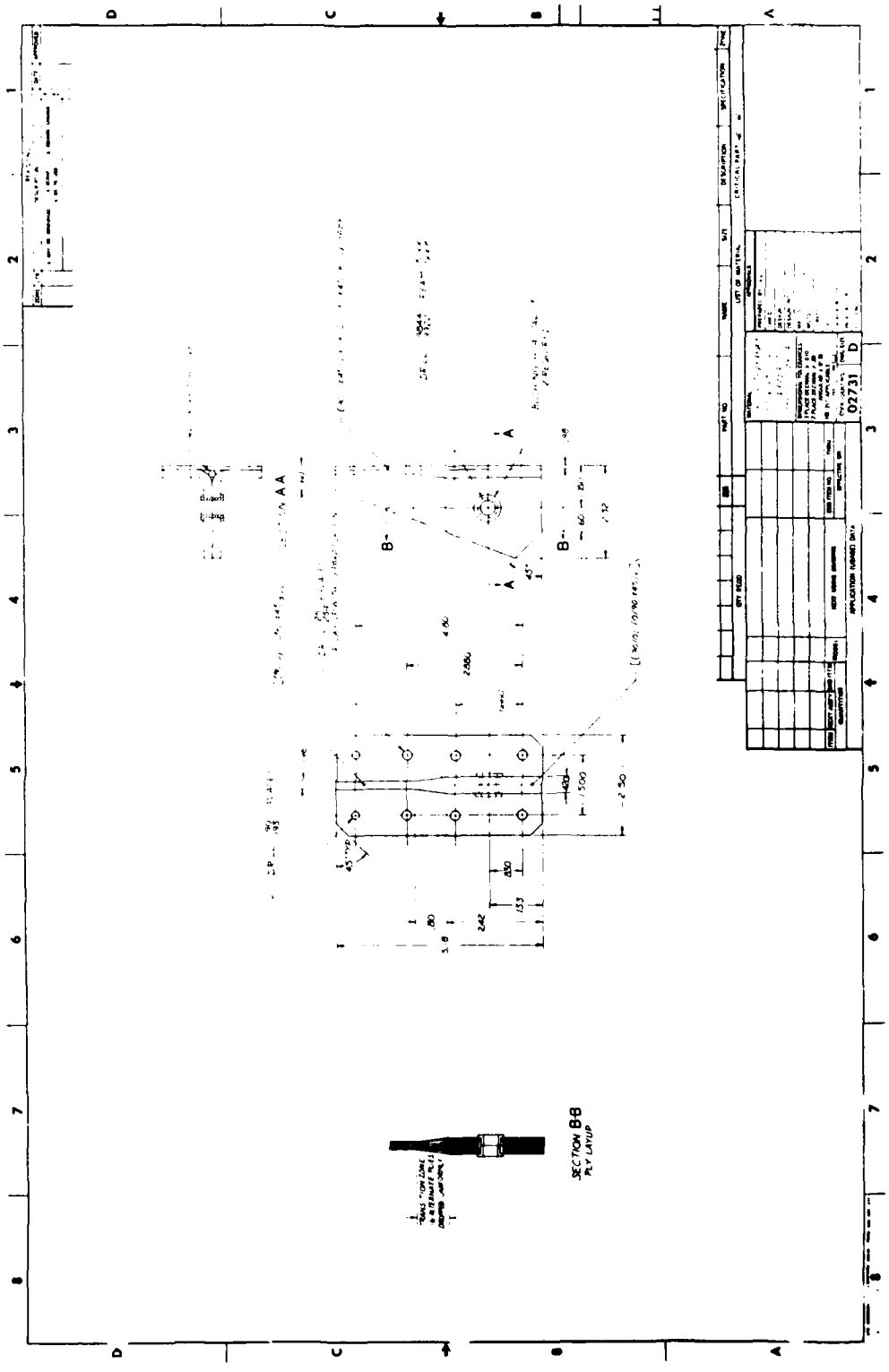

Figure 27. Type K Concept 2

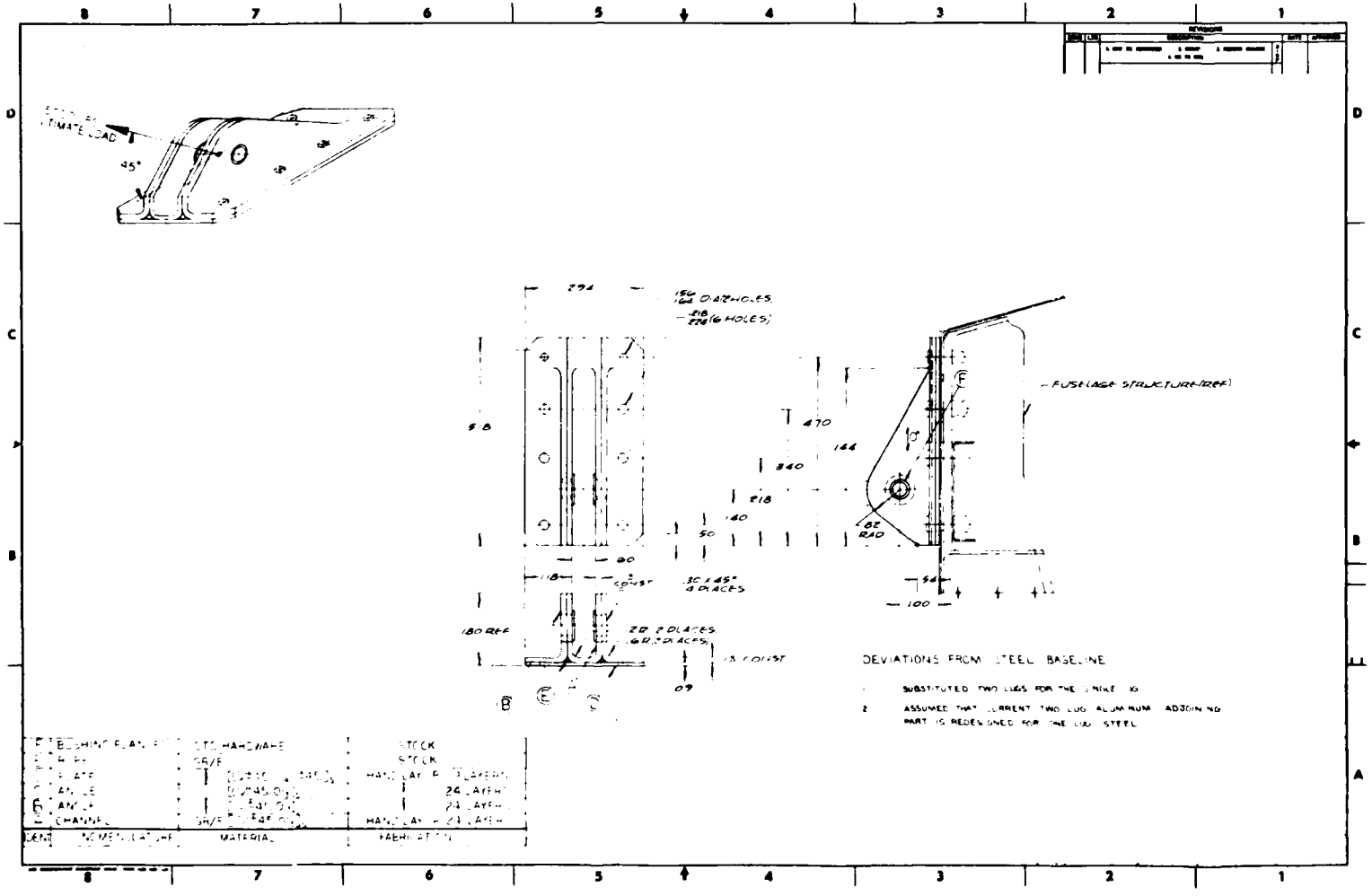

Figure 28. Type K Concept 3

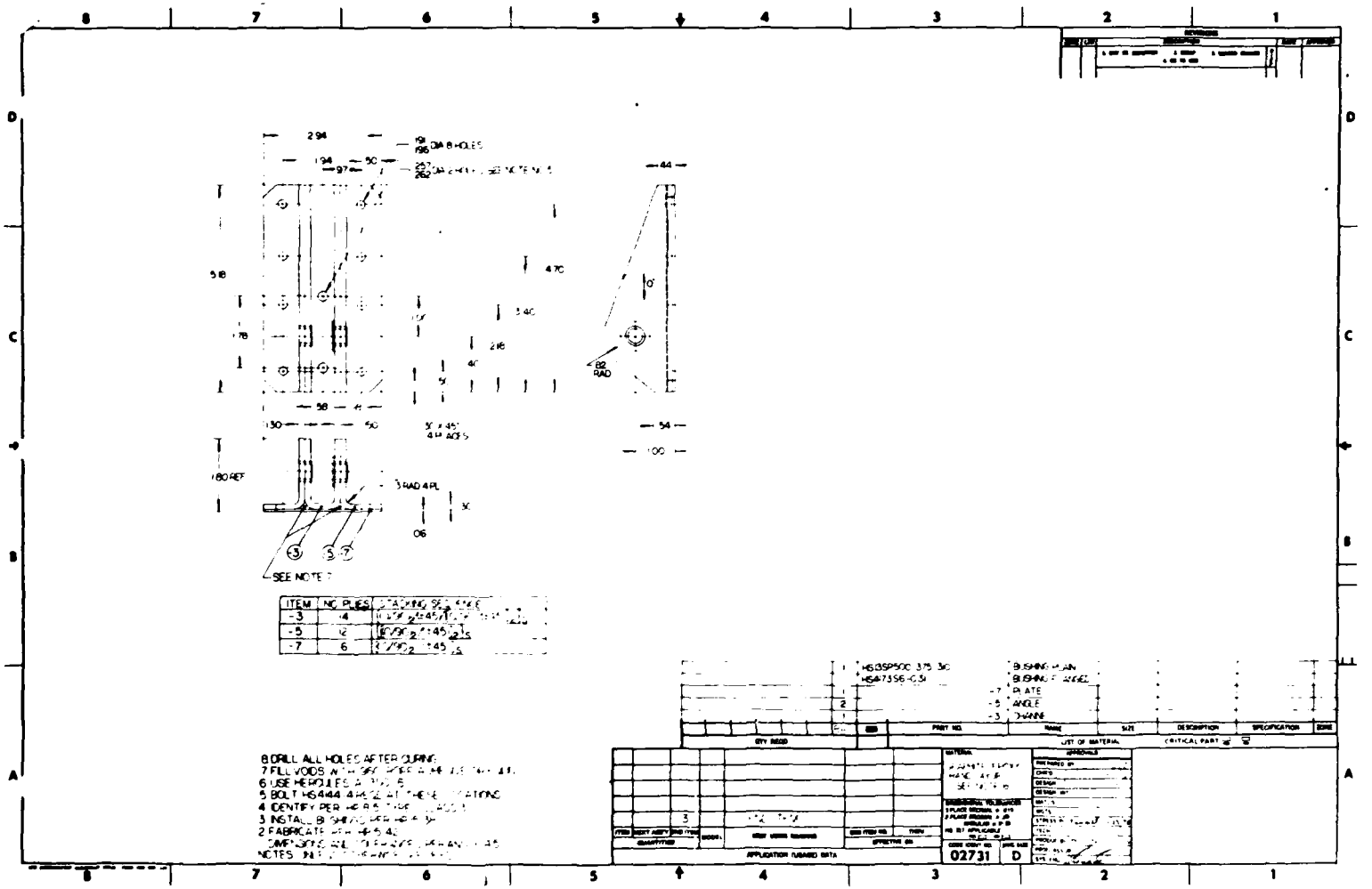

Figure 29. Final Detail Design: Type K

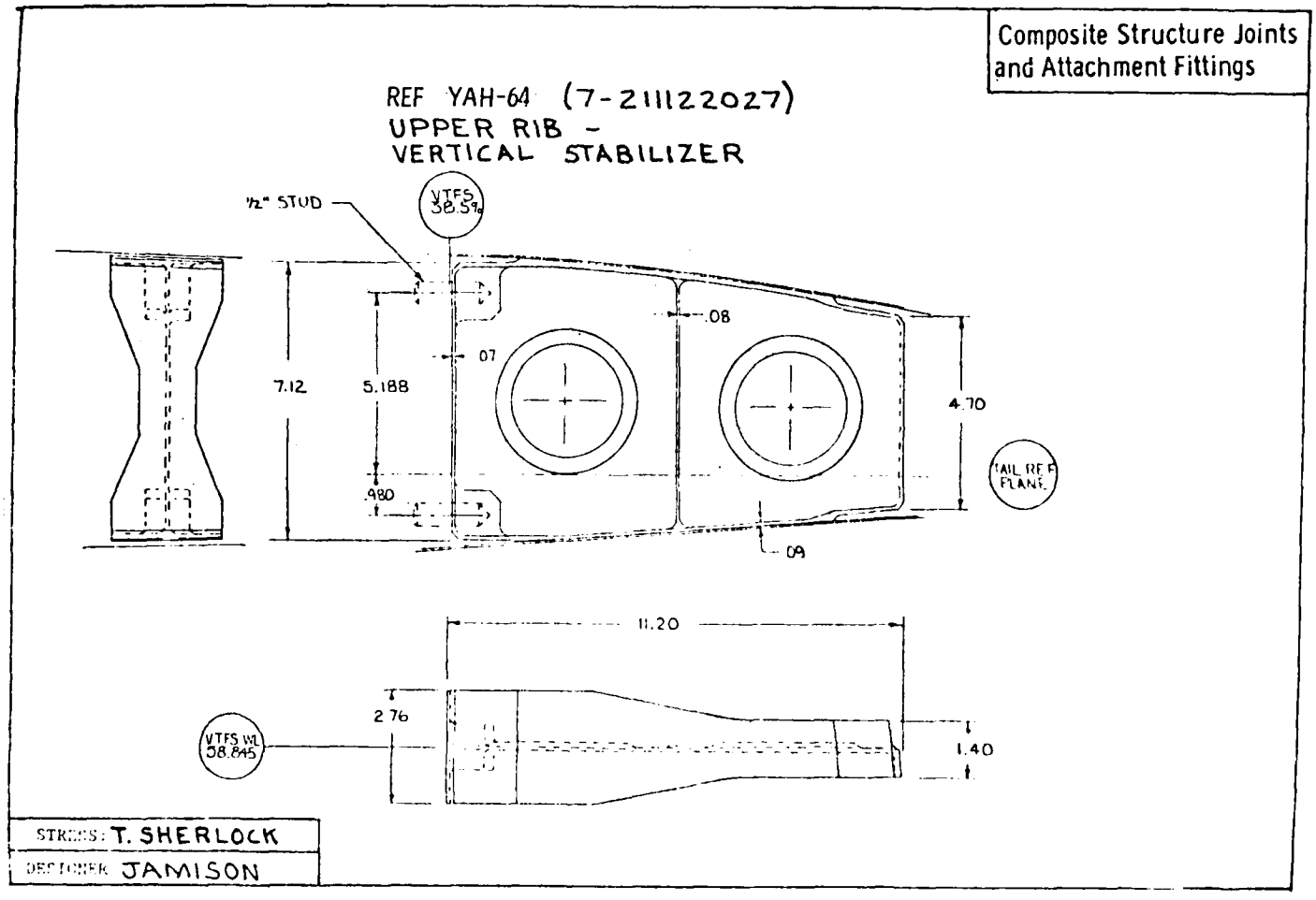

Figure 30. Baseline Metal Part Design: Gearbox Attachment Fitting (Type D)

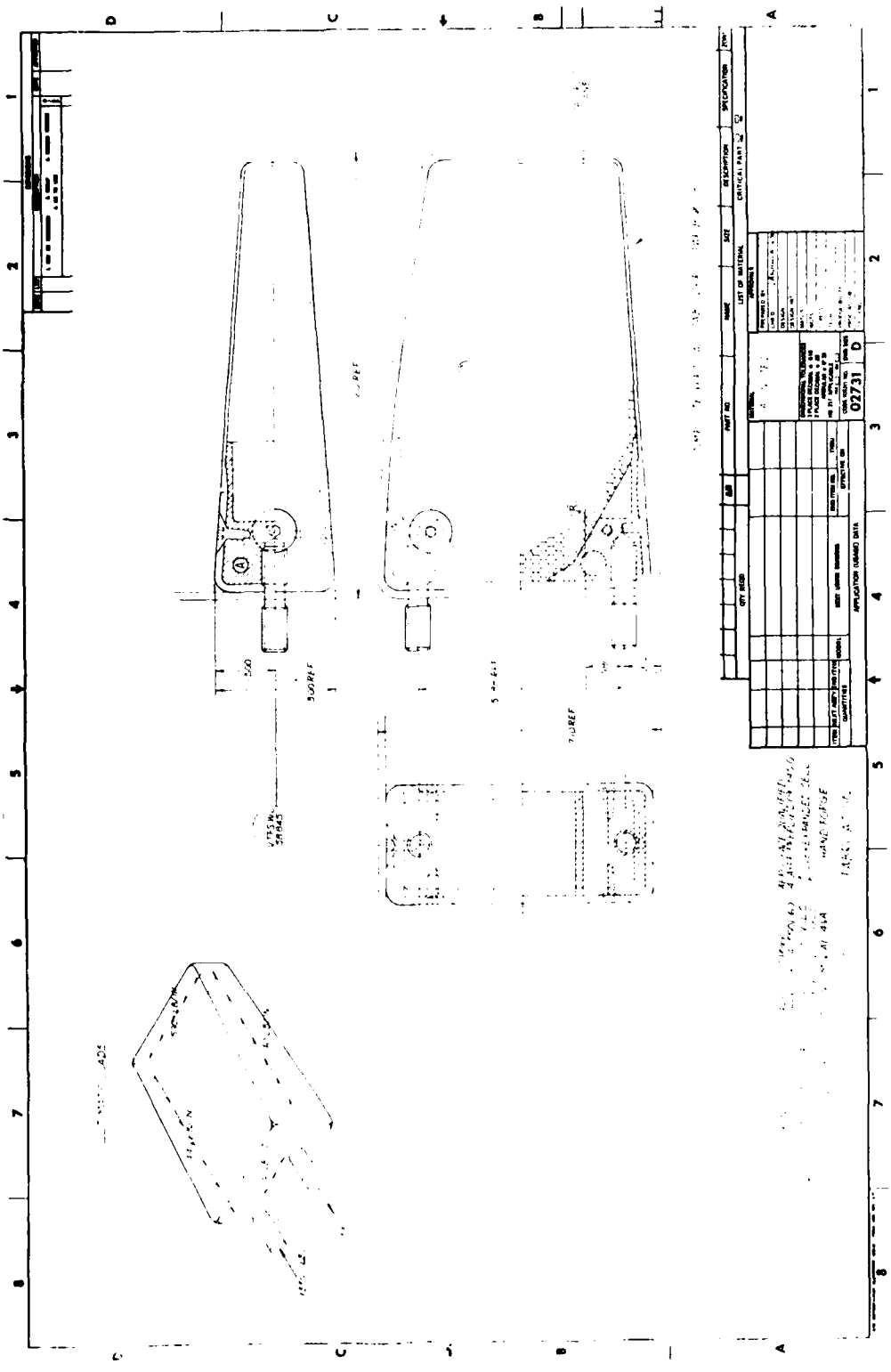

Figure 31. Type D Concept 1

Figure 32 illustrates Concept 2. This concept uses two metal anchors overwrapped with a filament-wound tube. The tube is mechanically trapped in the metal anchors and is bonded between the rib and spar box. The design is costly, and complex tooling is required to locate the flexible anchor block/tube assembly.

Figure 33 illustrates Concept 3. The metal anchors of Concept 2 were lengthened to provide sufficient area to bond directly to the graphite rib and spar box. Tapered doublers are used to control stiffnesses along the bond joint. The anchors are complex, and the fabrication of the tapered doublers is a labor-intensive operation.

Figure 34 shows the final Type D fitting design. Simplified steel fittings were used, and the tapered doublers were eliminated. The single shear web was replaced with a graphite/epoxy and foam sandwich. The solid laminate box was also replaced with a sandwich construction, with the bending material concentrated in corner caps to more closely simulate a composite vertical stabilizer design for the YAH-64 helicopter.

Type A – Wrapped Tension Fitting

Figure 35 shows the metal part from which the composite concepts were developed. Eleven of these "dagger fittings" form a tension joint between the fuselage and tailboom on the early versions of the YAH-64. The maximum loads on this joint occur during a tailwheel first crash landing.

Concept 1 is illustrated in Figure 36. This concept presumes a corrugated sandwich construction for the tailboom. The barrel nut is captive and cannot be replaced.

Figure 37 illustrates Concept 2. This design is similar to Concept 1 except that the sandwich core is honeycomb. The barrel nut is inaccessible for replacement.

Figure 38 shows Concept 3. This design also uses a honeycomb core, but the buried barrel nut has been replaced by a conventional nut. Access is assumed from inside the structure, and 24 fasteners are assumed rather than 11, as in the previous concepts. Local shear stresses around the corner are excessive.

Figure 39 illustrates Concept 4. The joint was refined by tapering the core to allow the inner and outer skins to join before making the turn. Eccentricity was reduced, as well as corner shear stresses. External access has been assumed on the fuselage (metal) side of the joint. This configuration

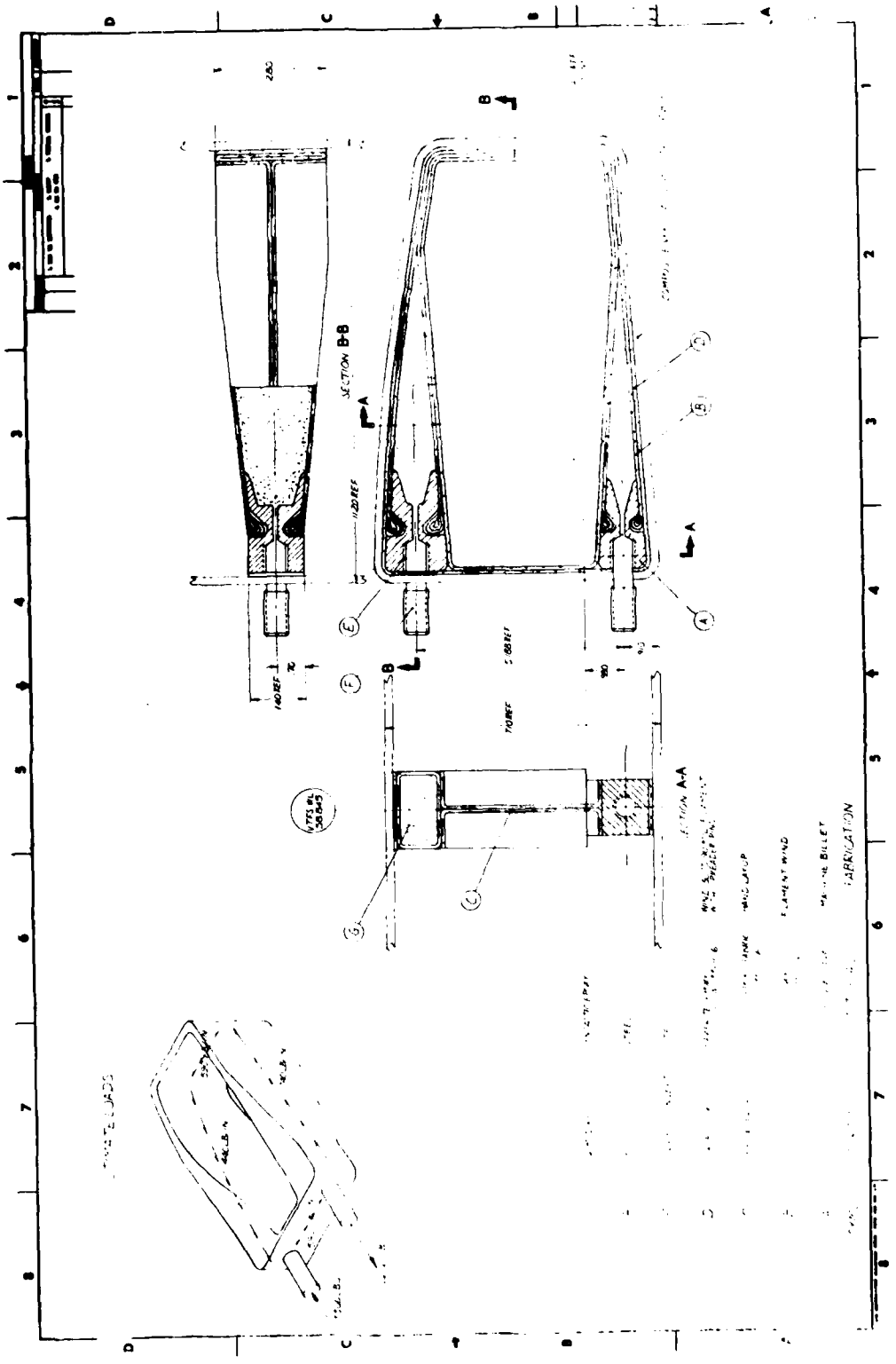

Figure 32. Type D Concept 2

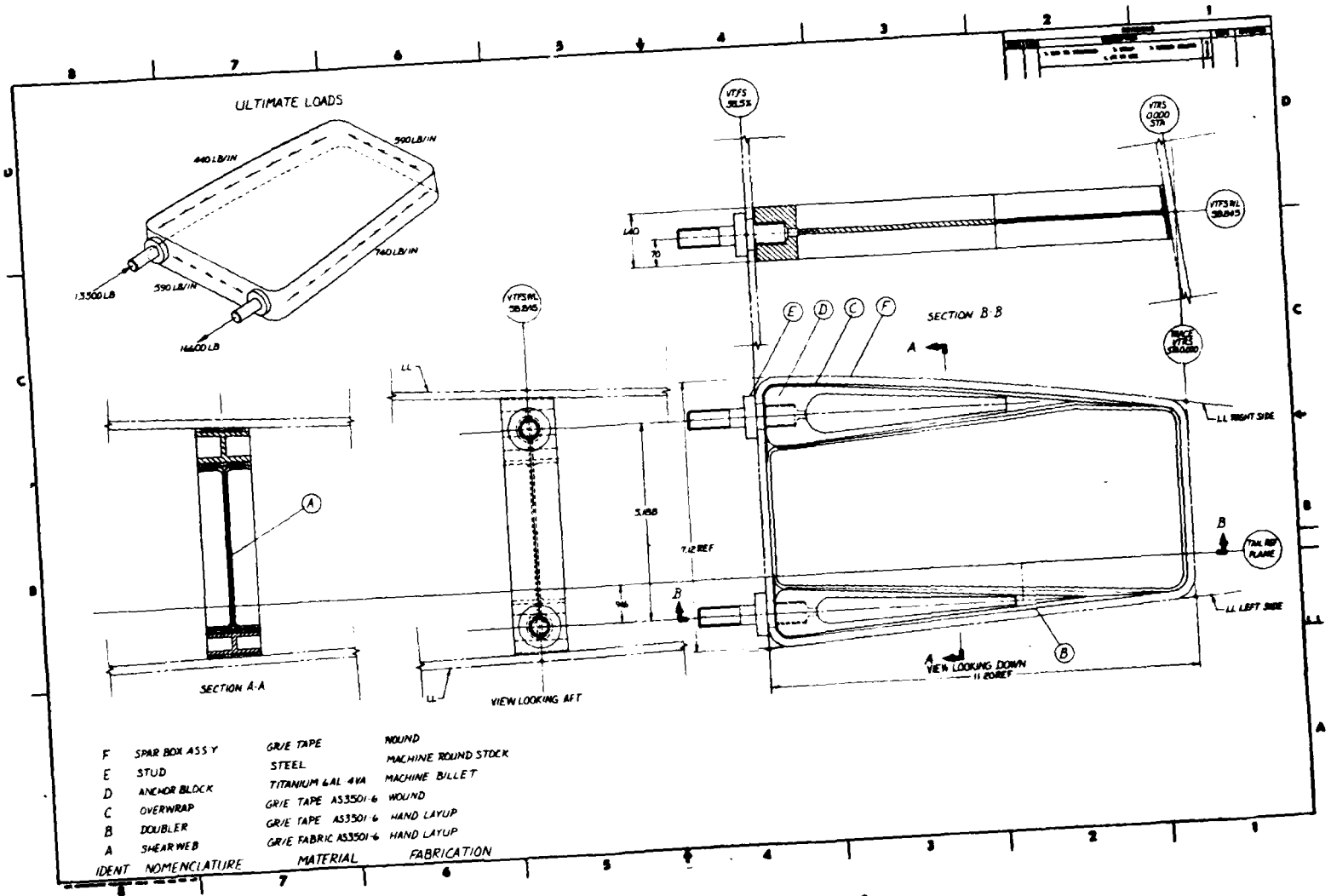

Figure 33. Type D Concept 3

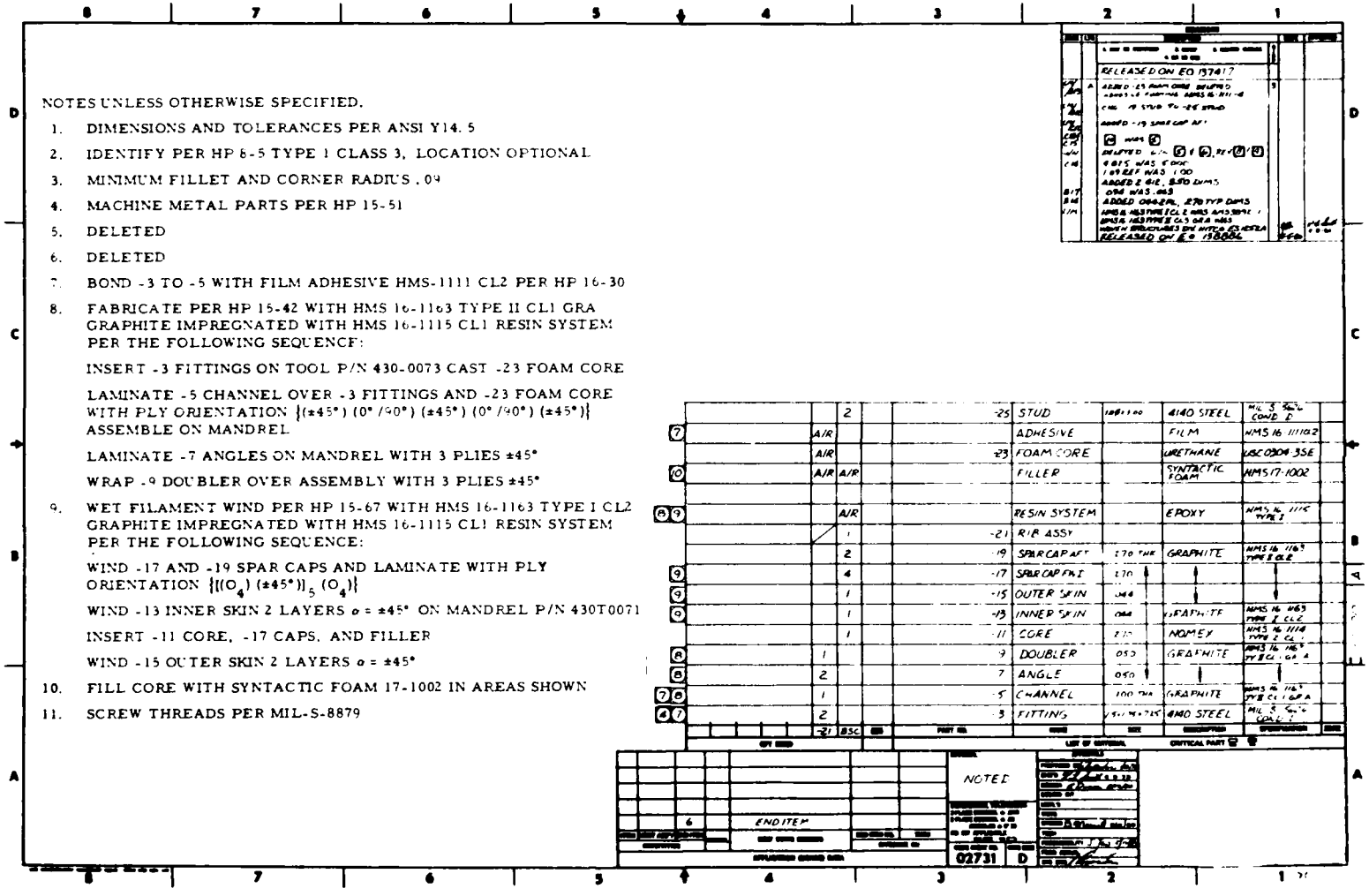

Figure 34. Final Detail Design: Type D (Sheet 1 of 2)

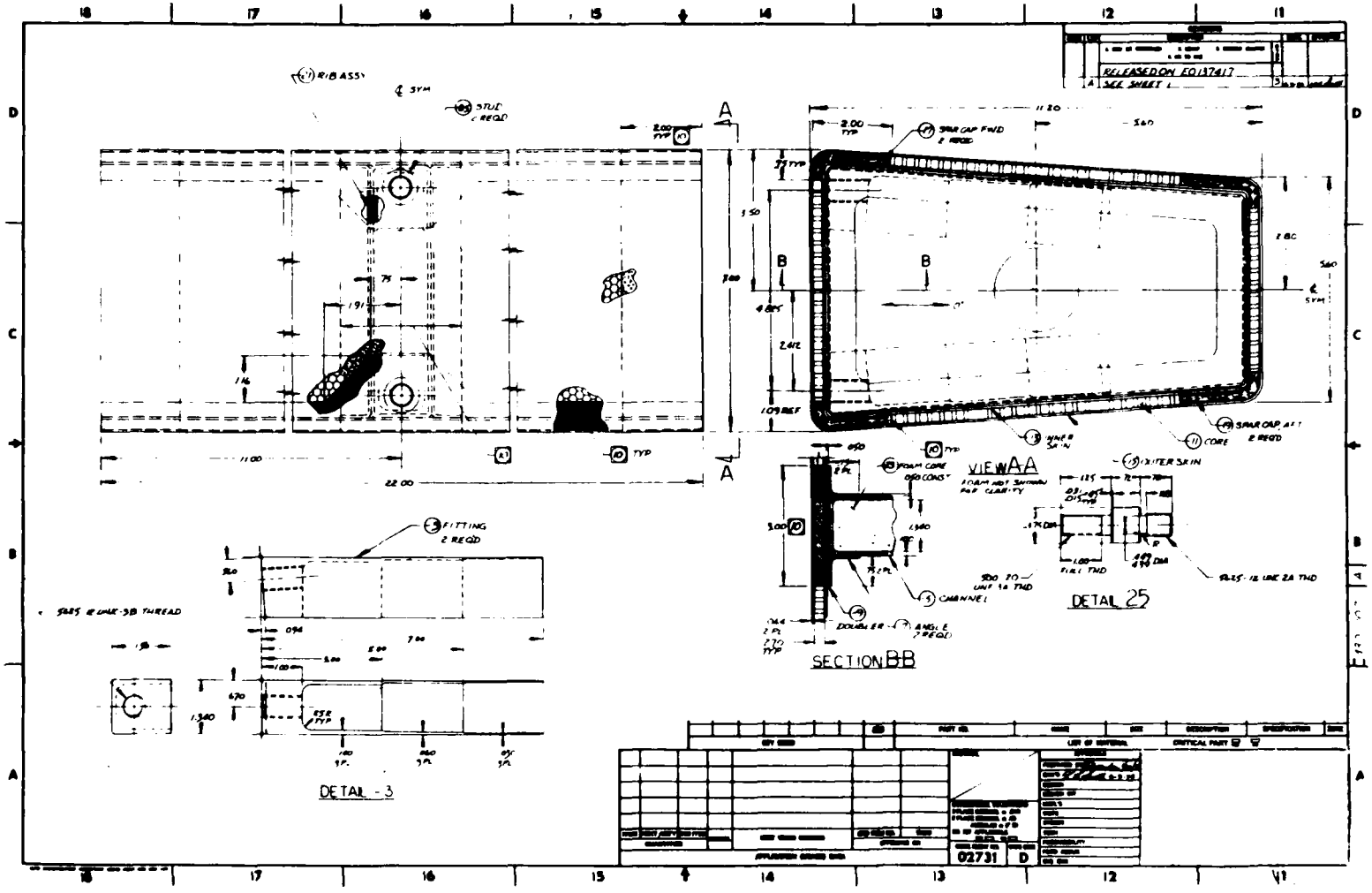

Figure 34. Final Detail Design: Type D (Sheet 2 of 2)

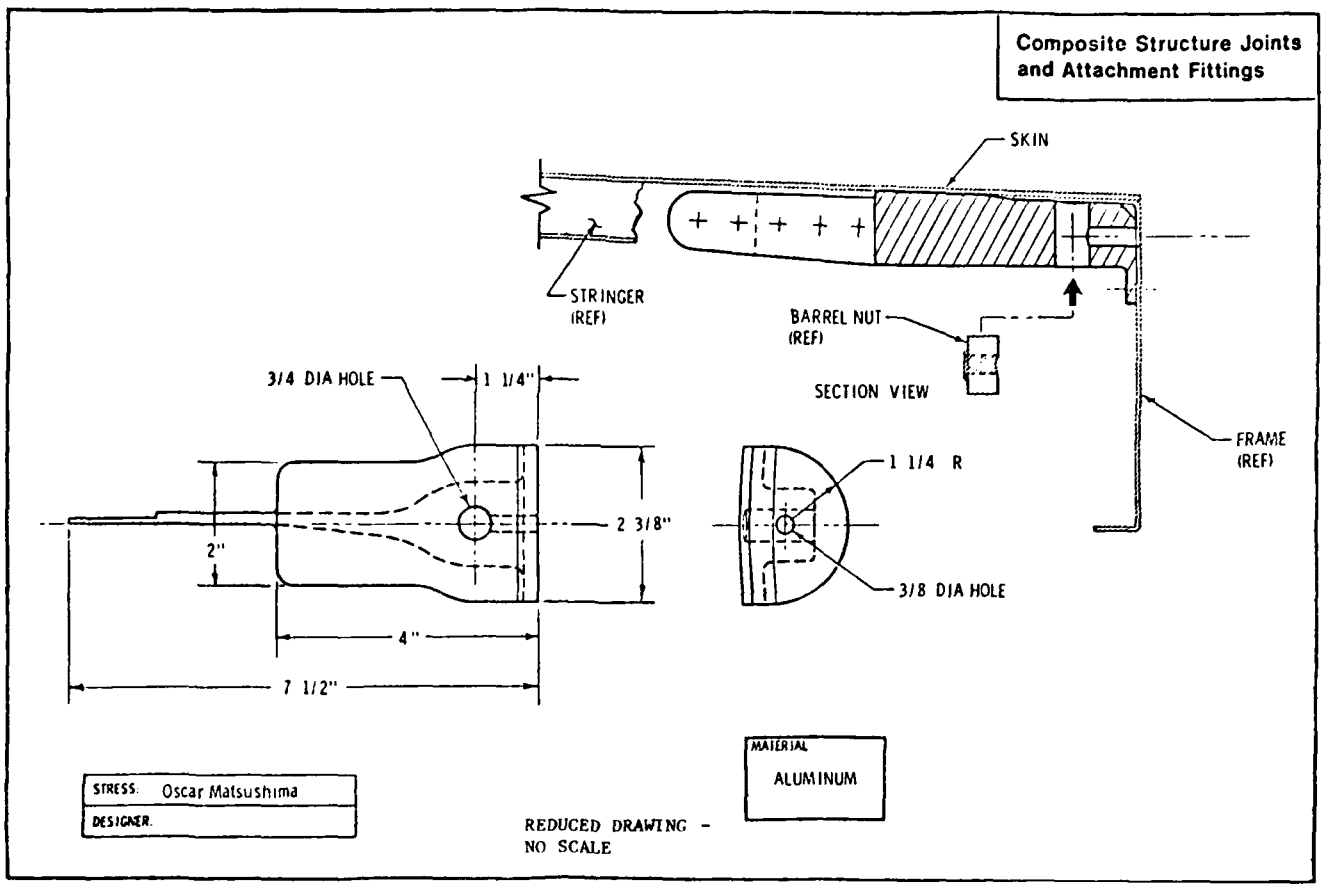

Figure 35. Baseline Metal Part Design: Wrapped Tension Fitting (Type A)

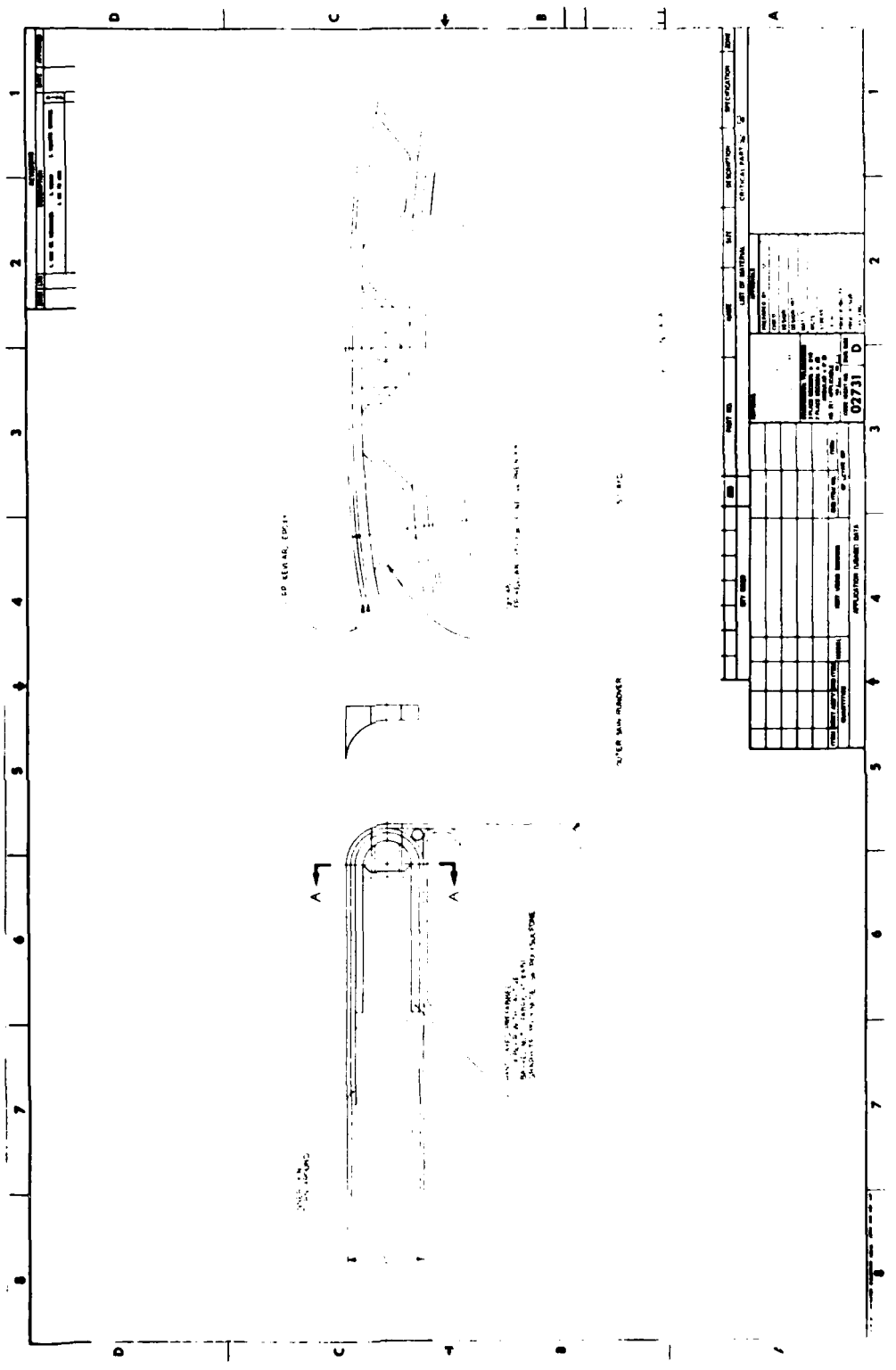

Figure 36. Type A Concept 1

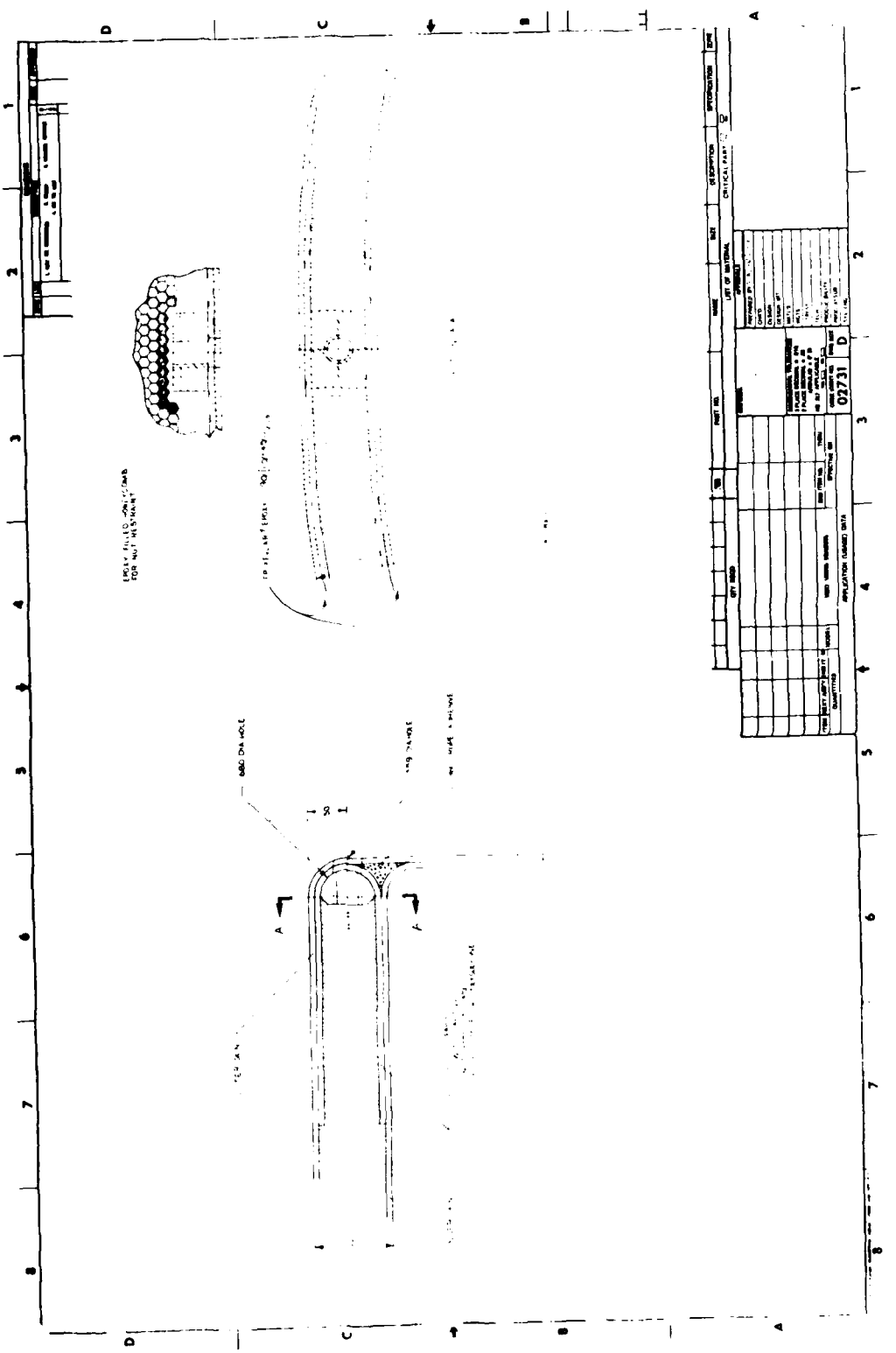

Figure 37. Type A Concept 2

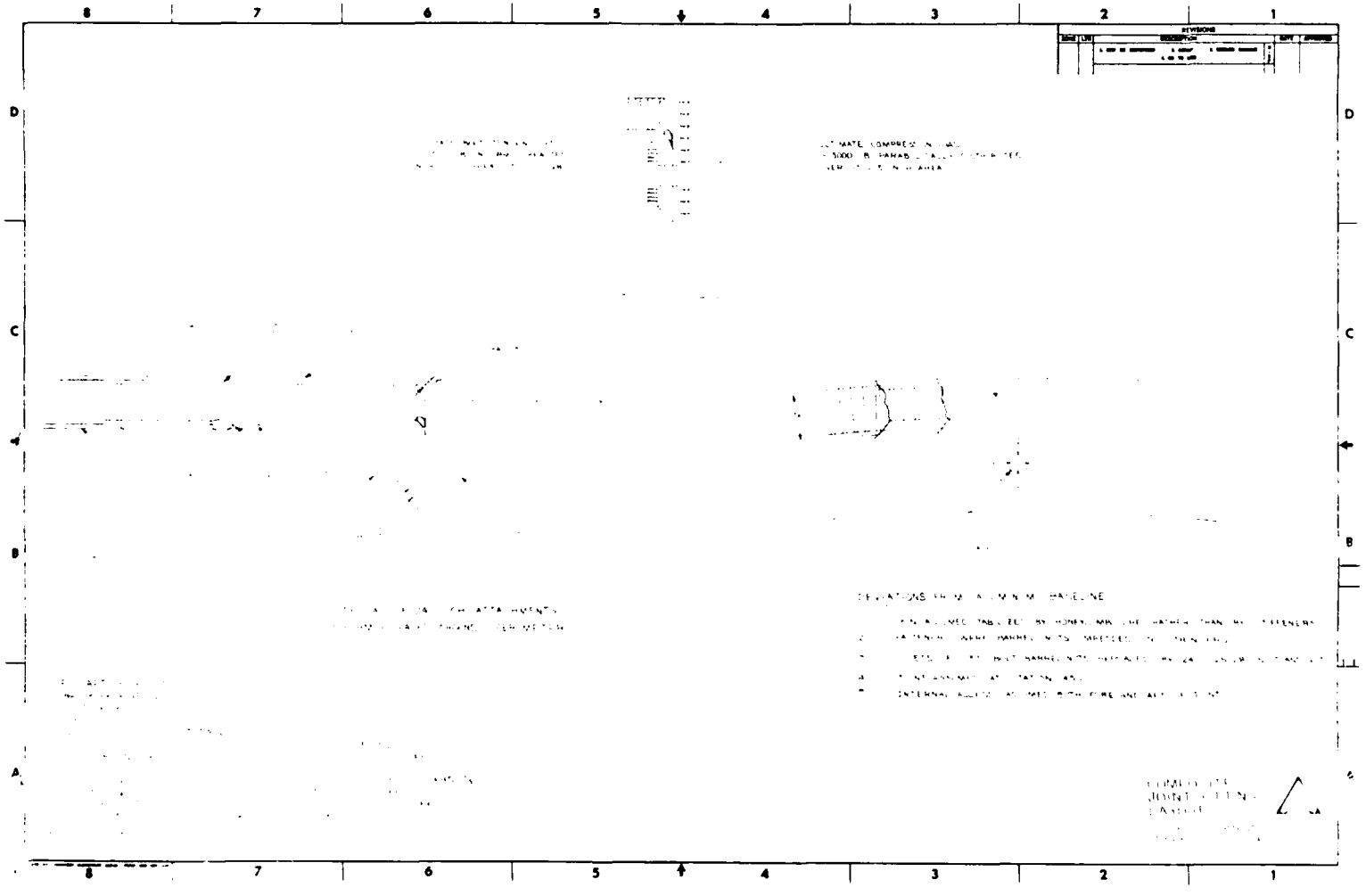

Figure 38. Type A Concept 3

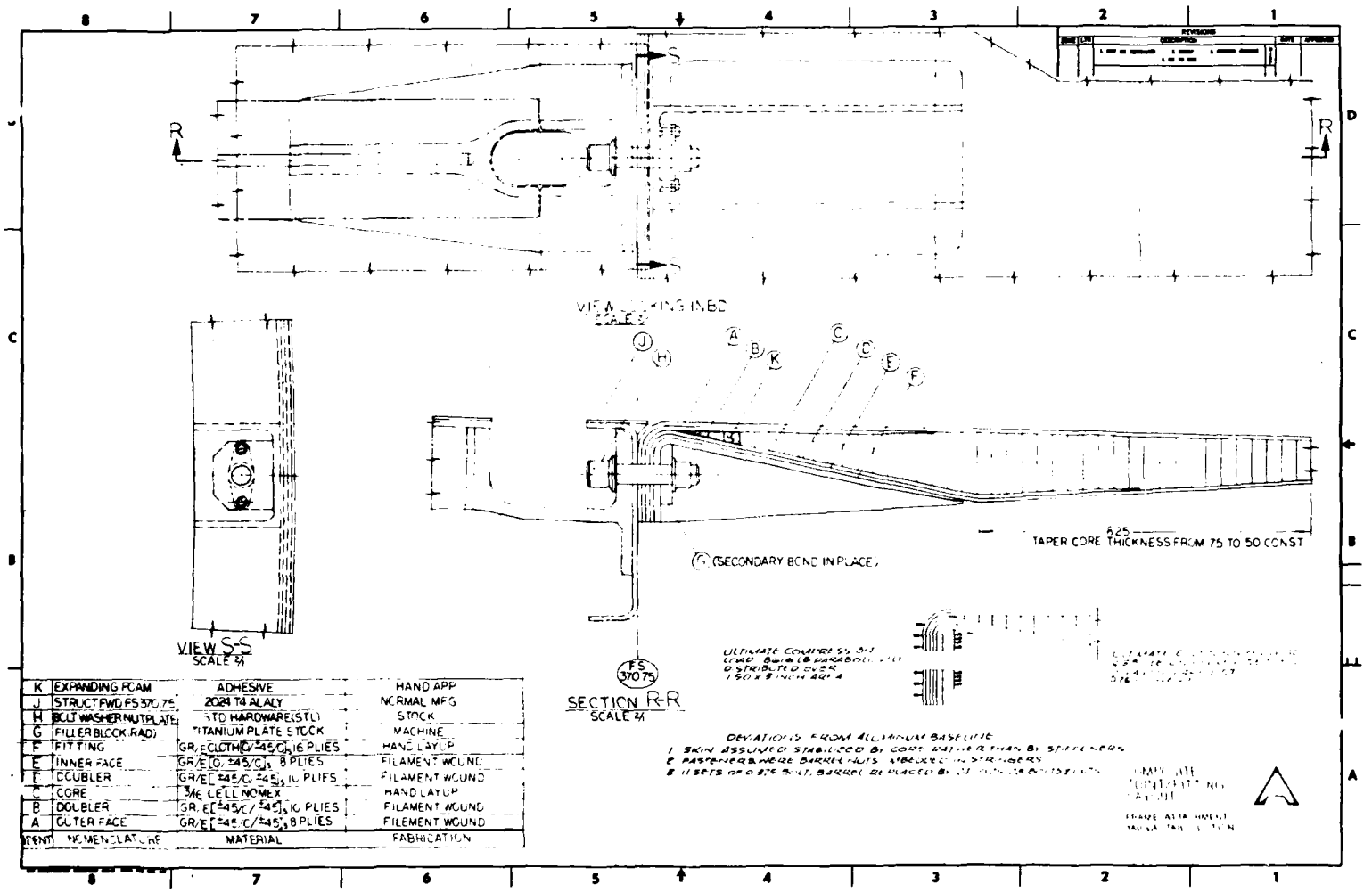

Figure 39. Type A Concept 4

was not considered an acceptable solution to the original problem. Twenty-four attachments were assumed, where the existing fuselage uses only 12 stringers, and external access on the forward fuselage would require extensive redesign of the metal fuselage.

The final design is shown in Figure 40. The internal bathtub and wrap-around skins were replaced by a channel closeout sandwiched between the skins. A pocket for bolt access is machined in the outer skin and the outer leg of the channel. The design utilizes the original geometry of the metal part, and is directly interchangeable.

DETAIL COMPARISON

This comparative analysis of the six joint/fitting types considers the inter-relationships of strength, weight, and projected cost, with emphasis on the strength vs weight and strength vs cost (material and labor) relationships. The comparative analysis for the metal baseline fittings and the composite fittings was done in three steps:

- Analysis of material cost vs total cost and total cost vs weight
- Comparison of strength vs weight and strength vs cost (material and labor) between baselines and composite designs
- Selection of the three most cost effective composite designs

The total costs for each unit are the cumulative average for a production run of 536 ship sets, and represent procurement costs to acquire the part per print (1978 dollars).

Analysis of Costs and Weights of Metal Baselines

The costs and weights of the six metal baselines are estimated in Table 4. Figure 41 plots material costs versus total costs and indicates that, for metal fittings, the cost of material stock comprises from one-fourth (for steel attachments) to over one-half (for the more intricate aluminum joints) of the total procurement costs.

The relation between cost and weight of the metal fittings in Figure 42 implies that the cost may be as low as $25 per pound for steel fitting F or as high as $210 per pound for aluminum fitting E.

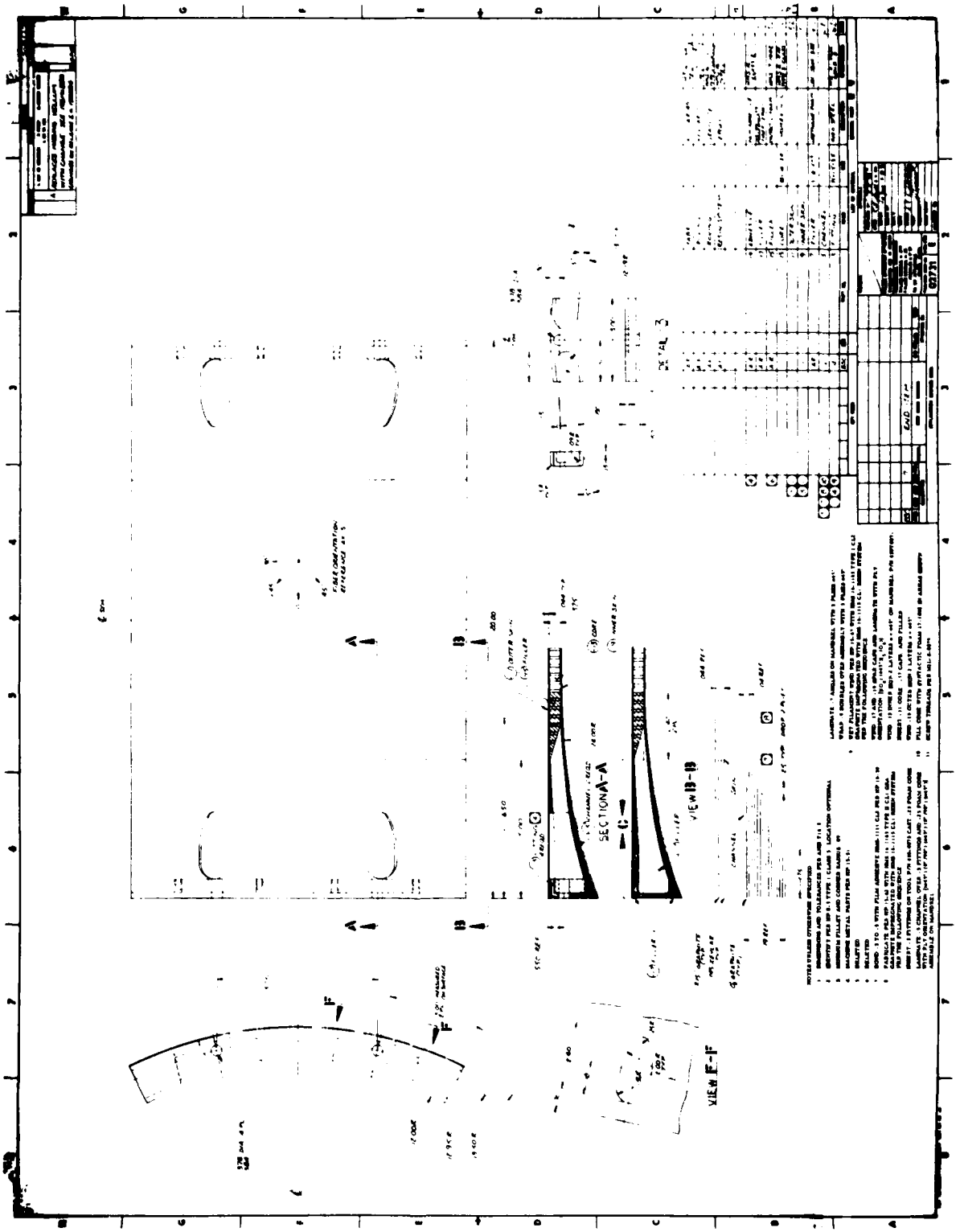

Figure 40. Final Detail Design: Type A

TABLE 4. METAL BASELINE COSTS AND WEIGHTS

Fitting	Material Cost, 1978 dollars (each)	Total Cost, 1978 dollars (each)	Weight, pounds
F – Composite Landing Gear Fitting	45	205	8.20
E – Integral Lug Fitting	22	105	0.50
G – Socket Attachment Fitting	70	130	2.84
K – Seat Attachment Fitting	33	135	0.65
D – Gearbox Attachment Fitting	41	110	1.55
A – Wrapped Tension Fitting	33	50	0.53

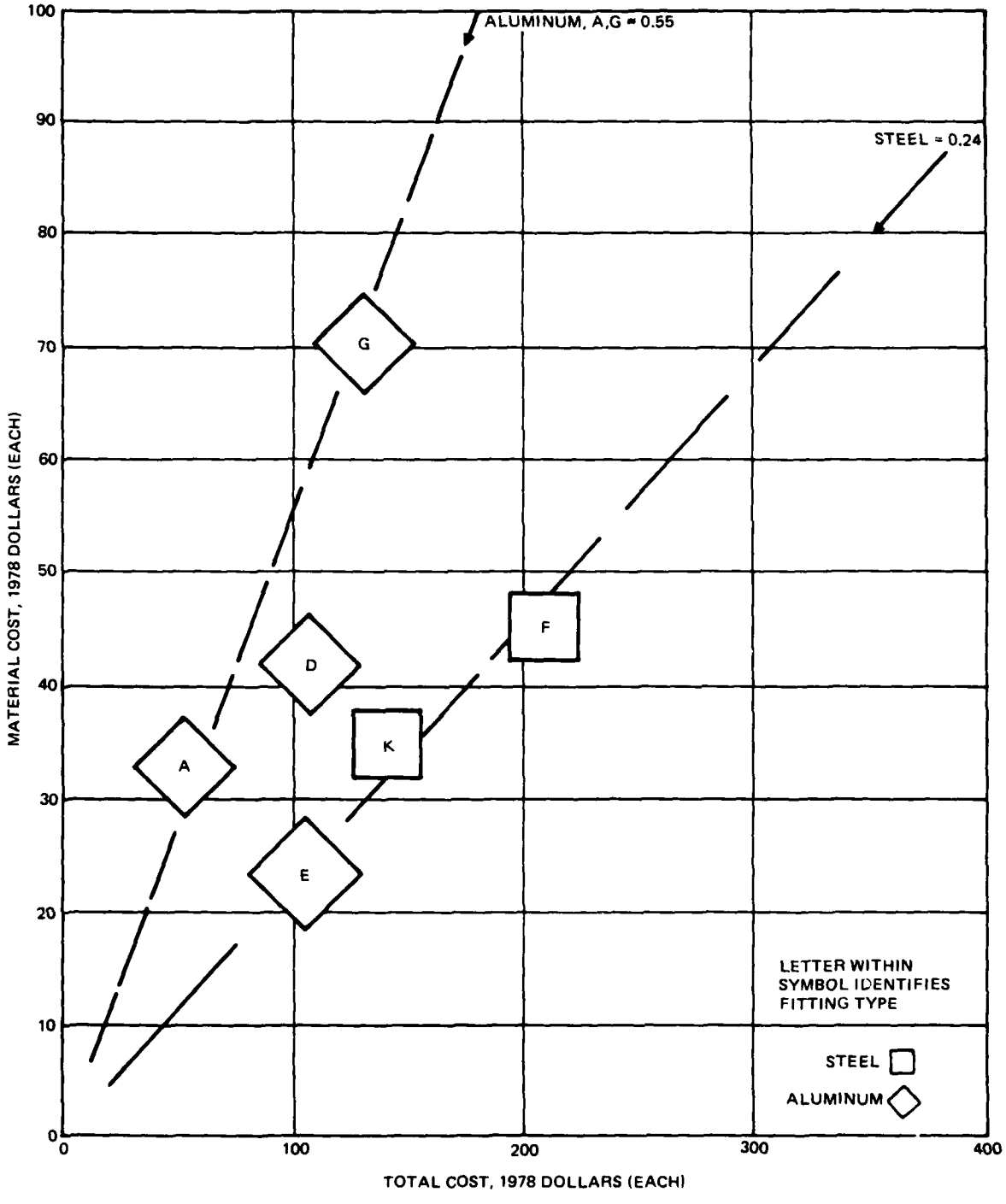

Figure 41. Cost Comparison of Metal Baselines

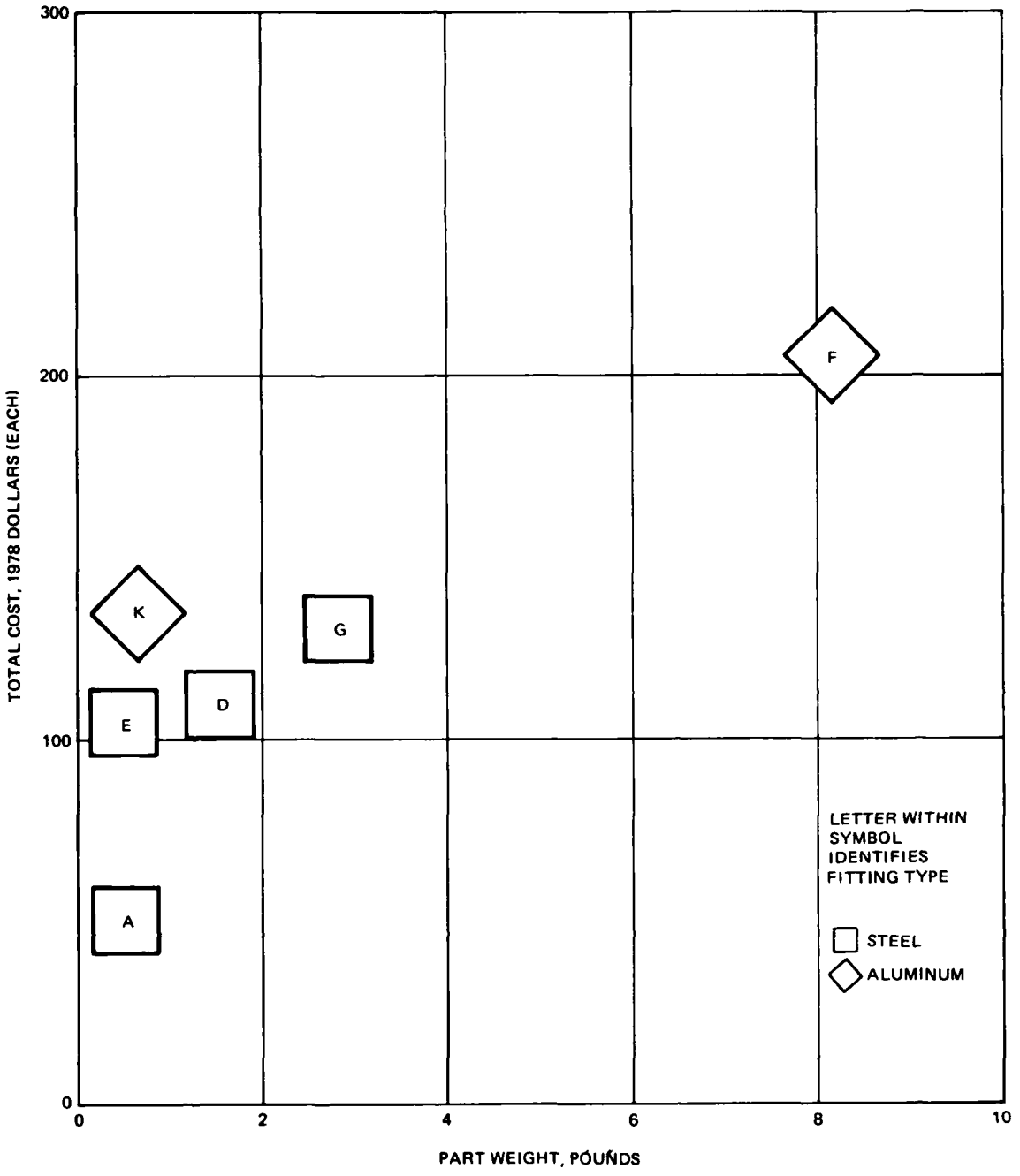

Figure 42. Cost-Weight Relationships of Metal Fittings

Cost and Weight of Composite Joints/Fittings

The cost and weight estimates of the composite attachment fittings are summarized in Table 5.

The Cost Analysis includes manufacturing labor costs, material costs, and nonrecurring costs.

Manufacturing labor costs consist of three types of labor man-hours:

a. Direct "hands-on" time in which personnel are actively engaged in fabrication of components, subassembly and final assembly operations, monitoring cure cycles, or engaged in finishing operations.

b. Time during which the personnel are required to be present, but are not contributing directly to the fabrication process.

c. Supervision, quality control, liaison engineering, and general observation of fabrication and assembly operation.

The Cost Analysis for fabricating the joint and fitting test specimens on a production basis is based on the R&D manufacturing experience gained on previous Advanced Composites programs that HH has conducted.

The cost estimates assume a quantity of 50 parts are released for fabrication at one time and are produced at a rate of 25 articles per month.

Labor and materials costs are both sensitive to production rate and quantity. Labor costs are based on a shop labor rate of $5.50 per hour.

Materials costs are based on a production scrap rate of 10 percent and are quoted as 1978 prices for comparison with the metal baseline costs.

Nonrecurring costs include amortization of tooling over the total production quantity of 536 articles.

Cost figures include a 150 percent burden and a 30 percent General and Administrative costs.

It is interesting to note that the composition (and thus the cost) of materials varies greatly from design to design. In general, all designs except F contain 79.5 percent or more composites (see Figure 43). (The exception of F stems from the material from which the metal baseline is made.) The 300-ksi maraging steel of F has a higher specific strength than orthotropic graphite/epoxy, thus negating the advantages of composites vis-a-vis steel and resulting in the small proportion of graphite/epoxy (26 percent) in the design of F.

TABLE 5. COST AND WEIGHT OF COMPOSITE FITTINGS

Attachment Fitting	Total Cost, 1978 dollars (each)	Material Cost, 1978 dollars (each)		Weight, pounds
		Metal	Composite	
F – Composite Landing Gear Fitting	950	103	201	7.07
E – Integral Lug Fitting	61	0	20	0.233
G – Socket Attachment Fitting	161	10	48	1.82
K – Seat Attachment Fitting	249	0	65	0.42
D – Gearbox Attachment Fitting	197	1	40	1.13
A – Wrapped Tension Fitting	74	5	17	0.31

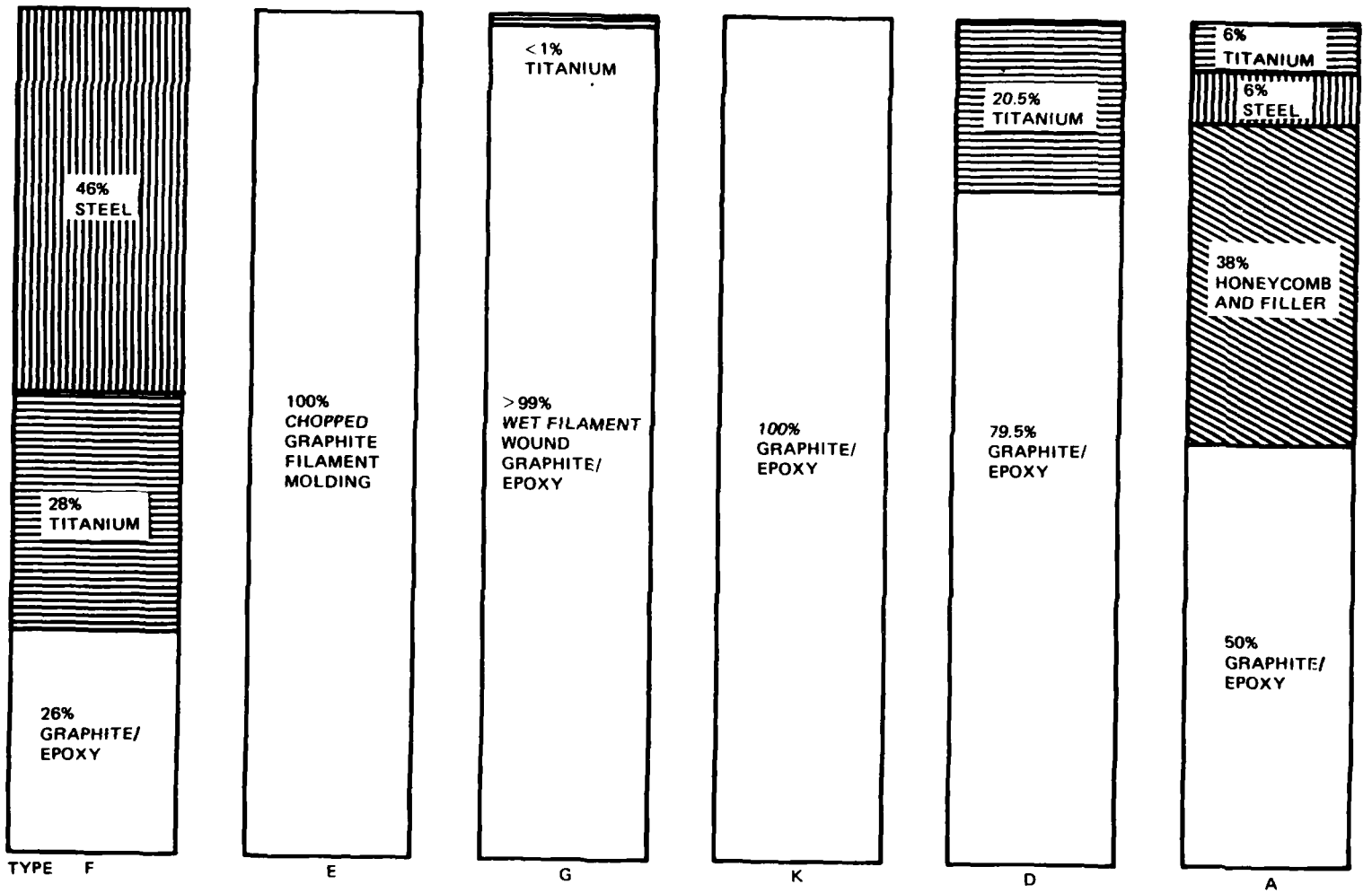

Figure 43. Material Proportions in Composite Fittings

Material (composite plus metal) costs versus total costs of the composite fittings are shown in Figure 44, which indicates that the average material costs are about 30 percent of the total and range from 20 percent (for D) to 36 percent (for G).

The relation between cost and weight of composite fittings in Figure 45 implies that total cost averages about $150 per pound but may be as low as $88 per pound (as in G) or as high as $593 per pound (as in K).

Strength Versus Weight and Strength Versus Cost Comparisons

The comparisons were carried out under the assumption that the composite designs were identical in static strength to the metal baselines but not necessarily identical in fatigue strength (Figure 46). It should be noted that because composites exhibit higher fatigue strengths than metals:

$$\left(\frac{F_{fatigue}}{F_{static}}\right)_{composite} > \left(\frac{F_{fatigue}}{F_{static}}\right)_{metal}$$

the fatigue strength of the composite joints will be equal to or greater than the fatigue strength of the corresponding metal baseline joints. It can be seen that weight reductions, which range from 14 percent (for F) to 53.4 percent (for E), average 33 percent.

These weight reductions, however, are achieved in most instances at a cost penalty. The cost difference when composite fittings are incorporated (Figure 47) ranges from a 42 percent savings (for E) to a 363 percent increase (for F), and averages out to about a 93 percent increase, or penalty, for the six fittings taken as a set.

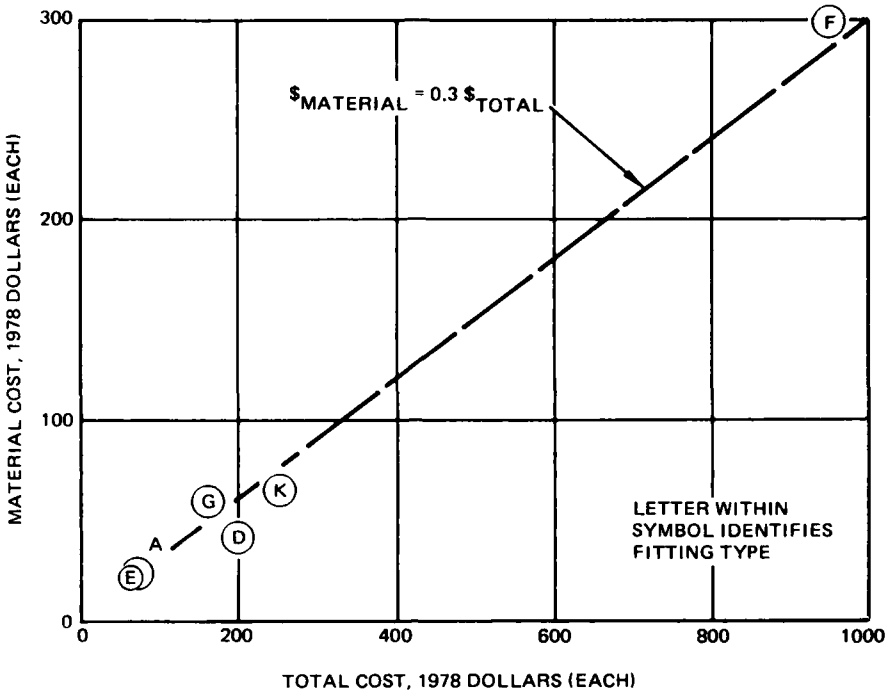

Figure 44. Cost Comparison of Composite Fittings

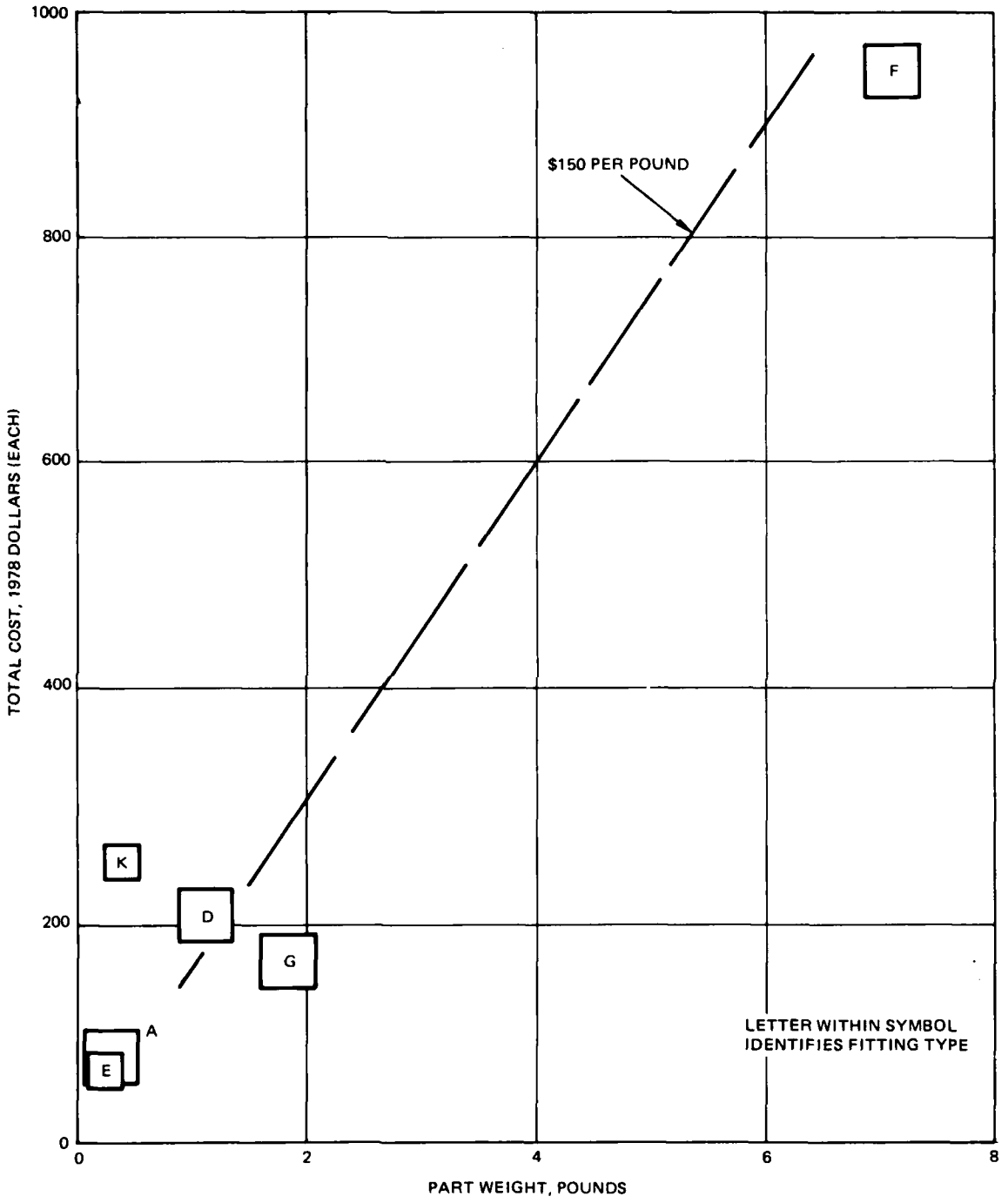

Figure 45. Cost-Weight Relationships of Composite Fittings

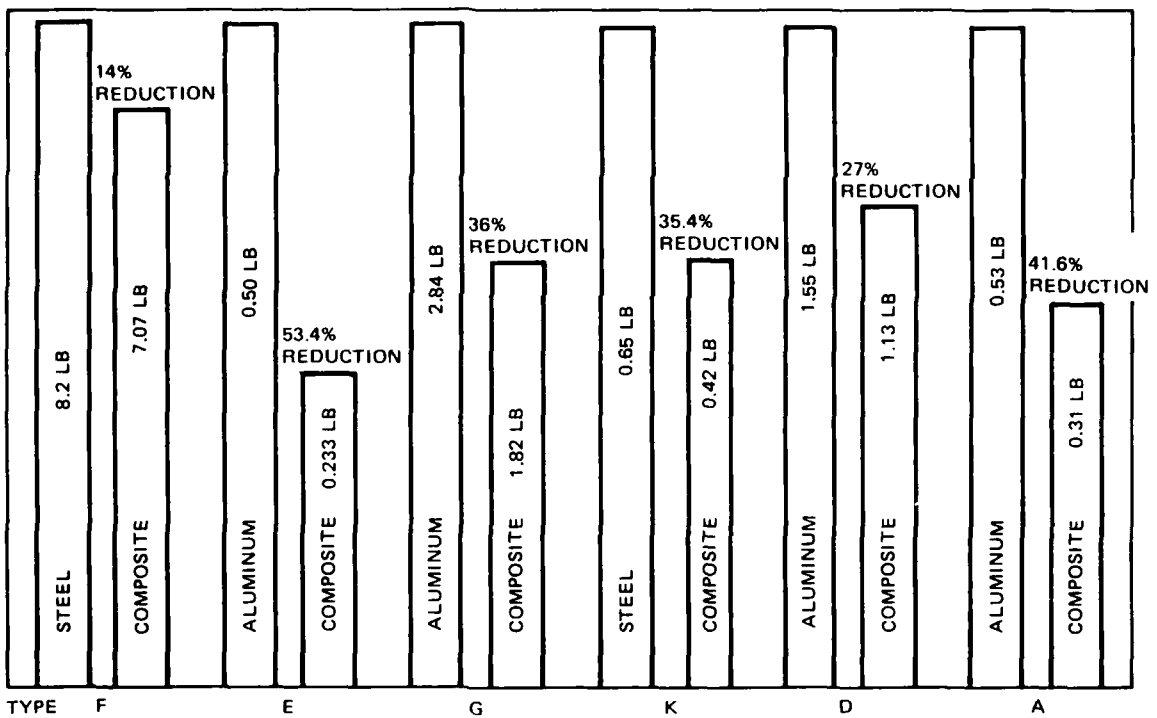

Figure 46. Weight Reduction Using Composite Fittings

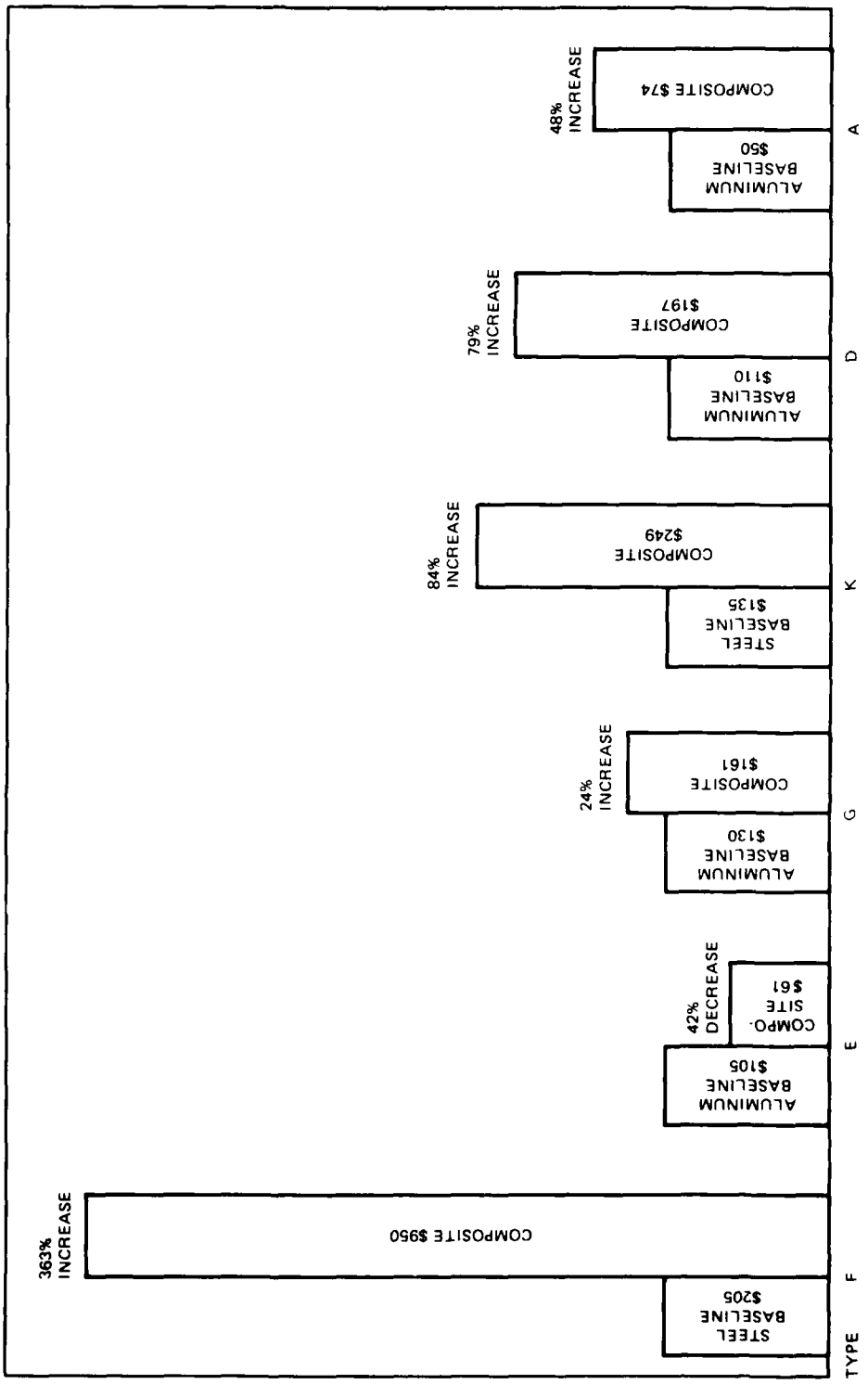

Figure 47. Cost Comparison of Metal Versus Composite Fittings (1978 dollars)

Selection of Three Cost Effective Composite Fittings

The cost effectiveness of each composite fitting design was measured by considering the individual weight reductions afforded by going to composi and the cost increments entailed vis-a-vis the metal baseline. To differe tiate between cost effective and cost ineffective designs, the cost differen (six increases and one decrease) and weight reductions are plotted in Fig ure 48 to indicate cost efficiencies. The cost efficiency of each fitting de is shown for a production run of 536 articles. The cost efficiency of Typ is also shown for a run of 10 articles to illustrate the effect of production quantity on the cost of weight reduction.

The population of cost-versus-efficiency points is divided into two domai by the cost effectiveness break-even line, with cost effective designs res to the left and above the break-even lines. These cost effective designs possess features whose value added in the form of weight elimination mo than offsets the extra expenses incurred. The slope of the economic bre even line is the unit monetary value (in life-cycle dollars), or the worth t the Army of eliminating a pound of structure from a helicopter without al ing its structural performance. The figure shows two break-even lines f this value to the user, $200 per pound and $300 per pound, to reflect two opinions as to the worth of helicopter structural weight reduction progra

It may be seen from Figure 48 that composite fitting types G, D, A, and are to the left and above the break-even lines and are therefore cost effe designs. If only 10 of the Type E test specimens were to be made, the $2,000 die cost would add $200 to the unit cost and bring Type E far belo break-even line. For this reason, Type E was assessed as cost ineffecti and not recommended for fabrication and testing.

Recommended Fittings

Six joint/fitting types were designed in detail, and three were recommen for fabrication and test:

- Type G – Socket attachment fitting
- Type D – Gearbox attachment fitting
- Type A – Wrapped tension fitting

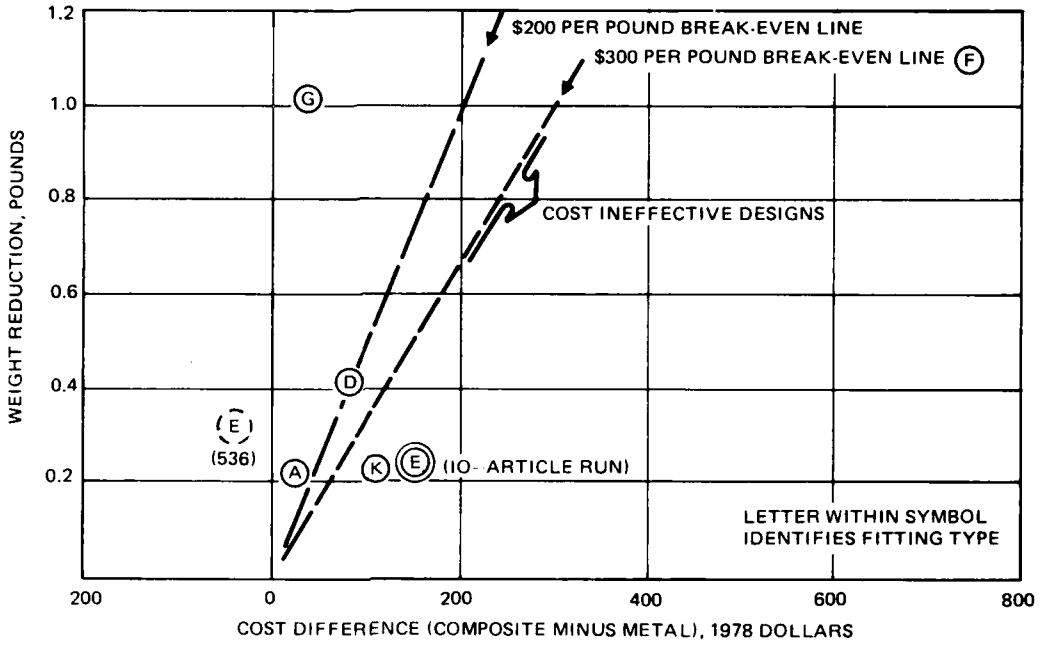

Figure 48. Break-even Partitioning of Composite Fittings

Types G, D, and A were selected because:

6
F

- All are applicable to large primary structures
- All have near-term implementation potential (e.g., YAH-64 composite tail section program and future all-composite fuselage)
- All provide weight reduction compared with the metallic baseline
- All are cost effective
- The Type A joint has the turn-the-corner feature, sized with the help of the interlaminar shear computer program.

Selected Fittings

Of the three joints and fittings recommended for fabrication and testing (Types G, D, and A), Types D and A were approved by the Army Contracting Officer. A decision was made to fabricate and test the Type K fitting instead of Type G. Various reasons for this change were cited, the majority of which were manufacturing considerations (Type K is a manual layup and does not require any special tooling or equipment for fabrication).

FABRICATION

A Fabrication Plan was developed to define the procedures to be employed in manufacturing the three selected fittings (Types K, D, and A, as illustrated in Figures 29, 34, and 40 respectively). The manufacturing plans are described below.

TYPE K

The manufacturing plan is illustrated in Figure 49. Precut materials were laminated onto individual tools for each detail. The details were then assembled and cocured in an autoclave. After cure, the part was removed from the tool and machined to final dimensions. The tool was designed to make all three specimens in one operation. A photograph of the finished part appears in Figure 50.

TYPE D

The manufacturing plan is illustrated in Figure 51. The -5 channel detail was fabricated and precured with the -3 metal fittings in place. The -17 and -19 spar caps were also precured. In the final assembly sequence, the -5 channel was assembled on the mandrel. The two -7 angles and the -9 doubler were then laminated on the mandrel. The inner skin was wound over these details, after which the -11 honeycomb core and -17 and -19 spar caps were installed. Winding the outer skin completed the assembly, which was vacuum bagged and oven cured. The part was removed from the mandrel and trimmed to drawing dimensions, and the attachment studs were installed. A photograph of the finished specimen appears in Figure 52. Six of the Type D specimens were fabricated.

6
B

TYPE A

The manufacturing plan is illustrated in Figure 53. The two -5 channels were fabricated and precured over a plaster mold with the -3 metal fittings in place. The plaster mold was removed and the -7 filler (urethane foam) was poured in its place. The inner skin was wound, after which the two -5 channels and the -13 honeycomb core were assembled on the mandrel. The outer skin was then wound to complete the assembly. Pressure plies (hoop windings) were wound to provide laminating pressure, and the part was oven

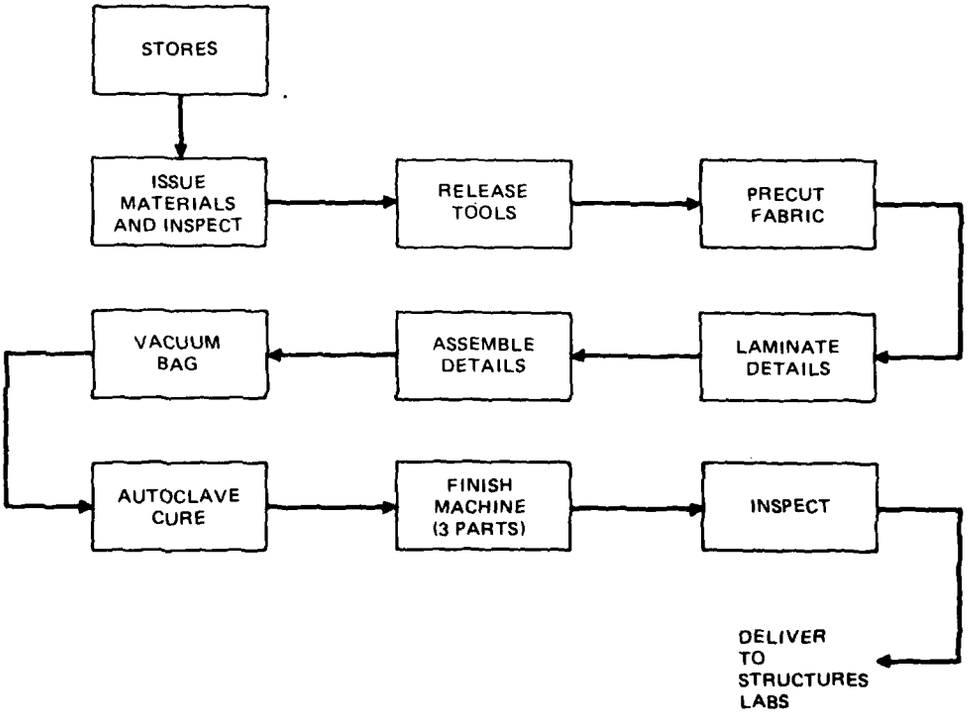

Figure 49. Manufacturing Plan (Type K)

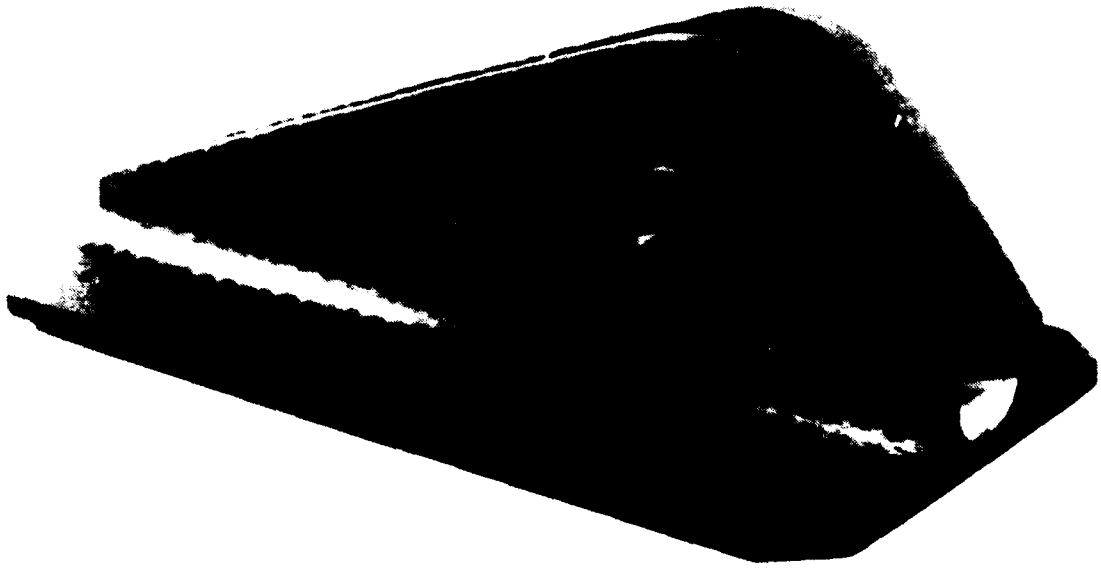

Figure 50. Type K Specimen

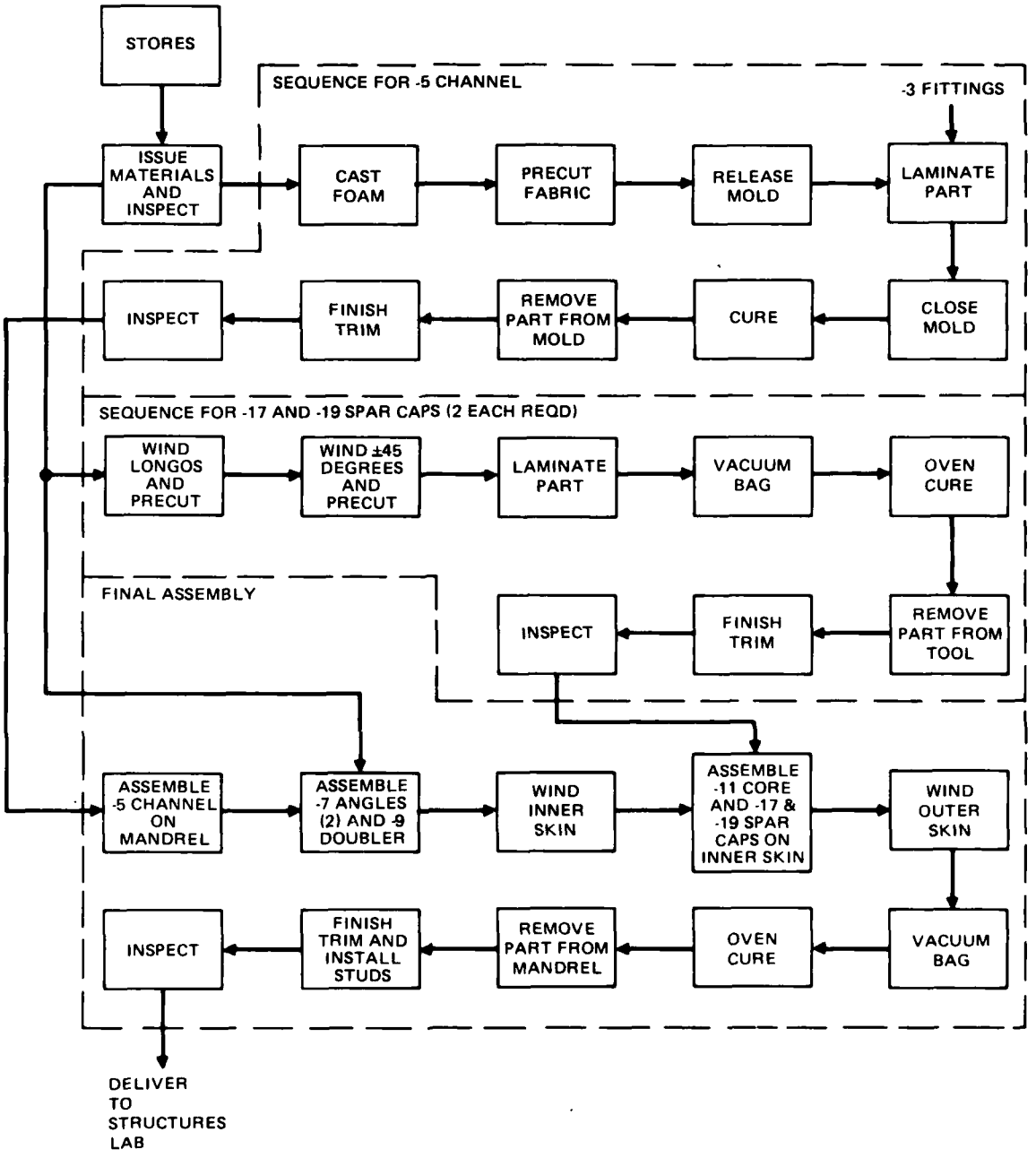

Figure 51. Manufacturing Plan (Type D)

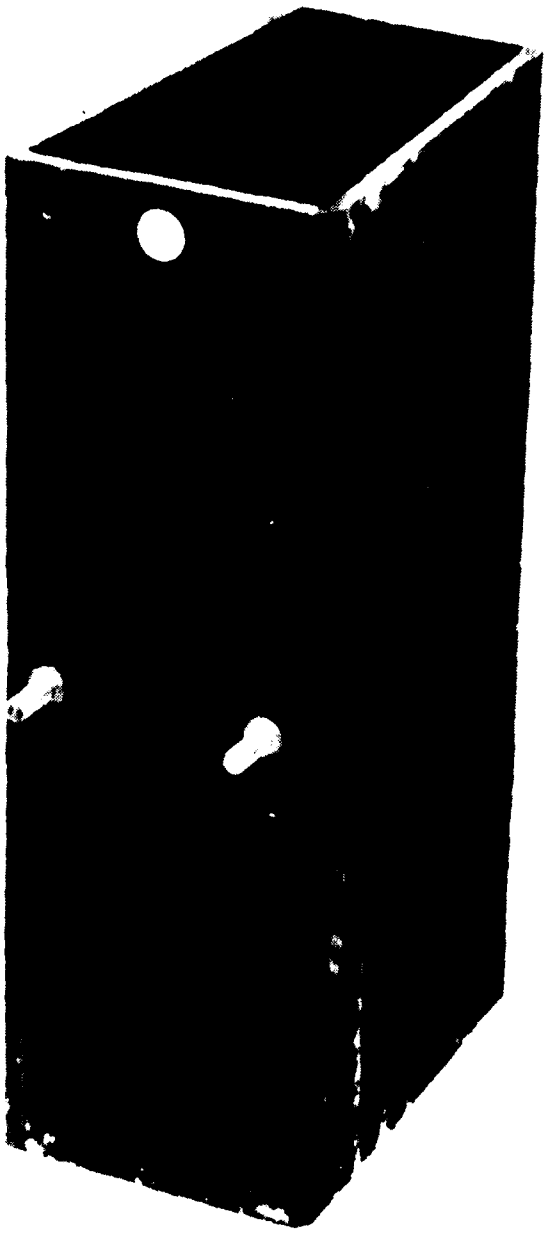

Figure 52. Type D Specimen

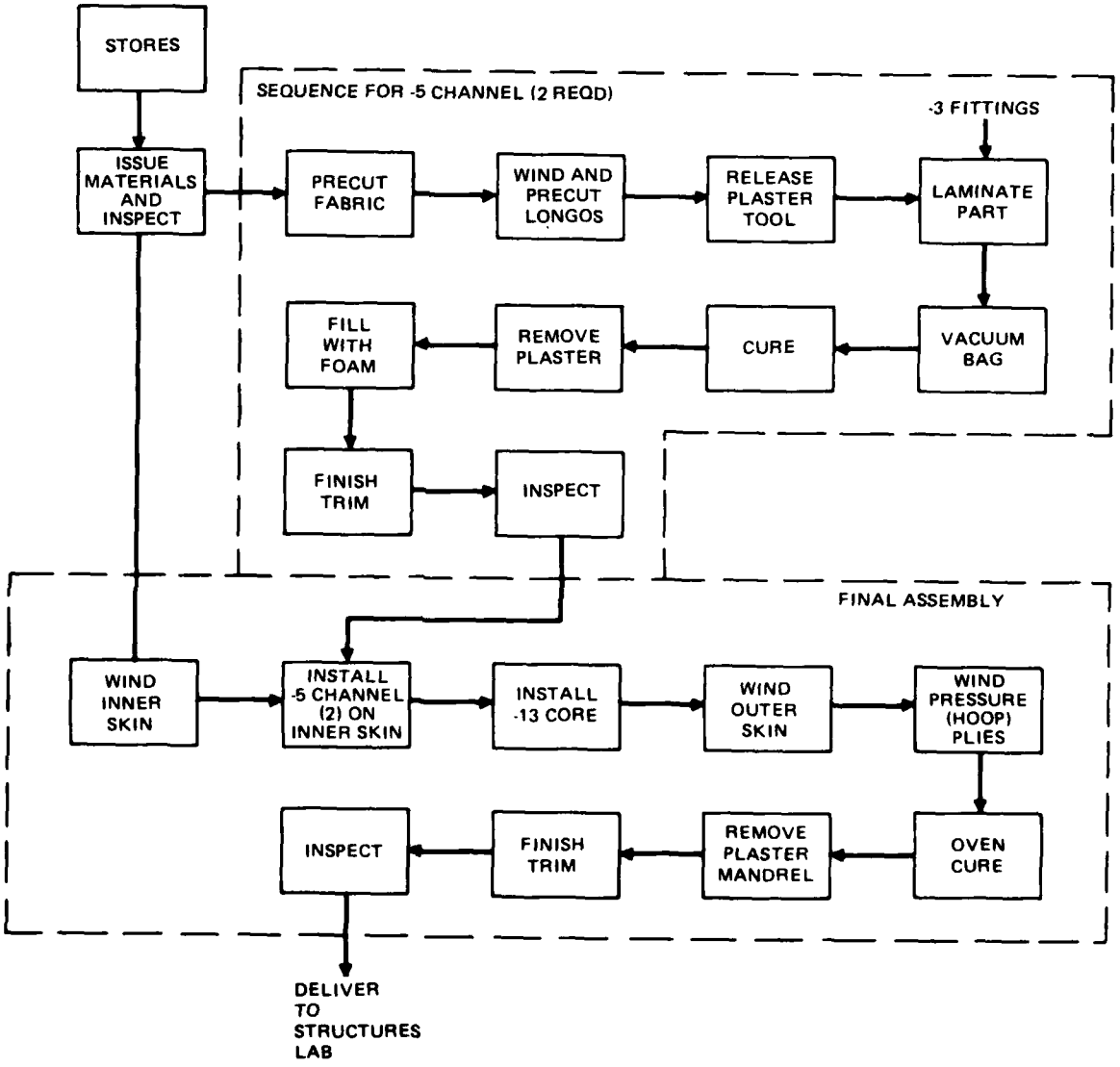

Figure 53. Manufacturing Plan (Type A)

cured. After cure, the seven test specimens were cut from the assembly and finished to drawing dimensions. A photograph of the finished specimen appears in Figure 54.

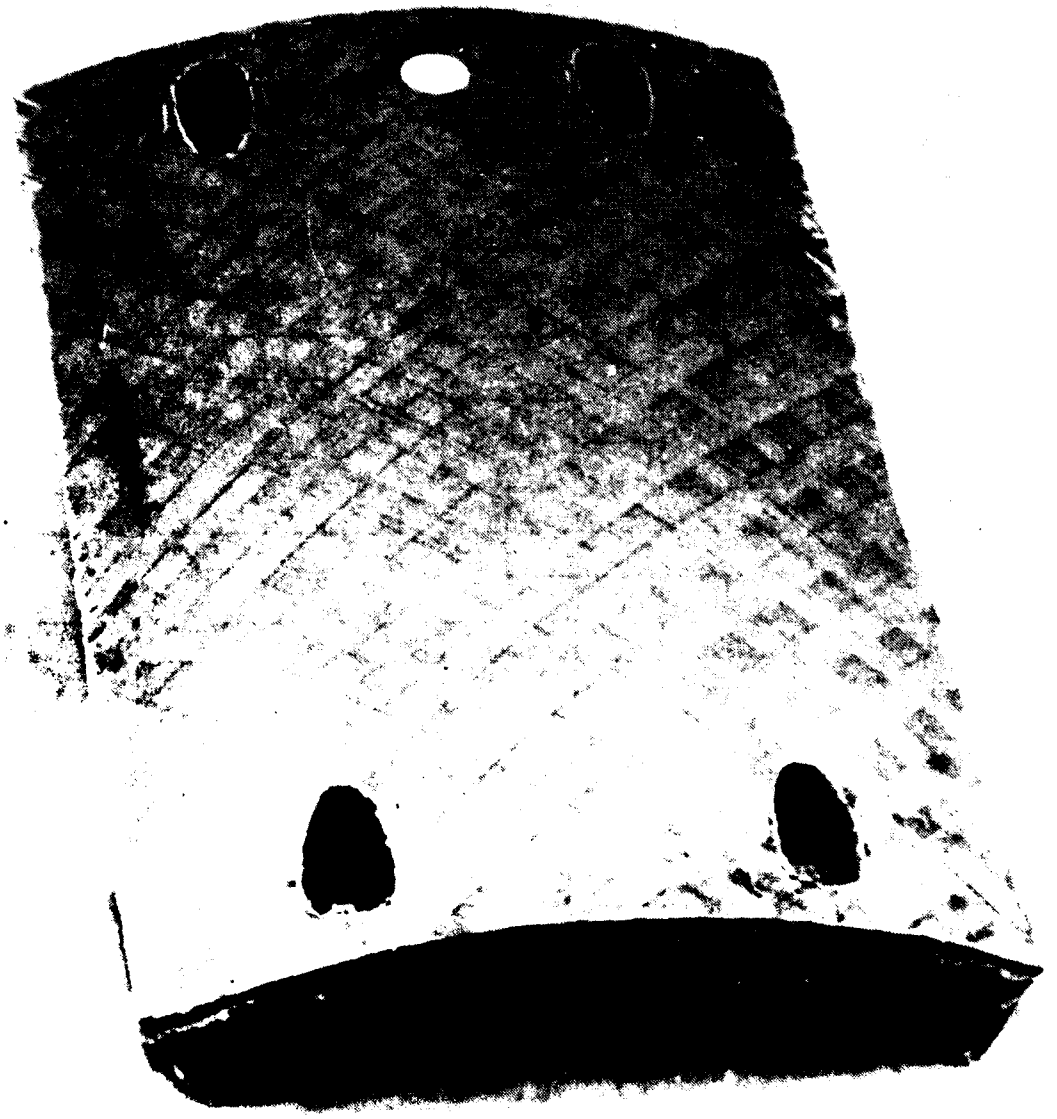

Figure 54. Type A Specimen

TESTING

SPECIMENS

Sixteen specimens of Types K, D, and A were fabricated--three for tool proofing, six for static testing, and seven for fatigue testing:

		Number of Specimens			
Type	Drawing No.	Tool Proof	Static Test	Fatigue Test	Total
K	430-010	1	2	0	3
D	430-007	1	2	3	6
A	430-009	1	2	4	7

Dimensions and Weights

One test specimen of each type was used for tool proofing. A dimensional inspection was performed to verify that the dimensions were within the design tolerances, and the part weight was determined and recorded. The weights and critical dimensions of the test articles were used to establish a first approximation of the manufacturing tolerance range to be expected for that part. Some part-to-part variation is to be expected due to the interaction of the various manufacturing materials and process operations, tooling fitup, layup size and fiber angle variations raw material inconsistencies, fiber and resin variations, and modifications to the cure cycle and machining techniques that become imperative as each part is processed.

Loading Conditions

Since these three types of test fittings could be used in the YAH-64 helicopter, the static and fatigue loads that these fittings could be expected to withstand in that helicopter are well understood.

Tables 6, 7, and 8 delineate the static test conditions for Types K, D, and A. Figures 55 and 56 show the derivation of fatigue loads for Types A and D. Figures 57 through 59 depict the loading fixtures and the estimated ultimate loads, and Figures 60 through 62 specify the type and location of the test instrumentation. The results of these tests are given in the next section.

NONDESTRUCTIVE INSPECTION (NDI)

NDI was carried out to determine the size, type, and location of defects that occurred during fabrication of the three joint and fitting types selected for testing (Types K, D and A). Defects detected by NDI were recorded for use in analyzing the static and fatigue test data, to determine the extent to which strength and reliability are degraded by the presence of a known defect. These could include:

- Delaminations
- Unbonded areas
- Porosity or voids
- Resin-rich/starved areas
- Geometry of internal details
- Thick bondlines
- Position and bond of metal inserts
- Foreign object inclusions

The importance of these defects varies with their size and location in relation to the size and geometry of the particular joint/fitting design in which they occur.

In manufacturing these joints and fittings, an attempt was made to cocure as many components as possible. While this method of assembly has significant advantages from a manufacturing standpoint, it makes it difficult

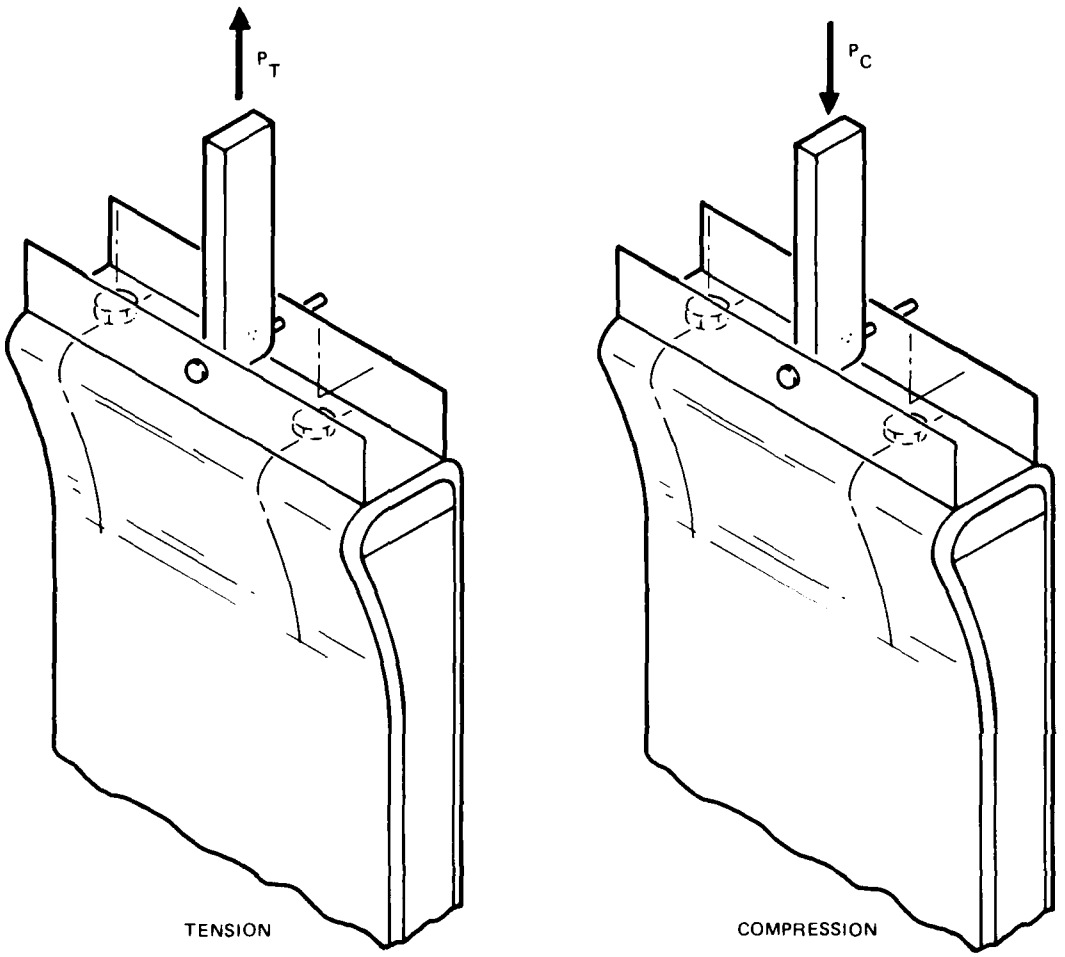

Figure 55. Derivation of Fatigue Loads – Type A

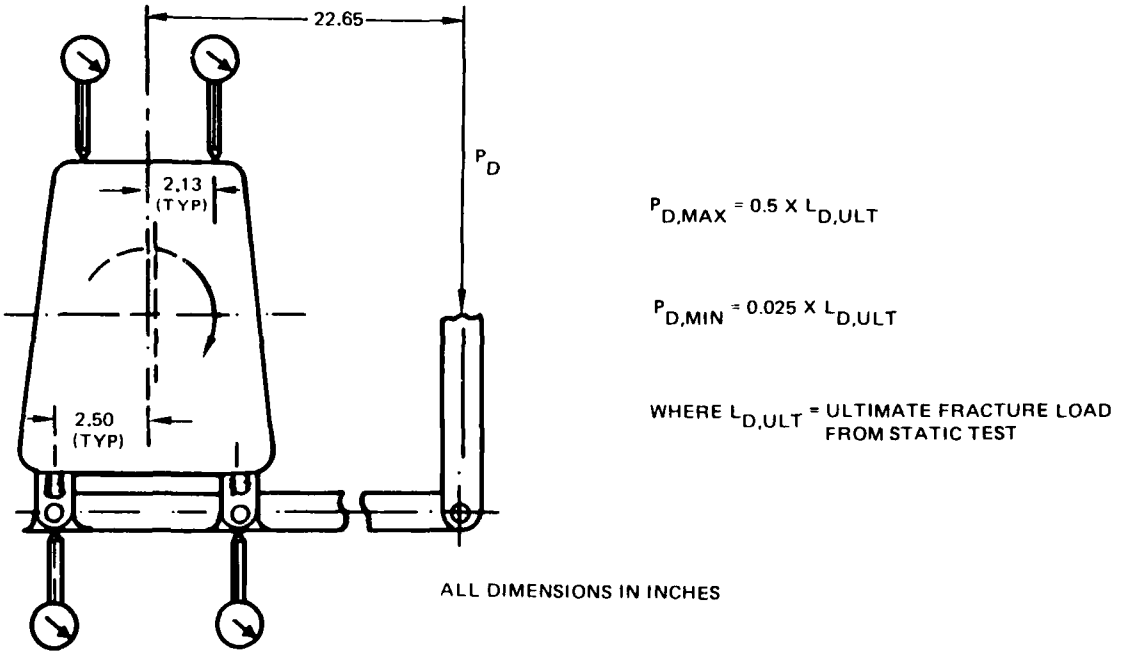

Figure 56. Derivation of Fatigue Loads – Type D

TABLE 6. STATIC STRENGTH, LUG TENSION – TYPE K

Material: Graphite/epoxy
Test Conditions: Ambient temperature and humidity
Pre-test Measurements: Deviations from drawing size tolerances, weight
Pre-test NDE: Visual inspection for surface quality and flaws, tap for delaminations
Instrumentation: Load force, deflections shown in Figure 60
Expected Maximum Load: 16,000 pounds
Deflection: 0.4 inch
Expected Failure Mode and Location: Interlaminar shear and midply filament breakage at midway plane through plate at A or B points
Measurements Required: Load force, deflection, failure location, and description of fracture mode for both incipient and ultimate fracture
Data Reduction: Load versus deflection plots
Number of Tests: Two replicates of rod pull tension

AD-A110 212 HUGHES HELICOPTERS CULVER CITY CA F/G 1/3
ADVANCED CONCEPTS FOR COMPOSITE STRUCTURE JOINTS AND ATTACHMENT--ETC(U)
NOV 81 J V ALEXANDER, R H MESSINGER DAAJ02-77-C-0076
UNCLASSIFIED HH-80-402-VOL-1 USAAVRADCOM-TR-81-D-21A NL.

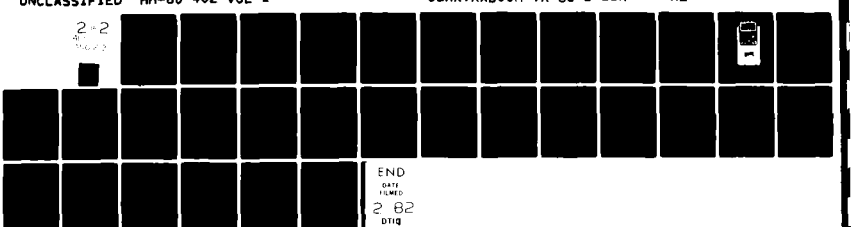

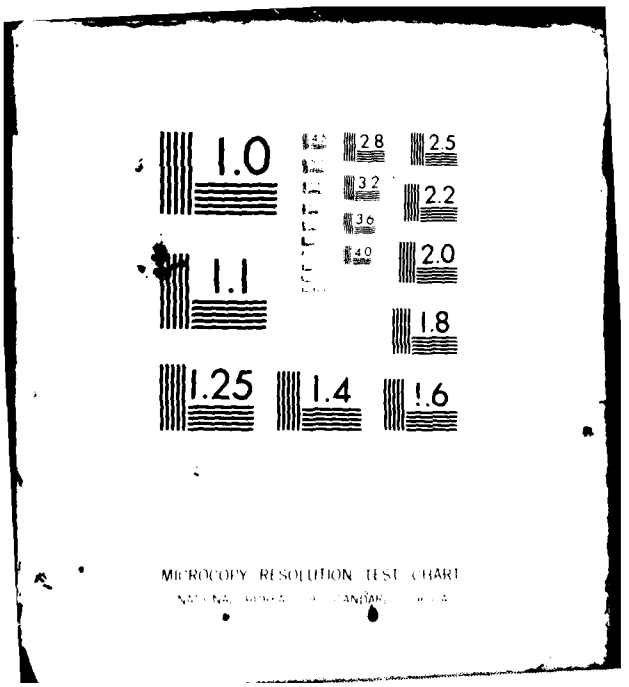
1.0
1.1
1.25
1.4
1.6
1.8
2.0
2.2
2.5
2.8
3.2
3.6
4.0
MICROCOPY RESOLUTION TEST CHART

TABLE 7. STATIC STRENGTH, STUD TENSION AND COMPRESSION – TYPE D

Material: Graphite/epoxy, Nomex honeycomb core, steel studs and anchors

Test Conditions: Ambient temperature and humidity

Pre-test Measurements: Deviations from drawing tolerances, weight

Pre-test NDE: Visual inspection for surface quality and flaws, tap for delaminations

Instrumentation: Load force on pivot push bar, deflections at points shown in Figure 61

Expected Maximum Load: 3,500 pound on push rod

Deflection: Up to 0.9 inch

Expected Failure Mode and Location: Stud/steel anchor push-through into composite and debond or stud tearout

Measurements Required: Loads with accompanying deflections between opposed gauges in two sets of readings, description of failure mode and location for both incipient (limit) and ultimate fracture

Data Reduction: Load versus net displacement plots

Number of Tests: Two replicates of rod compression

TABLE 8. STATIC STRENGTH, TENSION AND COMPRESSION – TYPE A

Material: Graphite/Kevlar/epoxy hybrid over Nomex core, aluminum washer fittings under steel bolts in bathtubs

Test Conditions: Ambient temperature and humidity

Pre-test Measurements: Deviations from drawing tolerances, weight

Pre-test NDE: Visual inspection for surface defects and flaws, tap for debonds and delaminations

Instrumentation: Load force, deflection at load pin connection and points shown in Figure 62

Expected Maximum Load: 23,000 pounds tension and 30,000 pounds compresion

Deflection: 0.5 inch

Expected Failure Mode and Location: Push-through of metal insert, bulge or delamination in skins, corner fiber breakage

Measurements Required: Load with displacements recorded at first noise of incipient failure, visual damage, first load drop, location and types of failure (incipient, ultimate, etc.)

Data Reduction: Load versus deflection plots

Number of Tests: One with panel in tension (no lateral restraints) and one with panel in compression with damped restraints for a total of two nonreplicate static tests

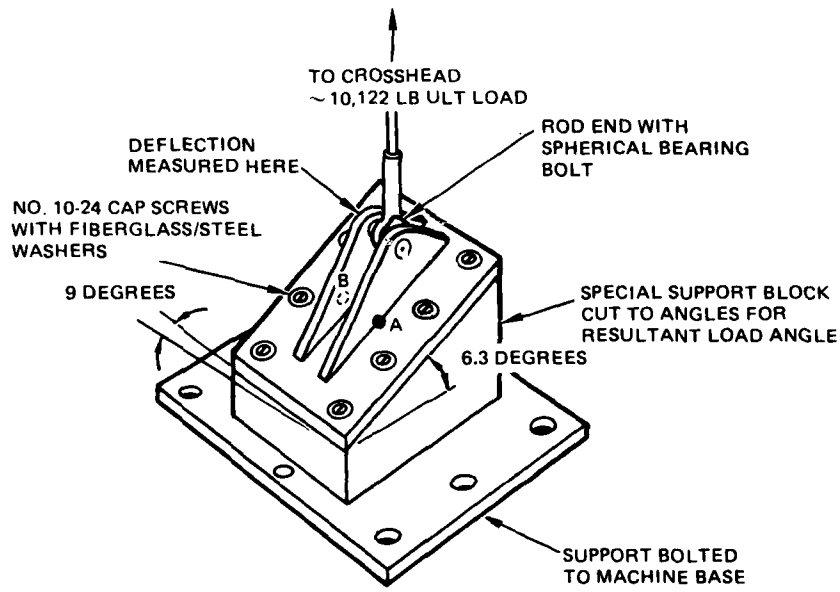

Figure 57. Loading Fixtures and Estimated Ultimate Loads – Type K

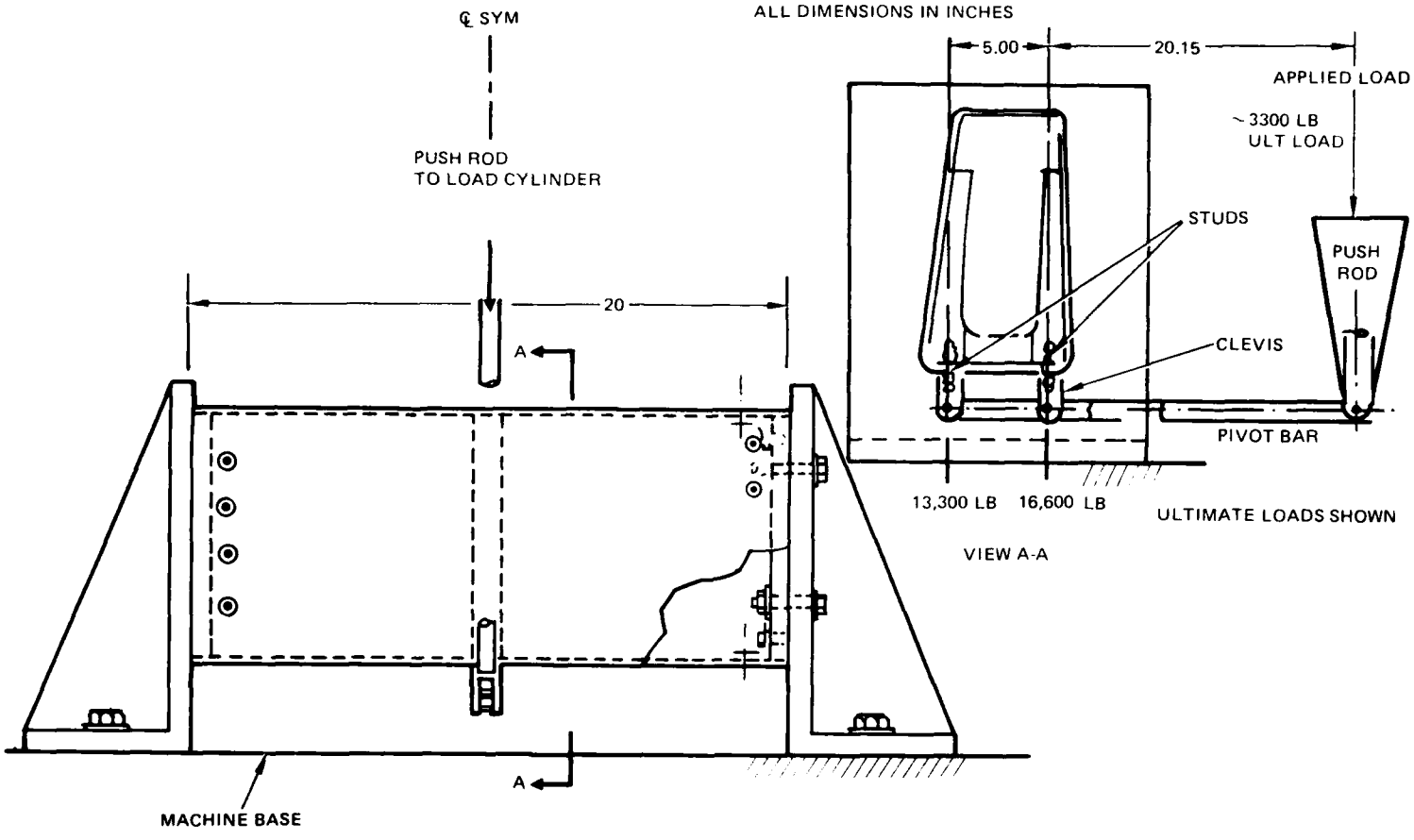

Figure 58. Loading Fixtures and Estimated Ultimate Loads – Type D

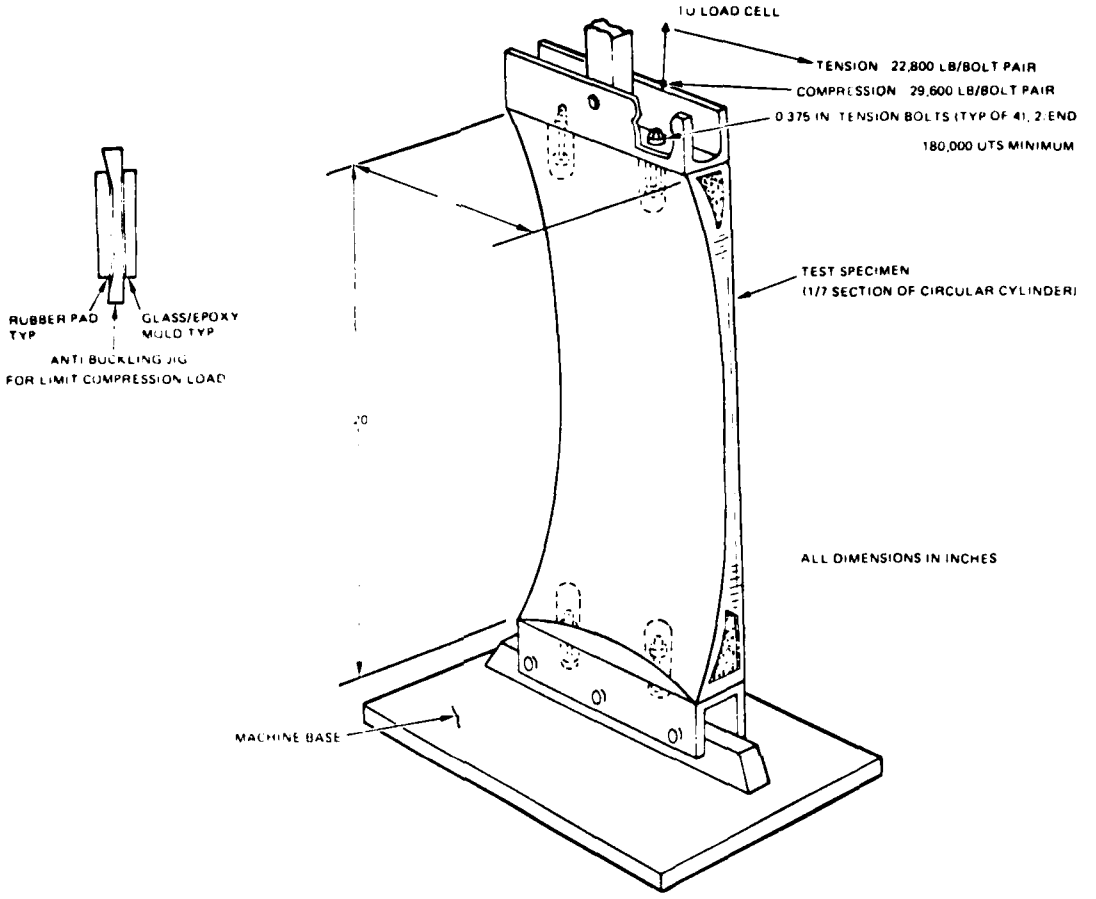

Figure 59. Loading Fixtures and Estimated Ultimate Loads – Type A

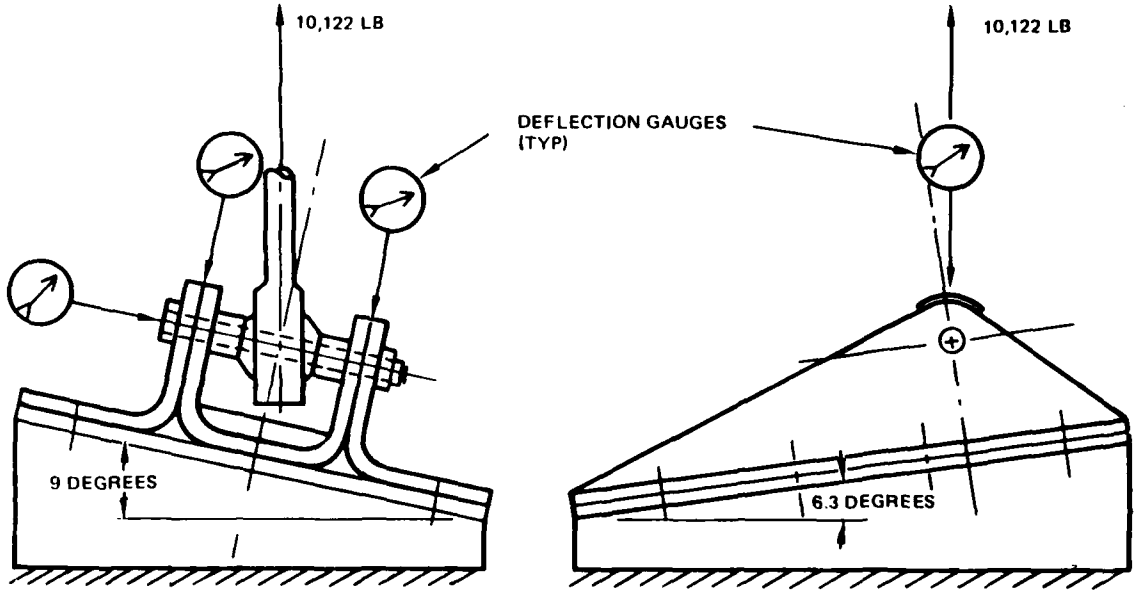

Figure 60. Load Test Instrumentation – Type K

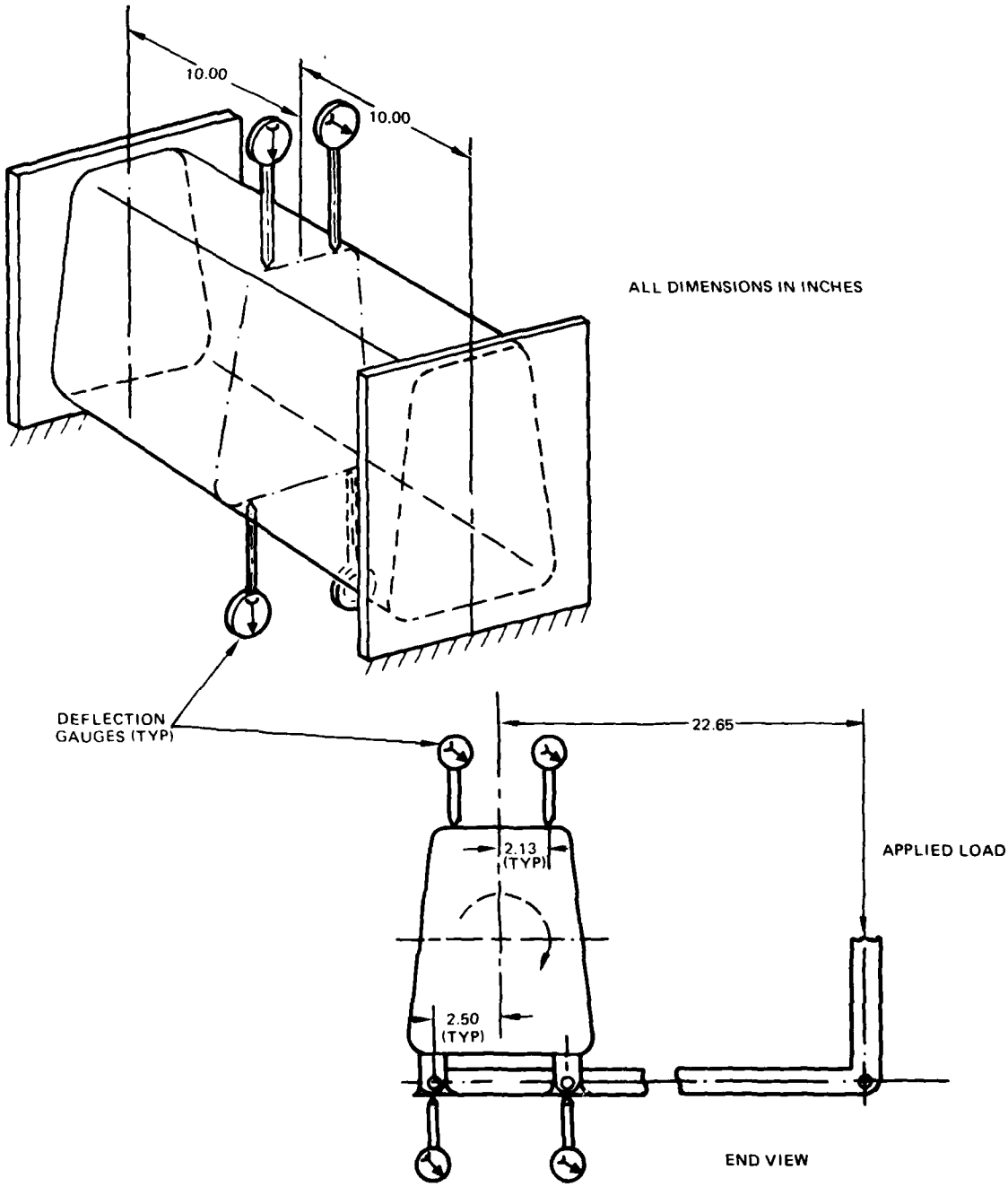

Figure 61. Load Test Instrumentation – Type D

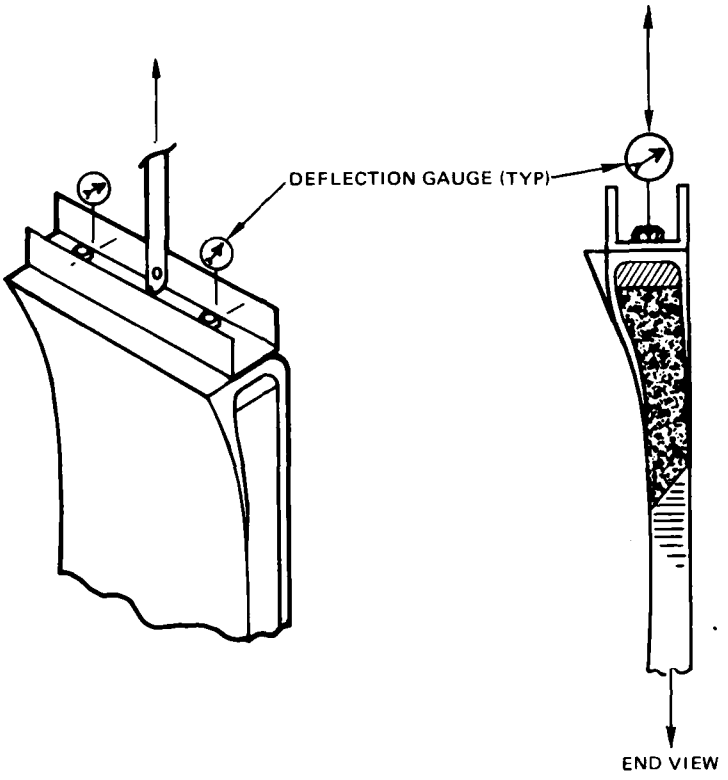

Figure 62. Load Test Instrumentation – Type A

to examine or inspect the various components (that make up an assembly) individually. Assurance that the finished part has been fabricated free of internal defects and has the proper internal geometry can only be obtained using one or more NDI techniques.

Early in the fabrication and test phase, NDI specimens were fabricated using materials and layups like the joint and fitting test specimens with known defects built in (Figure 63). These specimens were used to establish the NDI techniques and equipment settings to be used on precured details and final assemblies. They were also used as a reference for side-by-side comparisons as anomalies occurred in parts under examination.

Visual inspections were performed on detail parts during layup and after cure, in conjunction with hammer tapping prior to incorporation into final assembly.

Wet filament winding operations were inspected visually while in progress, and completed specimens were subjected to inspection using hammer tapping and scanned with the Shurtronics harmonic bond tester (Figure 64).

In the hammer tapping method, a small hammer is used to tap the surface of the composite component. The flat sound produced by tapping over an unbonded area or void is easily detected, even by an untrained ear, and an experienced inspector can readily determine and mark the boundaries of the unbonded area or void. Subsequent tapping can determine the growth of an unbonded area if it occurs.

The Shurtronics harmonic bond testing equipment operates by physically transmitting high-frequency vibrations into bonded materials and monitoring the resulting acoustical response with a small hand-held transducer. The instrument is calibrated with a sample specimen of the same materials and layup as the part under examination, with known defects built in for a reference. With the instrument calibrated for a known density and thickness, a reduction in local thickness caused by an unbonded area or other defect results in an amplitude or phase change in the received signal. Liquid coupling is not required for testing, and the probe can easily be used in any position. This equipment has been used for several years to inspect the bondlines on rotor blades for HH's Series 300 and 500 helicopters.

Records of the results of NDI testing were made and retained by part number and serial number. Sample record forms, with damage detected, are shown in Figures 65 and 66.

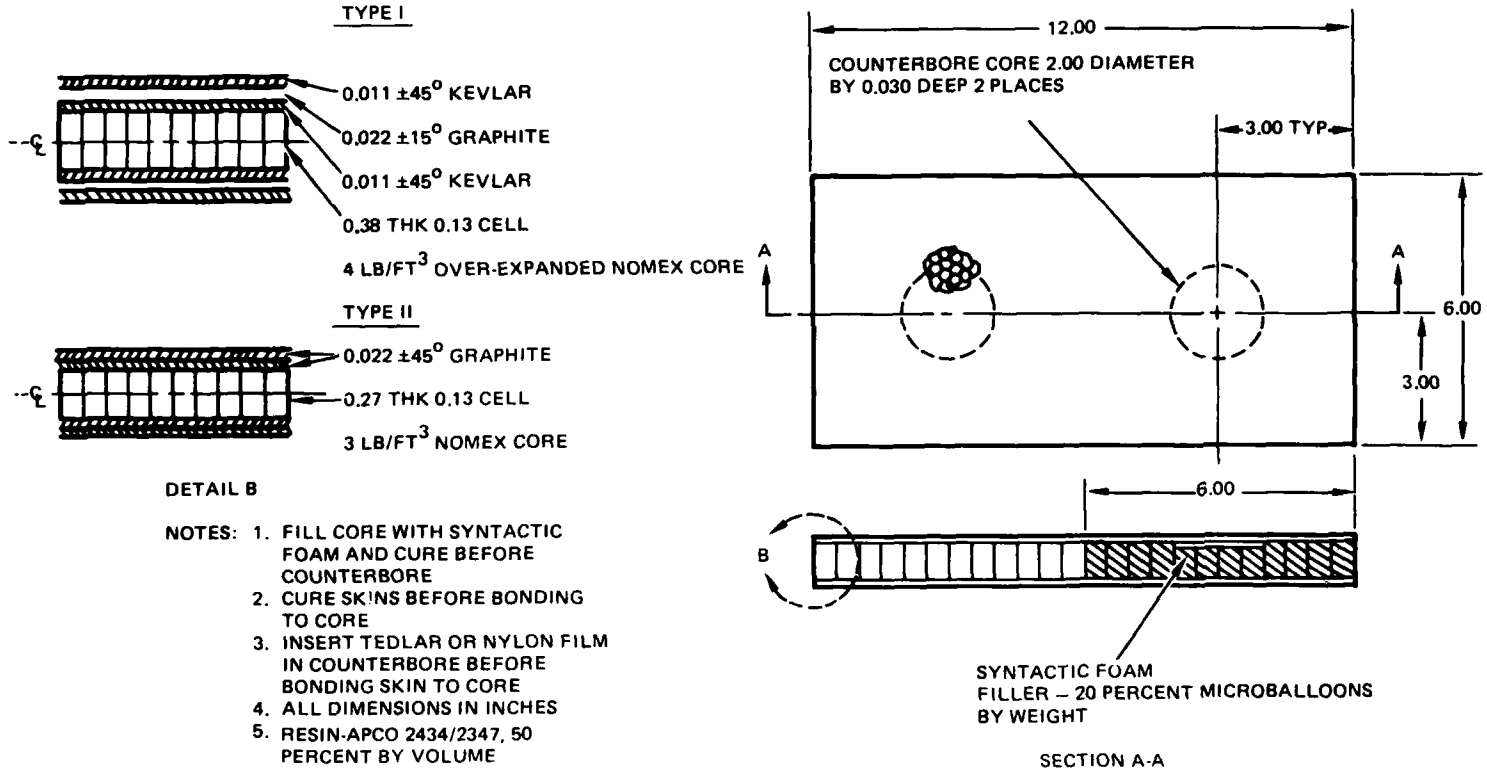

Figure 63. NDI Test Specimen

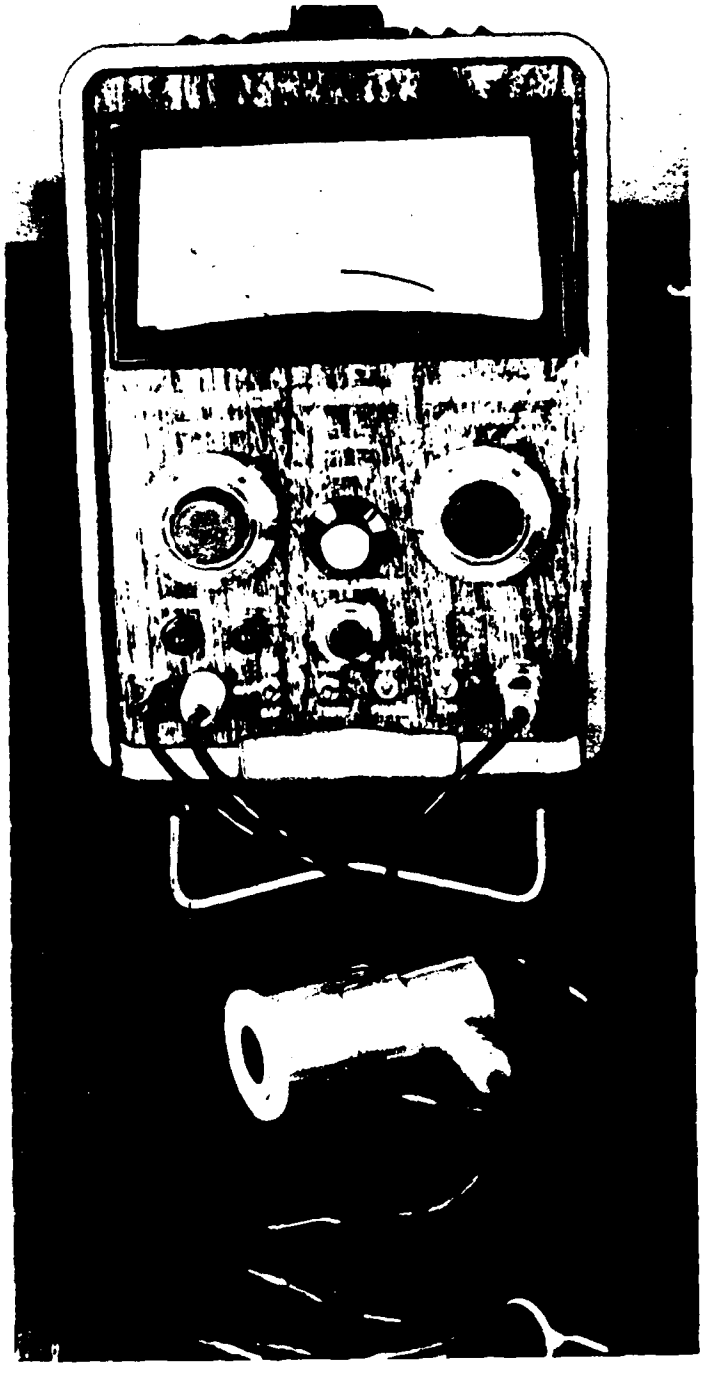

Figure 64. Shurtronics Harmonic Bond Tester

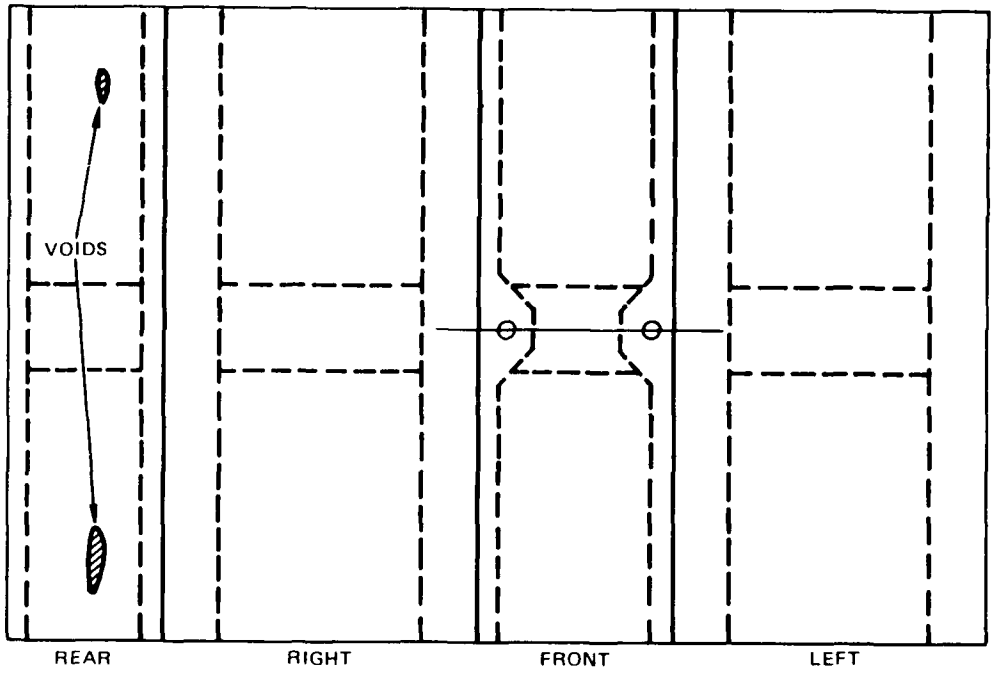

Figure 65. NDI Record – Outer Skin Damage (Type D)

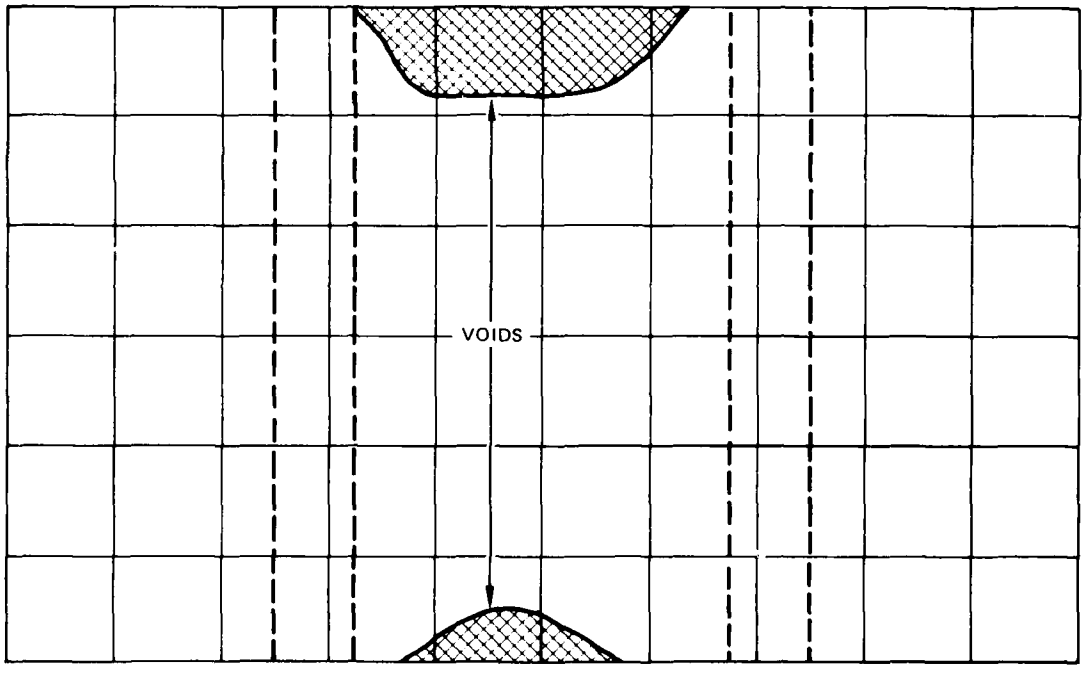

Figure 66. NDI Record – Upper Skin Damage (Type A)

Test Specimen Evaluation

The overall appearance of the Type K specimens was excellent due to all external surfaces being tool faces. The bases of all three parts were bowed slightly, probably due to the lack of locating pins between the various tool pieces permitting relative movement during the autoclave cure cycle. The fabrication process was straightforward and proceeded without problems. Nondestructive inspection did not uncover any delaminations, voids, or other defects.

The external skins of the Type D specimens were slightly wavy, typical of vacuum bagged surfaces. In some specimens the skin joggles where the honeycomb core transitioned to the spar caps due to variations in the thickness of the spar caps. The internal structure of the spar box was excellent. Refinement of the rib fabrication process greatly improved producibility. The knock-out plaster layup tool was replaced by a molded foam core which remains in place to become part of the finished rib. Nondestructive inspection of the specimens using the harmonic bond tester revealed minor skin-to-honeycomb disbonds in four of the six specimens, the largest of which was approximately 2 square inches (see Figure 65). The disbonds were in noncritical areas and were not cause for concern.

The appearance of the Type A specimens was similar to that of the Type D specimens. The outer skin surface exhibited a fairly course texture with some waviness. This is typical of a vacuum bagged surface. Some mismatch was apparent at the transition from the honeycomb sandwich to the precured channel at each end of the specimens. The inner skin looked excellent due to the smooth mandrel surface against which it was cured. The fabrication of the channels could have been improved by using a washout or melt-out plaster layup mold, or by precuring the foam core and laying up the detail directly on the foam. The break-out plaster was difficult to remove due to the limited access. The original outer skin started to gel before sufficient bonding pressure had been applied, leaving a very porous skin. This skin was subsequently removed and a new skin was wound and bonded to the core. The second skin quality was much better. Nondestructive inspection revealed disbonds between the skins and the honeycomb core in three of the seven specimens. This is probably due to insufficient filleting of the resin to the cell walls. The largest of these were approximately 10 square inches and occurred in the upper skin along the panel edges (see Figure 66). Since these disbonds were not located near the joint area under investigation, they were not considered critical.

STRUCTURAL TESTING

Thirteen specimens were structurally tested in accordance with the Test Plan prepared during detail design. Two specimens of each of the three types of joints fabricated (K, D, and A) were statically tested. Seven fatigue tests were performed, three on Type D and four on Type A specimens. The remaining specimen of each type was a tool proof article, which was not subjected to structural tests. A summary of the test results is given in Table 9. Loads are based on percent of design limit load (DLL).

Static Testing

The static tests were conducted in a similar manner for all three types. The load on the specimen was applied in increments of 20 percent up to 100 percent of DLL. The load was reduced to 20 percent to permit checking for permanent deformation and was reapplied in 20 percent increments up to 100 percent DLL, and then in 10 percent increments up to 150 percent DLL (150 percent DLL equals the design ultimate load). If no failure occurred, the load was increased until failure did occur. The failure load was recorded, and the mode of failure was determined.

Type K. The static tests of the Type K specimens (Figure 29) consisted of two tension tests (Figure 57). The load deflection curves for the two specimens are plotted in Figure 67. The failure load of the first specimen was 143 percent DLL. The first sign of damage was an audible cracking sound at 74 percent load.

At 104 percent load a second cracking sound was heard. Brooming around the bushings appeared at 119 percent load, followed by tensile failure of one leg of the -3 channel at 143 percent load. The -5 angle of the same leg also failed by peeling and transverse shear around the washers.

The second specimen, tested in the same manner, failed at 161 percent DLL. This specimen first showed signs of damage at 30 percent load (resin crazing), followed by a loud crack (delamination) at 71 percent load. Faint cracking and elongation of the bushing hole appeared at 89 percent load. Faint cracking began again at 119 percent load and continued until failure occurred at 163 percent load. The mode of failure was the same as for the first specimen.

TABLE 9. TEST SUMMARY

E Specimens		Test Load			
No.	Type	Static Load, pounds	Fatigue Load, pounds	$\frac{PT}{PD}$[1]	Remarks
1	Tool Proof				
2	Static	9,500		1.43	Tension Failure of -3 Channel
3	Static	10,840		1.63	Tension Failure of -3 Channel
D Specimens					
1	Tool Proof				
2	Static	4,100		1.86	Metal-Composite Bond Failure
3	Static	2,770		1.26	Metal-Composite Bond Failure
4	Fatigue		1,385	0.63	Runout - 3×10^6 Cycles
5	Fatigue		1,662	0.76	Runout - 3×10^6 Cycles
6	Fatigue		1,939	0.88	Metal-Composite Bond Failure - 586,500 Cycles
A Specimens					
1	Tool Proof				
2	Static Tension	29,220		1.92	Skin-to-Core Delamination, Bolt Failure
3	Static Compression	11,760		0.60	Panel Buckling Failure
4	Fatigue Compression		5,880	0.30	Runout - 3×10^6 Cycles
4	Static Compression	16,900[2]		0.86	Skin Buckling Failure
5	Fatigue Compression		7,056	0.36	Runout - 3×10^6 Cycles
5	Fatigue Compression		10,140[3]	0.52	Skin Buckling Failure - 908,400 Cycles
6	Fatigue Tension		14,610	0.46	Runout - 3×10^6 Cycles
7	Fatigue Tension		17,[illegible]2	1.15	-5 Channel-to-Skin Bond Failure - 949,200 Cycles

[1] Test load design limit load.

[2] Residual strength test on Specimen 4 after fatigue test.

[3] Second fatigue test on Specimen 5.

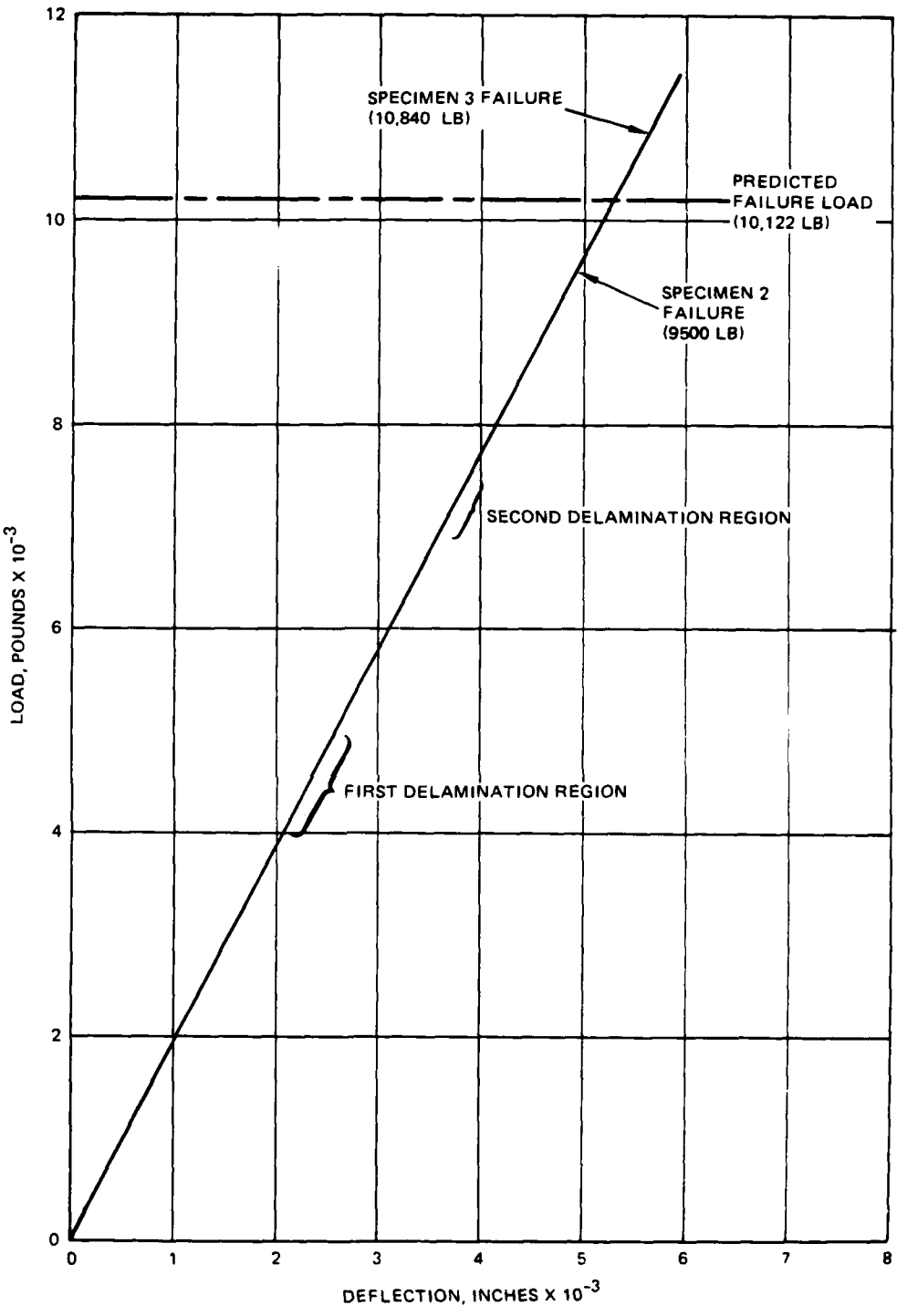

Figure 67. Load-Deflection Curves – Type K

Type D. The static tests of the Type D specimens (Figure 34) consisted of two torsion tests (Figure 58). The load-deflection curves of the two specimens are plotted in Figure 68. The failure load for the first specimen was 186 percent DLL. The first sign of damage was an audible crack at 127 percent load. At 150 percent load the stud loaded in tension failed. This stud was replaced with a higher strength part, and the loading procedure was repeated. No further damage was evident until 158 percent load, when audible cracking began. Failure occurred at 186 percent DLL, with a shear bond failure between the -3 steel insert and the -21 composite rib.

The second specimen was tested in the same manner, with the first audible cracks occurring at 120 percent load, continuing until ultimate failure at 126 percent DLL. The mode of failure was the same as for the first specimen.

Type A. The static tests of the Type A specimens (Figure 40) consisted of one static tension test and one static compression test (Figure 59). The load-deflection curves are plotted in Figure 69. The failure of the tension specimen occurred at 192 percent DLL. The first audible cracking occurred at 66 percent, followed by cracking at 86 percent, 112 percent, and 138 percent. At 192 percent DLL, a skin-to-core disbond appeared, and one of the four attachment bolts broke, causing local buckling damage in the skins along the panel edge.

The compression specimen failed immediately at 60 percent DLL, by compressive buckling of the panel. This failure was a general buckling failure due to the eccentric loading condition inherent in this design. The design of the tailboom-fuselage joint consists of a tapered cylinder loaded in bending. The failure of the curved panel specimen corresponds to an outward buckling of the cylinder. In a cylindrical section this buckling mode is resisted by a circumferential tension stress, but in the curved test panel this resisting stress cannot be generated. For this reason the compression test was determined to be unrepresentative of the actual conditions present in a tailboom-fuselage joint of this type. After runout of the first compression fatigue test, this specimen was tested in compression using a jig fabricated and installed to prevent general panel instability. The result of this test was a compressive failure load of 86 percent DLL. The failure mode was local crippling of the skins in the sandwich section of the specimen.

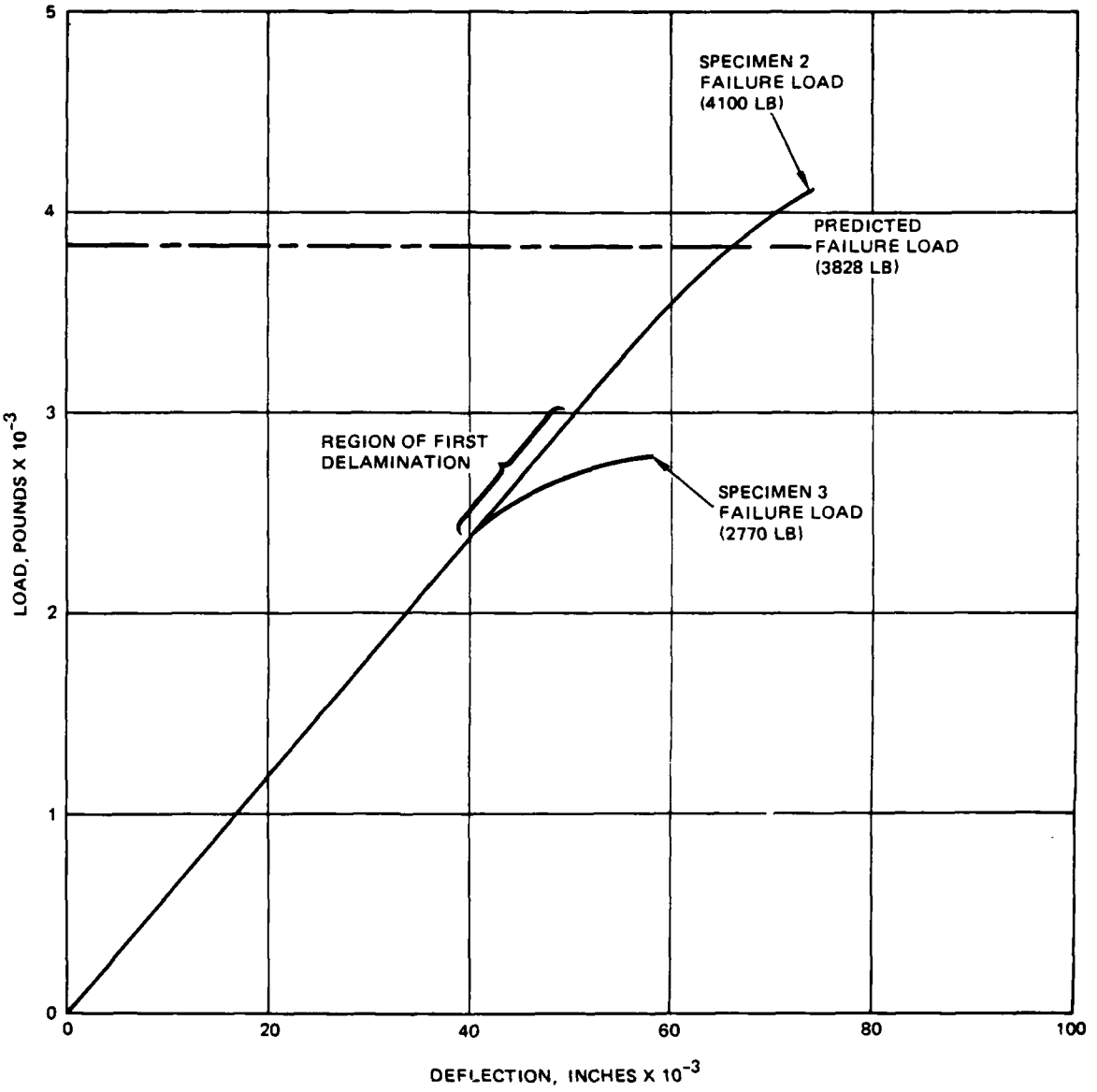

Figure 68. Load-Deflection Curves – Type D

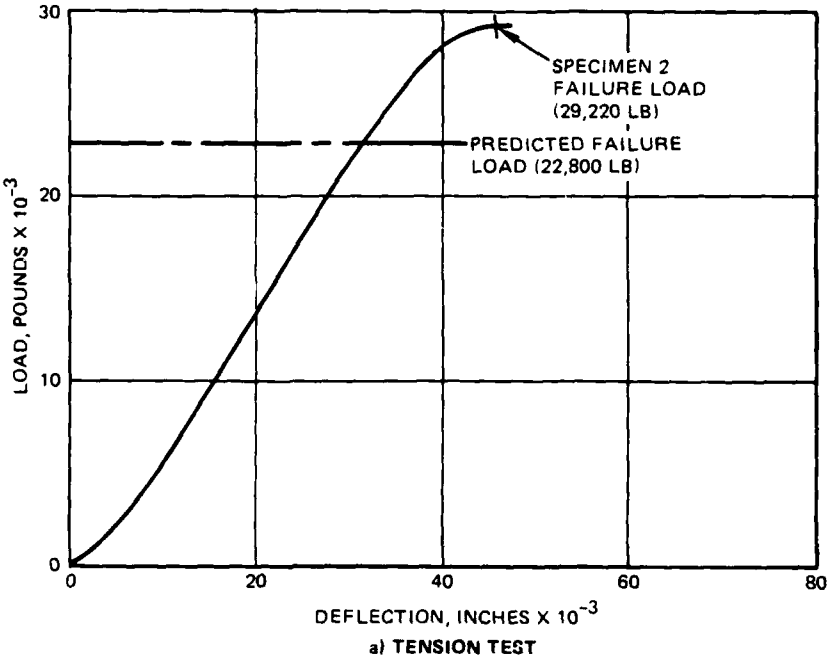

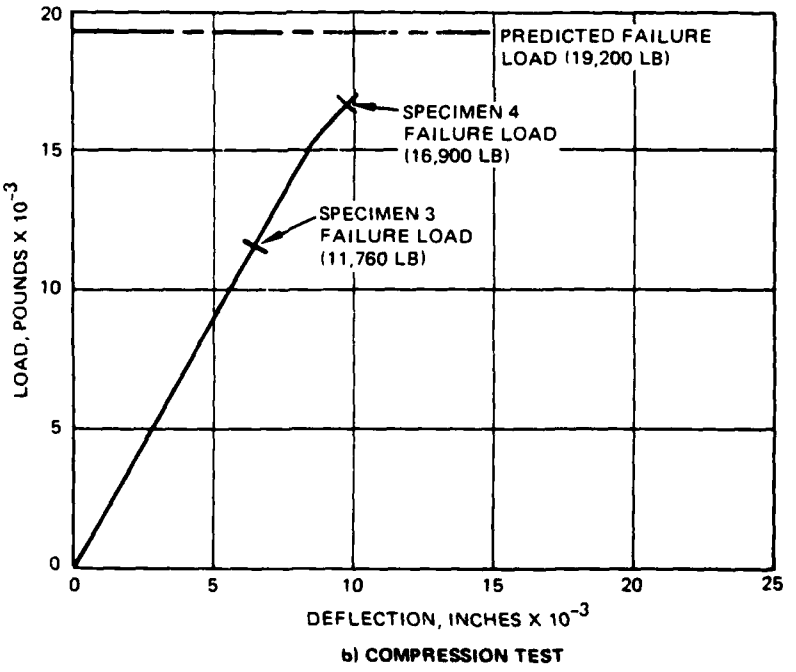

Figure 69. Load-Deflection Curves – Type A

Fatigue Testing

Seven fatigue tests were performed, three on Type D and four on Type A. The fatigue tests on all specimens consisted of the application of a constant amplitude, nonreversing load with the minimum/maximum load ratio equal to 0.05.

The objective of the fatigue testing was to generate fatigue data to be presented in the form of load versus cycle curves (S-N diagrams) for each of the composite joint types. In order to generate this type of data and concurrently limit testing time, an accelerated fatigue test program was used. First, if a specimen endured three million cycles without failure, it was considered a "runout" test and terminated. Second, load levels were set higher than would normally be encountered in service to precipitate failures before runout. This step was undertaken to ensure that the data obtained would develop the required curves.

The load levels used for fatigue testing were based on the failure load in the corresponding static test. Fatigue tests were initiated at 50 percent, 60 percent, and 70 percent of the corresponding static failure loads.

Type D. Fatigue testing of the Type D joint design was carried out on three specimens. This type underwent two static tests with considerably different static failure loads. The decision was made to use the lower of the two static failure loads as a basis for determining the fatigue test load levels.

The first Type D fatigue test specimen was cyclically loaded to 50 percent of the static failure load (this load level corresponds to 63 percent DLL). Application of such a high cyclic load level created problems with the steel studs in the specimen. Fatigue failures in the studs necessitated removal and replacement with larger diameter, higher strength units. This procedure proved successful, and was applied to the remaining two specimens before application of fatigue loads. No damage was detected in the first specimen during the test, and the specimen endured the required three million cycles to runout.

The second Type D fatigue test specimen, according to the Test Plan, was tested at a load level equal to 60 percent of the static failure load (76 percent DLL). As with the first specimen, no damage was detected, and the test was terminated at three million cycles (runout).

The last Type D fatigue specimen was tested at a load level equal to 70 percent of the static failure load (88 percent DLL). This specimen experienced a metal-to-composite bond failure at 586,500 cycles. The failure was the same mode as the two static test failures.

A load-cycle curve for the Type D joint is given in Figure 70. Two static and three fatigue test points are plotted.

Type A. Fatigue testing of the Type A joint design was carried out on four specimens, two tension and two compression. Static failure loads were again used as a basis for fatigue test load levels. The compression tests were all run with the stabilizing jig in place. The first compression specimen was subjected to a load level equal to 50 percent of the first static compression failure load (30 percent DLL). No damage was detected, and the test was terminated at three million cycles (runout). This specimen was then subjected to a static compression test as detailed in the static test section of this report.

The second compression fatigue test specimen was subjected to a fatigue load level equal to 60 percent of the first static failure load (36 percent DLL). This test was also a runout at three million cycles. No noticeable damage was seen in this test. This specimen was then subjected to a second fatigue test using the second static test failure load (86 percent DLL) as a basis for determining the fatigue load level. For this test 60 percent of the second static load was chosen (52 percent DLL). This test terminated due to specimen failure at 908,400 cycles. The mode of failure was compression buckling of the inner and outer skins in the sandwich section of the specimen.

The first tension fatigue test was run at 50 percent of static tension failure load (96 percent DLL). As a result of the high level of this test load, several tension bolt failures were experienced. To alleviate this problem, the specimen was removed from the test fixture and drilled to accept half-inch bolts instead of the original three-eighth-inch bolts. Damage that developed during the test was limited to cracking of the panel edge filler (milled glass/epoxy). The test was terminated at three million cycles (runout).

The second tension fatigue test was performed at 60 percent of static tension failure load (115 percent DLL). Test specimen failure occurred at 949,200 cycles, with -5 channel-to-outer skin debonding at one end of the panel. Subsequent damage included shear failure of the -7 foam filler and delaminations in the skin-to-honeycomb bond.

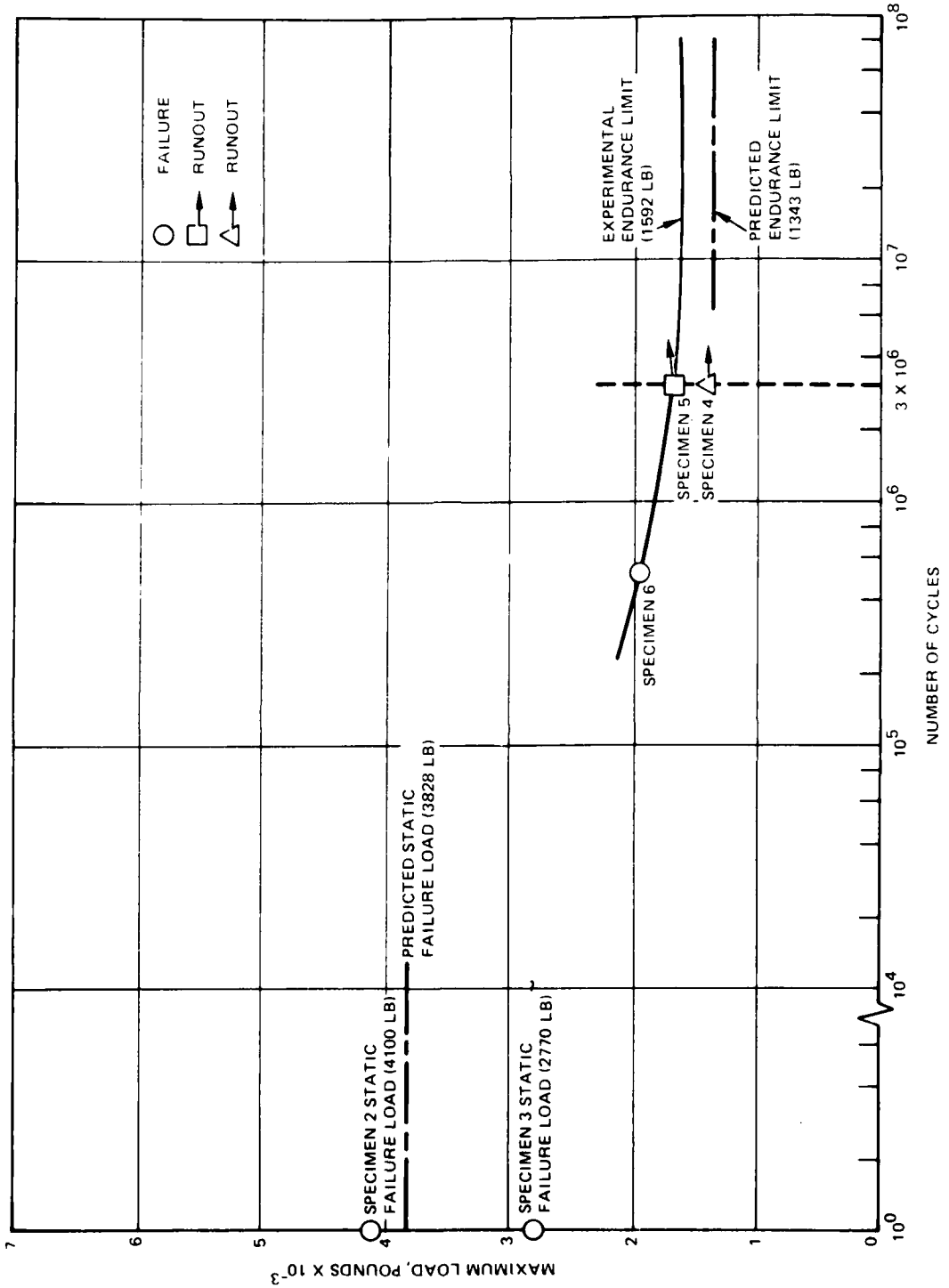

Figure 70. Load-Cycle Curve – Type D

Load-cycle curves for the Type A joint are shown in Figures 71 and 72. One static and two fatigue test points are plotted for tension, and two static and three fatigue test points are plotted for compression.

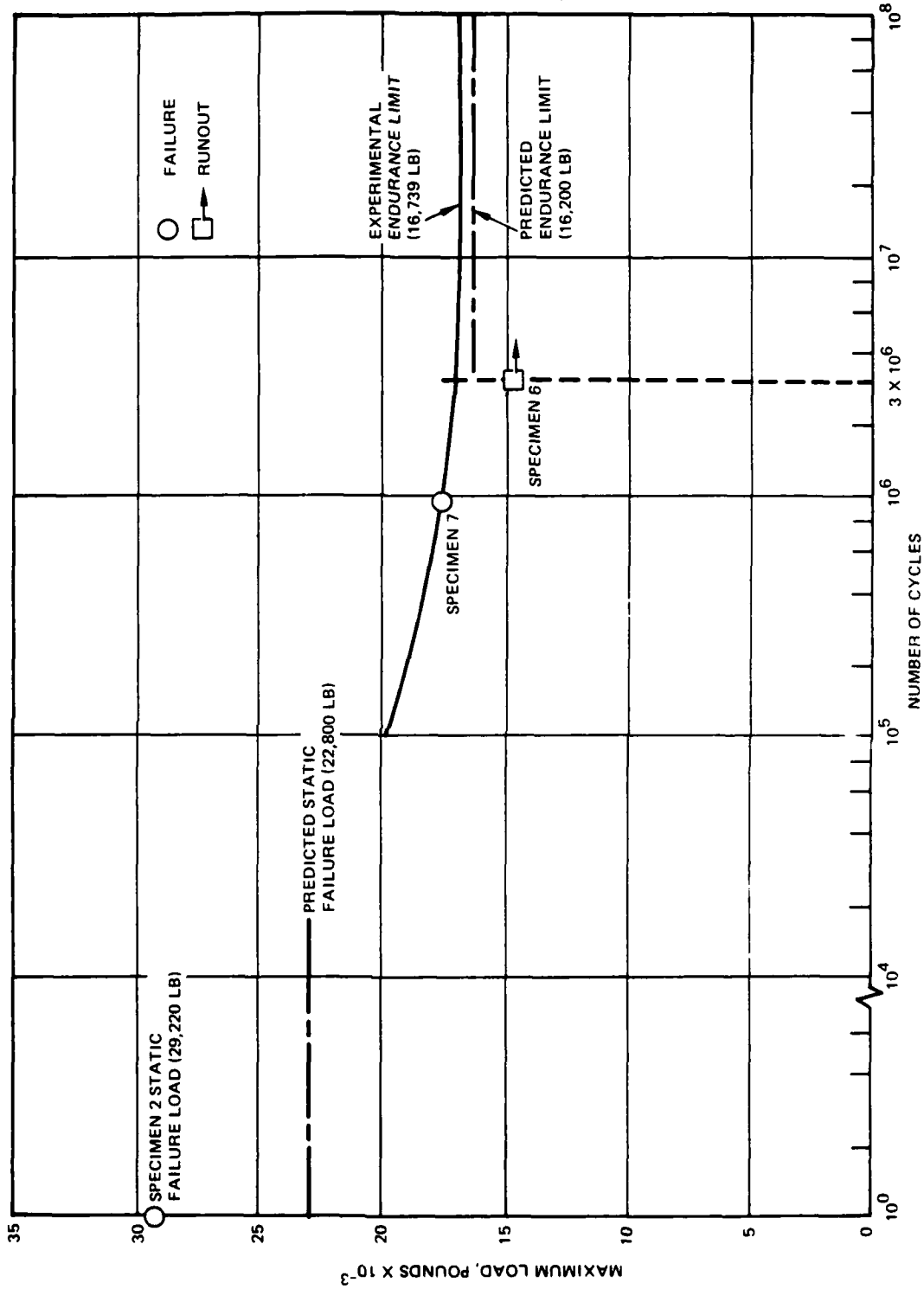

Figure 71. Load-Cycle Curve – Type A (Tension Fatigue Tests)

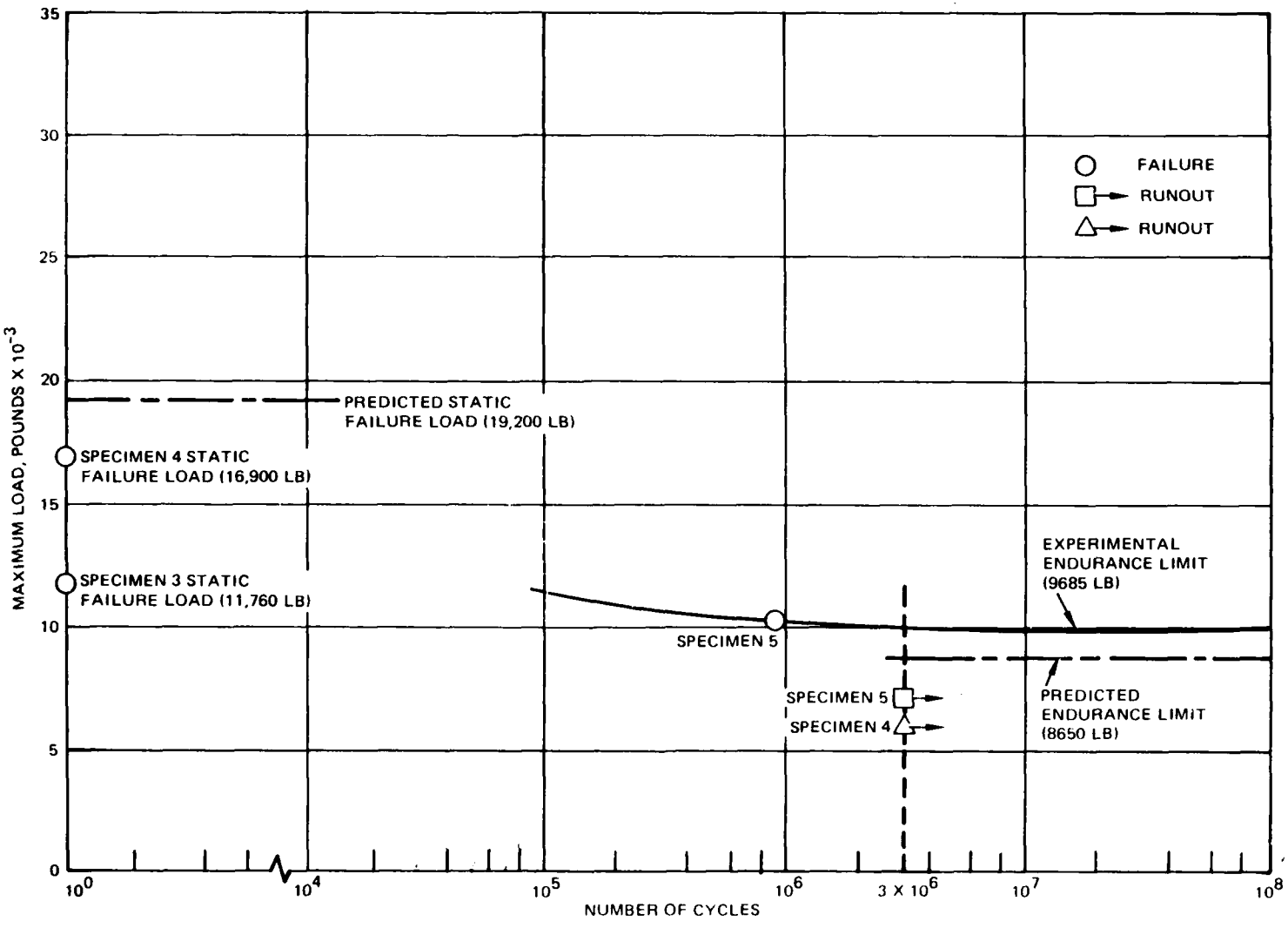

Figure 72. Load-Cycle Curve – Type A (Compression Fatigue Tests)

ANALYTICAL COMPARISONS

The results of the static and fatigue tests were compared with the performance predictions based on the stress analysis in Volume II (Appendix O) to validate the final design and to substantiate the structural analysis methods employed during detail design.

STATIC TESTS

The predicted and experimental failure loads for each of the static test specimens are presented in the upper portion of Table 10. Included in the table is the ratio of the predicted load divided by the experimental load.

Type K

The load-deflection curve (Figure 67) presents the experimental and predicted performance in graphic format. The predicted value (10,122 pounds) corresponds closely with the mean of the two experimental values (10,170 pounds). The difference between the high and low experimental failure load values is 13 percent.

Type D

The load-deflection curve (Figure 68) shows that Specimen 3 failed prematurely. This early failure was precipitated by poor control of the bondline (thickness and pressure) during the fabrication process. Specimen 2 failed at 107 percent of the predicted failure load. This test agrees well with the prediction.

Type A

The load-deflection curves are presented in Figure 69a for the tension load case and in Figure 69b for the compression load case. As the curves show, the part performed quite well in tension (128 percent of prediction) but poorly in compression. This poor performance was attributed to the design of the panel sandwich and not the design of the joint. The failure of Specimen 3 was due to buckling of the panel, which is loaded eccentrically in compression. The failure of Specimen 4 (tested with the anti-buckling jig in place) was due to local cripping of the sandwich face sheets.

TABLE 10. ANALYTICAL VERSUS EXPERIMENTAL COMPARISONS

Static					
Specimen		Load Type	Failure Load, pounds		$\frac{F_E}{F_P}$
Type	No.		Predicted (F_P)	Experimental (F_E)	
K	2	Tension	10,122	9,500	0.94
	3			10,840	1.07
D	2	Tension	3,828	4,100	1.07
	3			2,770	0.73
A	2	Tension	22,800	29,220	1.28
	3	Compression	19,200	11,760	0.61
	4			16,900	0.88
Fatigue					
Specimen		Load Type	Endurance Limit, pounds		$\frac{EL_E}{EL_P}$
Type	No.		Predicted (EL_P)	Experimental (EL_E)	
D	4	Tension	1,3[illegible]	1,592	1.19
	5				
	6				
A	4	Compression	8,650	9,685	1.12
	5				
	5				
	6	Tension	16,200	16,739	1.03
	7				

FATIGUE TESTS

The predicted and experimental endurance limit values for each of the specimen types are compared in the lower portion of Table 10. The table also includes the ratio of the experimental value divided by the predicted value for each type.

Type D

The load-cycle curve of Figure 70 represents the results of the three fatigue tests performed on the three Type D specimens. Included in the figure are the static failure loads and the predicted and experimental endurance limit values. The endurance limit values compare well. Based on the values for the endurance limit, the static failure load for Specimen 3 does not agree with the values obtained from the other four specimens. This indicates a defective part and reinforces the conclusion drawn during the static tests. The experimental value of the endurance limit is 39 percent of the Specimen 2 static failure load.

Type A

The fatigue tests consisted of both tension and fatigue tests. These will be compared separately because of the different failure modes.

The results of the Type A tension fatigue tests are given in Figure 71. The static failure loads (predicted and Specimen 2) are included for the purpose of comparison of static versus endurance strengths. As can be seen in the figure, the predicted and experimental values of the endurance limit agree quite closely (within 3 percent). The experimental value of the endurance limit is also seen to be quite high (57 percent of the static failure load for Specimen 2).

The results of the Type A compression fatigue tests are compared in Figure 72. The static failure load for Specimen 3 (the first static compression specimen) can be seen to disagree with the other four test points. This is due to the different mode of failure, as discussed in the static test section of the report. The static failure load for Specimen 4 is actually the residual strength of that specimen after three million cycles at a load of 5,880 pounds (31 percent of the predicted static failure load). As can be seen in the figure, the experimental endurance limit agrees well with the predicted value (within 12 percent).

DESIGN GUIDE

The Design Guide (Volume II) covers each of the types of fittings that were fabricated and tested. It includes recommendations for:

- Basic joint design considerations
- Criteria for selecting the joint configuration (load paths, strength and stiffness, materials, compatibility, and damage tolerance)
- Cost/weight trade-offs
- Allowable stresses (ultimate and endurance limit)
- Analytical methods (including NASTRAN and failure modes)
- Environmental considerations
- Fabrication and NDI methods
- Future tests

CONCLUSIONS

The Advanced Concepts for Composite Structure Joints and Attachment Fittings program met all of its goals. The design concepts that were developed and tested proved that reliable, efficient composite joints are practical in the design of primary aircraft structures. These concepts were generic and are readily adaptable to a variety of applications.

Future programs are necessary to develop additional test data pertaining to composite joint and fitting designs in order to incorporate the concepts developed during this program into the design of composite structures. During these programs data should be developed with regard to the effects of environmental degradation, foreign object and impact damage, and damage due to handling and storage, as well as field repair techniques.

BIBLIOGRAPHY

Advanced Composite Design Guide, Rev. 3, Air Force Materials Laboratory, 1977.

Dallas, R. N., "Mechanical Joints in Structural Composites," Lockheed-California Co., SAMPE Symposium, October 1967.

Eves, J., "Advanced Composite Bulkhead Concepts for Wing-to-Fuselage Trunnion Joints," Northrop Corp., SAMPE Symposium, April 1977.

Fant, J. A., et al., "Advanced Composite Technology Fuselage Program," Convair Aerospace Div., General Dynamics Corp., AFML-TR-71-41, Vol. VI, October 1973.

Fant, J. A., "An Advanced Composite Wing for the F-16," Fort Worth Div., General Dynamics Corp., SAMPE Symposium, April 1977.

Hart-Smith, L. T., "Bolted Joints in Graphite-Epoxy Composites," NASA-CR-144899, January 1977.

Head, R. E., "Flight Test of a Composite Multi-Tubular Spar Main Rotor Blade on the AH-1G Helicopter," USAAMRDL-TR-77-19A, January 1977.

Hille, A. A., "Joint Design Optimization by Discrete Element Computer Techniques," Douglas Aircraft Co., LB-33964, October 1967.

Hoffstedt, D. M., and Swatton, S., "Advanced Helicopter Structural Design Investigation," Boeing Vertol Co., USAAMRDL-TR-75-56A, Vol. I, December 1975.

Johnson, R., and McCarty, J., "Design and Fabrication of Graphite/Epoxy Bolted Wing Skin Splice Specimens," Boeing Commercial Airplane Co., NASA-CR-145216, May 1977.

Kutscha, D., and Hofer, K. E., Jr., "Feasibility of Joining Advanced Composite Flight Vehicle Structures," AFML-TR-68-391, January 1969.

Lehman, G.M., et al., "Advanced Composite Rudders for DC-10 Aircraft," Douglas Aircraft Co., NASA-CR-145068, Final Report, NASA Contract NASI-12954.

Lehman, G.M., "Advanced Composite Vertical Stabilizer for DC-10 Transport Aircraft," Douglas Aircraft Co., ACEE-03-PR-7177, Quarterly Progress Report, NASA Contract NASI-14869, June 1977.

Lehman, G.M., and Hawley, A.V., "Investigation of Joints in Advanced Fibrous Composites for Aircraft Structures," AFFDL-TR-69-43, Vols. I and II, June 1969.

Macander, A.B., "Joints for Advanced Composite Structures: A Technology Review and Evaluation Plan to Determine Marine Suitability," NSRDC Report 4275, April 1974.

Mayerjack, R., and Smyth, W., "Investigation of Advanced Structural Concepts for Fuselage," Kaman Aerospace Corp., USAAMRDL-TR-73-72, October 1972.

Miller, R.C., and Bellinger, T.P., "Fabrication of Advanced Composite Attach Lugs for Aircraft Structures," Vought Corp., SAMPE Journal, Vol. 13, September/October 1977.

Needham, J.F., "Design, Fabrication, and Testing of an Advanced Composite AH-1G Tail Section (Tail Boom/Vertical Fin), "USAAMRDL-TR-76-24, February 1976.

Pinckney, R.L., "Fabrication Techniques and Materials for High-Modulus, Filament-Reinforced Composites," AFML-TR-67-399, December 1967.

Reifsnider, K.L., and Louraitis, K.N., "Fatigue of Filamentary Composite Materials, ASTM Special Technical Publication 636, 1977.

Rich, M.J., et al., "Advanced Composite Airframe Structures," Journal of the American Helicopter Society, July 1975.

Schaeffer, W.H., et al., "Advanced Composite Wing and Empennage-to-Fuselage Attachment Fittings," Convair Aerospace Div., General Dynamics Corp., AFML-TR-74-5, January 1974.

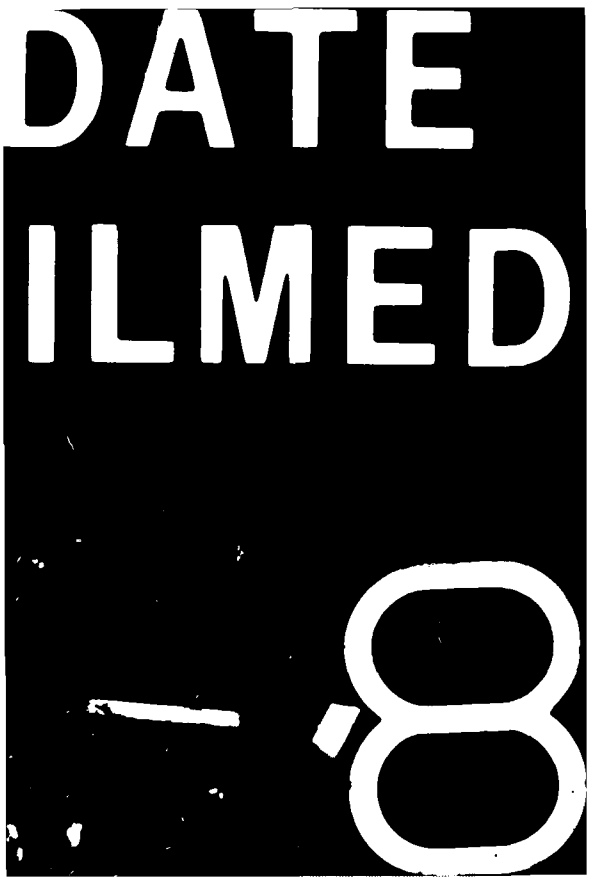
DATE
ILMED
-'8